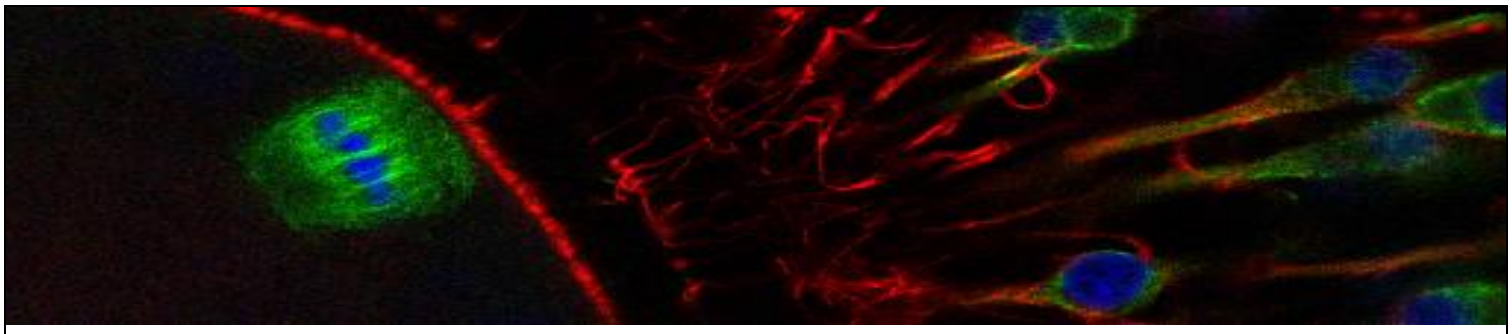

Colorado State University

14th Annual
College of Veterinary Medicine
and
Biomedical Sciences
Research Day Scientific Proceedings

The Fort Collins Hilton
January 26, 2013

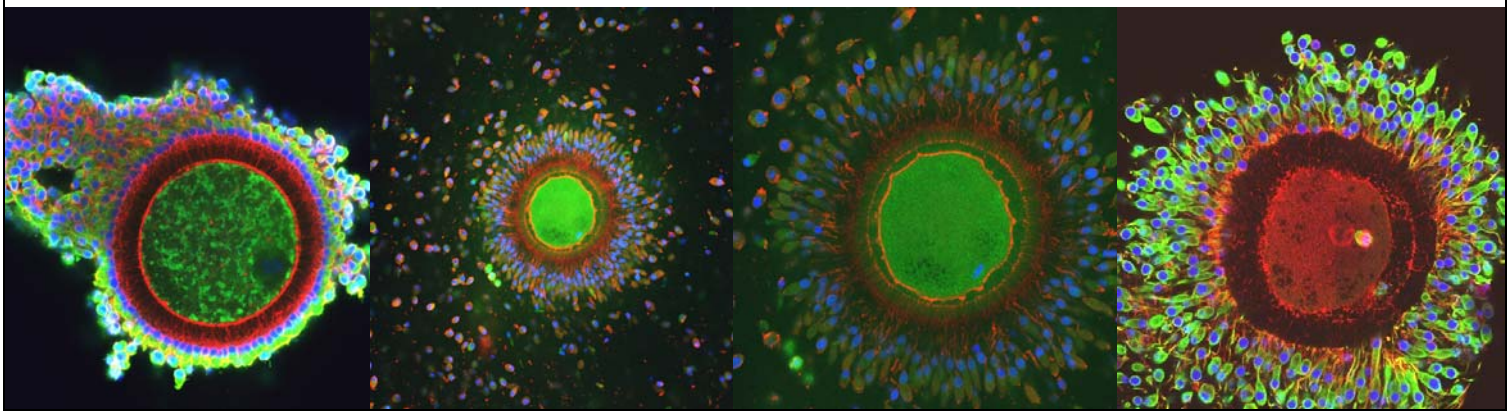

Thank you moderators and judges!!

Thank you to our sponsor!

Animal Health

Cover Art:
Top: close-up of the meiotic spindle of an equine oocyte
Bottom: Images of 4 different equine oocytes surrounded by cumulus cells
Courtesy of Elena Ruggeri (BMS, CSU) and Dr. David Albertini (University of Kansas Medical University)

CVMBS Research Day 2013

Schedule Of Events		Room
11:30-12:00	Poster set up	Salon III, IV
12:00	Opening remarks – Dr. Susan VandeWoude	Salon II
12:05	Pfizer Research Award Winner – Dr. Mark Zabel	Salon II
	"Prion Trafficking and Therapeutics: Tracking them down and stopping them in their tracks"	
12:45	Break	
1:00-5:00	Oral Presentation I: Clinical Sciences	Salon I
1:00-5:00	Oral Presentation II: Basic Sciences	Salon V
1:00-5:00	Oral Presentation III : Clinical/Basic Sciences	Salon II
1:00-3:00	Poster Session I Judging: Odd-numbered Posters	Salon III, IV
3:15-5:00	Poster Session II Judging: Even-numbered Posters	Salon III, IV
5:00-6:00	Social Hour, Remove Posters	Salon III, IV
5:30	Awards	Salon III, IV

Oral Presentation: - Please limit to a 10 minute talk with 1-3 minutes for questions and changeover. Oral presentations will be in Salons I, II, and V.

Poster Presentation: - Please hang your posters on Jan. 26 from 11:30-12:00 in Salons III and IV. Individuals presenting the poster must be in attendance to discuss their materials with judges as listed above.

PFIZER RESEARCH AWARD WINNER

CVMBS Research Day
Saturday, January 26, 2013

Dr. Mark Zabel, Ph.D.

"Prion Trafficking and Therapeutics: Tracking them down and stopping them in their tracks"

Dr. Mark Zabel established his prion research laboratory at CSU seven years ago and is currently tenured Associate Professor and Associate Director of the Prion Research Center. He received his PhD in experimental pathology from the University of Utah. Dr. Zabel was awarded the prestigious Human Frontiers in Science Long Term Research Fellowship and received postdoctoral training in prion biology, biochemistry and pathology from the laboratory of Dr. Adriano Aguzzi at the Neuropathology Institute, University Hospital of Zürich. He also received training in immunology in the laboratory of Nobel Prize winner Dr. Rolf Zinkernagel in the Immunology Department, also at the University Hospital of Zürich.

The Zabel laboratory employs molecular biological, immunological and biochemical techniques to explore peripheral pathogenesis, therapeutics and vaccines for prion diseases. Studying basic mechanisms of prion infection and dissemination provides translational information leading to diagnostic, therapeutic and vaccine targets. Dr. Zabel's research program focuses on the interaction of prions with cells and receptors of the immune system and lymphoid tissues in the early entry, trafficking, and pathogenesis phases of prion infections. He utilizes novel mouse models of Chronic Wasting Disease that have led to numerous publications detailing translational knowledge about the role of the Complement system in prion replication, disease progression and transmission. Dr. Zabel's laboratory currently collaborates with researchers from Fort Collins, the Front Range of Colorado, Wyoming, Nebraska, Montana, Ohio, Tennessee, Massachusetts, England, Scotland, Germany, Switzerland and Australia.

Dr. Zabel received the Univeristy of Utah Molecular Biology and Biochemistry Distinguished Alumni Award in 2010 and is an Academic Editor for PLoS One. Dr. Zabel has also distinguished himself as a meeting organizer and session chair at the Regional Rocky Mountain Prion Research Symposium, Fort Collins (2008), and the International Transmissible Spongiform Encephalopathy workshops in Montreal, Canada (2011) and Amsterdam, the Netherlands (2012).

His research is funded through USDA-APHIS and NIH-Neurological Disorders and Stroke.

Salon II
The Hilton Hotel
Fort Collins, CO

Oral Presentations

SESSION 1: CLINICAL SCIENCE
1:00-4:45PM

Salon I

1:00	Aanstoos-Ewen	Effects of Adipose-Derived Mesenchymal Stromal Cells on Osteosarcoma Growth and Metastasis	BIOM
1:15	Adams	Association of Thoracic Radiographs and Severity of Pulmonary Arterial Hypertension (PAH) Diagnosed in 66 Dogs via Doppler Echocardiography	ERHS
1:30	Daniel	Optimization of a technique to distend the digital flexor tendon sheath in horses and subsequent evaluation with ultrasound and MRI	CS
1:45	Edmondson	Prognostic molecular markers and immunohistochemical characterization of canine renal cell carcinoma	MIP
2:00	Ellis	Differentiation between Healthy Cattle and Cattle Infected with Mycobacterium bovis using the Volatile Organic Compound Profiles Present in Breath	BMS
2:15	Enroth	Differentiating Nasal Chondrosarcoma From Nasal Adenocarcinoma On Computed Tomography	ERHS
2:30	Forster	Dry bean consumption modulates metabolic byproducts in overweight dogs undergoing weight reduction	CS
2:45	BREAK		
3:00	Griffenhagen	Evaluation of a Novel Formulation of Propofol Containing 2% Benzyl Alcohol in Cats	CS
3:15	Hay-Roe	Coccidioidomycosis at the Phoenix Zoo, 2006-2011	BMS
3:30	Lear	Evaluation of Serum Vitamin E and Cholesterol Levels in Alpacas	CS
3:45	Loeber	Incorporation of FDG-PET/CT into Radiation Therapy Planning to Improve Treatment of Canine Nasal Tumors	CS
4:00	Magnuson	Validation of molecular techniques for rapid detection of tuberculosis in elephants	CS
4:15	Nelson	Multimodal diagnostic approach to stifle disease in Quarter horses	CS
4:30	Noland	The alveolar-arterial oxygen gradient of primiparous dairy heifers is associated with total milk production	CS
4:45	Noyes	Pen-level associations between antimicrobial use and resistance in feedlot cattle	CS

Oral Presentations

SESSION 2: BASIC SCIENCE
1:00-4:45PM

Salon V

1:00	Barnhart	The Commandeering of the HuR Protein by Alphaviruses Affects Cellular Post Transcriptional Gene Regulation	MIP
1:15	Brackney	Autophagy functions in a pro-viral manner during West Nile virus infection of mosquitoes	MIP
1:30	Bumgardner	Effects of NOD2 on the Immunogenicity of Lactobacillus as a Mucosal Vaccine Vector	MIP
1:45	da Silveira	Exosomal miRNAs regulate TGFß family members during equine ovarian follicular development	BMS
2:00	Fowles	Comparative analysis of MAPK and PI3K/AKT pathway activation and inhibition in human and canine melanoma	CS
2:15	Frahm	Prenatal dexamethasone impacts the blood vessels within the paraventricular nucleus of the hypothalamus	BMS
2:30	Frawley	The Effect of Sample Storage Media, Refrigeration, and Time on Urine Culture Accuracy in Canine Urine Experimentally Inoculated With Known Bacterial Quantities	CS
2:45	BREAK		
3:00	Gallagher	µ-opioid receptor mediated modulation of intrinsically photosensitive retinal ganglion cells	BMS
3:15	Garner	Correlation of Mast Cell Tumor Aggressiveness with Degree of Cutaneous Mucinosis in Chinese Shar-Pei Dogs	MIP
3:30	Hoon-Hanks	Highly Sensitive In Vitro Evaluation of Cervid Field Samples for Chronic Wasting Disease Infection	MIP
3:45	Hoxmeier	Mosquitoes and Mycobacteria: A forbidden love	MIP
4:00	Linke	A novel RNAi delivery system engineered to target epithelial cells and prevent avian influenza replication	CS
4:15	Miller, C.	Viral excretion and tissue tropism of feline immunodeficiency virus in saliva and oral tissues	MIP
4:30	Morges	Evaluation of artemisinin analogs in canine and human tumor cell lines	CS
4:45	Nie	Metnase Regulation of DNA Integration	ERHS

Oral Presentations

SESSION 3: CLINICAL/BASIC SCIENCE
1:00-4:45PM

Salon II

1:00	Palomares	Assessment of diagnostic tests for identification of Giardia spp. and Cyptosporidium spp. detection in dogs and cats, in the absence of gold standard: A Bayesian approach	CS
1:15	Raabis	Changes in alveolar-arterial oxygen gradient in dairy calves from one week to one month of age	CS
1:30	Ruterbories	Computed Tomography evaluation of metastatic lymph nodes from head or neck cancers of canine and feline patients and the initial development of indirect CT lymphography	ERHS
1:45	Saklou	Environmental infectivity of Equid Herpesvirus type 1	CS
2:00	Selmic	Oncologic outcome and prognostic factors in 1134 dogs with appendicular osteosarcoma treated at a single institution	CS
2:15	Weishaar	Correlation of Nodal Mast Cell Infiltration Pattern with Clinical Outcome in Dogs with Mast Cell Tumors	CS
2:30	Parkinson	Establishing a Reference Interval for Fibrinogen in Box Turtles (Terrepene ornata ornata)	CMB
2:45	BREAK		
3:00	Ochola	Comparing Radiation-Induced DNA Damage Response in Lung Tissues of Recombinant Congenic Strains of Mice	CS
3:15	Parks	Tuberculosis in elephants in the United States: an assessment of risk factors, diagnostic test performance and treatment outcomes.	BMS
3:30	Regan	Losartan Repurposed as Novel Monocyte Migration Inhibitor for Treatment of Cancer Metastasis	MIP
3:45	Shoeneman	Survivin Inhibition in Canine Lymphoma and Osteosarcoma cell lines via EZN-3042	CS
4:00	Sishc	Roles of caspase 3 and telomerase in the radiation induced reprogramming of non-cancer stem cells into cancer stem-like cells	ERHS
4:15	Sullivan	Endogenously-generated lipid peroxidation products dilate rat cerebral arteries by activating TRPA1 channels in the endothelium	BMS
4:30	Wang	The retinal ganglion cell distribution and visual acuity in alpacas	CS
4:45	Yore	Determination of the Flea Species Infesting Dogs in Florida and Bartonella spp. Prevalence Rates	CS

Departmental Abbreviations

BMS: Biomedical Sciences
BIOM: Biomedical Engineering
CMB: Cell and Molecular Biology Program
CS: Clinical Sciences
ERHS: Environmental and Radiological Health Sciences
MIP: Microbiology, Immunology, and Pathology

Poster Presentations

Session 1-Odd Numbered Posters 1:00-2:45PM
Session 2-Even Numbered Posters 3:15-4:45PM

#1	Akin	Single-particle tracking of Nav1.6 suggests a novel anchoring mechanism and demonstrates direct trafficking to the AIS	BMS
#2	Allaband	Quantitative measurement of NF-kB and IRF3 nuclear translocation in individuals with a hypomorphic NEMO mutation	NIH
#3	Barnard	The Effect of Autophagy Inhibition on Anchorage Independent Growth	CS
#4	Bender	Determining the Efficacy and Treatment Regimen of an siRNA Therapeutic for Prion Disease	MIP
#5	Birkenheuer	RV-cyclin and CDK8: the interaction and implication	MIP
#6	Brown	Development and validation of a method to induce and quantify local saddle pressures	CS
#7	Burden	Administration of daily deslorelin acetate throughout mid-diestrus does not increase serum progesterone levels in the mare	CS
#8	Burgess, B.	Serotype reactivity of commercial immunoassays for Salmonella enterica identification in experimentally-inoculated equine fecal samples	CS
#9	Burgess, W.	Emergence of Disinfectant Resistant Mycobacteria Infections	MIP
#10	Cartwright	A simple and rapid fluorescence in situ hybridization microwave protocol for reliable dicentric chromosome analysis	ERHS
#11	Carver	Perioperative changes in the Pa02/Fi02 and SaO2/Fi02 ratio in ovariohysterectomized dogs recovering on room air versus nasal oxygen insufflation	CS
#12	Chang	Use of equine bone marrow derived mesenchymal stem cells to enhance keratinocyte migration and proliferation in an in vitro model of wounding	CS
#13	Cleys	Androgen Exposure Leads to Global DNA Methylation and Gene Expression Changes in Sheep Placental Cells	BMS
#14	Cloninger	Outcome of serum amyloid A and fibrinogen in horses with colic before and after surgery : A preliminary study	CS
#15	Colbath	Spatial morphology of the abdominal reproductive tract in 6 mares	CS
#16	Dang	Local L-type Calcium Channel Signaling in alpha T3-1 Cells	BMS
#17	Davidson	Speciation of Airborne Bacteria Collected by Novel and Traditional Samplers in a Cantaloupe Processing Facility: A Pilot Study	ERHS
#18	Doepker	Effects of handling time on the leukocyte profile of wild rodents	BMS
#19	Eck	Evaluation of the transcription factor, Nrf2, and the antioxidant response during an in vitro infection model of Mycobacterium tuberculosis	MIP
#20	Eitel	Microfluidic strategy for spatiotemporally resolved molecular sampling from organotypic tissue slices	BMS
#21	Elder	Misfolded Prion Protein Detection Using Real Time-Quaking Induced Conversion for Brain and Blood	MIP
#22	Enriquez	Ovarian cancer cell-secreted exosomes induce molecular and phenotypic changes in cells	BMS
#23	Erales	Development of a community - based livestock syndromic recording system for animal disease surveillance in silvopastoral production system in Mexico	CS

#24	Evans	U.S. Army Human Medical Event Data Collection: A Comparison of Existing Systems Using Zoonotic Disease	CS
#26	Fox, K.	Bighorn sheep sinus tumors are associated with co-infections by pneumonia-causing bacterial agents in the upper respiratory tract	MIP
#25	Fox, P.	Endoplasmic reticulum/plasma membrane junctions function as membrane protein trafficking hubs	BMS
#27	Garner	Histologic Characterization of Experimental Brucellosis Infection in Elk (Cervus canadensis)	MIP
#28	Gates	Survey Assessment of Empirical Antimicrobial Use by Veterinarians	CS
#29	Gullberg	The Dengue Virus NS5 RNA Capping Enzyme is Activated by Redox Conditions	MIP
#30	Gurol	Functinal Genomics of Hybrid Vigor	ERHS
#31	Gwynn	Effectiveness of monosodium alpha-luminol (Galavit or GVT) as an adjunctive medication in the treatment of chronic superficial keratitis	CS
#32	Halleran	Prenatal androgenization and its effects on the placenta	BMS
#33	Henao Tamayo	Characterization of immunity against Mycobacterium tuberculosis in C3Heb/FeJ and C3H HeOuJ mice	MIP
#34	Herman	Genetic Analysis of a Quarantined Yellowstone National Park Bison Herd	CS
#35	Hetrick	Characterizing the Dose Fields of the Radionuclide Cu-64-ATSM in Canines using PET	ERHS
#36	Hoover	Mitigation of Prion Pathogenicity by Heat Shock Protein 72 in Vitro	MIP
#37	Jalkanen	Regulation of zinc finger protein mRNA stability in induced pluripotent stem cells	MIP
#38	Johnson	Evaluation of Immunogenicity of Prion Vaccine Administered Together with Vaccine Enhancing Agent	MIP
#39	Kalet	IGF2 mRNA Binding Protein 1 Drives Growth, Metastasis and Chemoresistance in Osteosarcoma	CS
#40	Kaplan	Immunophenotypic Characterization of Canine CD8 T cell Lymphoproliferative Disorders	MIP
#41	Khamsi	The role of CCDC3 in canine osteosarcoma cell proliferation, clonogenicity, and chemotherapeutic resistance	CS
#42	Kick	Instrumentation and Technique for Improved Implantation of Osteochondral Grafts	VRS
#43	Ko	Optimization of Electroretinogram Parametric Amplitudes through Monochromatic Filter Combination Challenge in the Normal Dichromatic New Zealand White Rabbits	CS
#44	Kouri	Development of a New Transgenic Line of Mice for Evaluating Ovine GnRH Receptor Expression in vivo	BMS
#45	Krajacich	Demonstration and Analysis of a Safe, Novel, Human-baited Tent Trap for the Collection of Anthropophagic Culex and Anopheles Disease Vectors	MIP
#46	Lake	Oral, Subcutaneous and Intravenous Pharmacokinetics of Ondansetron in Healthy Cats	CS
#47	Larson	Examining the role of Dengue Virus NS4B as a potential suppressor of RNAi in Aedes aegypti	MIP
#48	Lishnevsky	Detection of pulmonary vascular micro-hemorrhages in PECAM-1 deficient FVB/n mice using hemosiderin-positive macrophages and deposition of fibrin	MIP
#49	Lordan	Risk Factors Associated with Colic in Horses Undergoing Elective Procedures Under General Anesthesia	CS

#50	Maeda	Genomic instability and telomere fusion of canine osteosarcoma cells	CMB
#51	Matthews	Does tensile strain induce cellular proliferation in cultured mitral valves?	CS
#52	Meyerett Reid	Prion Strain Adaptation: Breaking and Building Species Barriers	MIP
#53	Miller, J.	NF-kB Activation in the Hippocampus During Multiple Sub-threshold Exposures to Seizuregenic Compounds	ERHS
#54	Minor	Coxiella burnetii in Northern Fur Seals and Steller Sea Lions of Alaska	CS
#55	Moon	Dysregulation of host mRNA stability by flaviviruses: implications for pathogenesis	MIP
#56	Neff	Differential regulation of mRNA stability in human induced pluripotent stem cells	MIP
#57	Nelson	Use of a cationic contrast agent predicts glycosaminoglycan content in equine femoropatellar joint cartilage in horses undergoind contrast enhancing computed tomography	CS
#58	Nelson	V-loc vs Biosyn in Equine Jejunal Anastomosis	CS
#59	Nylund	Validation of a novel radiographic method for tibial plateau angle measurement in large and giant breed dogs	CS
#60	Orr	Ultrasound guided transversus abdominus plane block in routine ovariectomies in dogs	CS
#61	Penman	Equine Mesenchymal Stem Cell Characteristics; differences in sternum and ilium	CS
#62	Petri	In vitro differentiation of canine mesenchymal stem cells into cells with functional hepatocyte-like properties	CS
#63	Podell	Increased severity of tuberculosis in a guinea pig model of type 2 diabetes	MIP
#64	Potter	Evaluation of coliphage dynamics in bighorn sheep, domestic sheep and cattle: implications for bacteriophage therapeutics	MIP
#65	Prasad	Production of non-ping pong dependent PIWI RNA-like small RNAs in the mosquito midgut in response to West Nile virus infection	MIP
#66	Preisner	Evaluation of an outpatient protocol in the treatment of canine parvoviral gastroenteritis	CS
#67	Randall	Cellular Localization of PenA ß-lactamase in Burkholderia pseudomallei	MIP
#68	Rauhauser	Streptococcus agalactiae Mastitis: a Molecular Approach to Investigating Re-emergence in the Dairy Industry	CS
#69	Reagan	Investigation into the role of Aedes aegypti in the transmission of Bartonella clarridgaie and Mycoplasma hemofelis to cats	CS
#70	Romero, A.	ATM Mouse Strain-Dependent Variations in Sensitivity to Induction of Gamma-H2AX Foci after Continuous Low Dose-Rate Irradiation	ERHS
#71	Romero, J.	Delivery of interferon-tau into the uterine or jugular vein induces genes hypothesized to protect the corpus luteum from luteolysis	BMS
#72	Rout	Plasma exosomes as a diagnostic tool for canine iron deficiency, hemangiosarcoma, and osteosarcoma	MIP
#73	Rowland	Therapeutic plasma lidocaine concentrations in horses	CS
#74	Ruggeri	Meiotic Spindle Configurations in Metaphase II Oocytes from Young and Old Mares	BMS
#75	Ruple-Czerniak	Risk factors for the development of malignant histiocytosis in Bernese Mountain Dogs	CS
#76	Sadowski	A novel role for Bouvardin as an inhibitor of canine tumor cell proliferation	CS
#77	Schilling	A Similar Role for LIN28 in Placental and Cancer Cells	BMS

#78	Selariu	Evidence for vertical transmission of chronic wasting disease (CWD)	MIP
#79	Sessions-Bresnahan	Altered gene expression in equine granulosa cells associated with aging	BMS
#80	Shields	The Role of Synaptotagmin in Asynchronous Vesicle Release	BMS
#81	Shropshire/ Lappin	Evaluation of the association between Bartonella species antibodies and azotemia in client-owned cats	CS
#82	Shropshire	Evaluation for associations between Leptospire species antibodies and azotemia in client-owned cats	CS
#83	Soisson	Regulation of Human Trophoblast Cell Differentiation by LIN28A and LIN28B	BMS
#84	Spencer	Genes relevant to left ventricular hypertrophy are differentially expressed according to dietary fatty acid composition	BMS
#85	Steel	Subgenomic Reporter RNA System for Detection of Sindbis Virus Infection in Live Mosquitoes	MIP
#86	Swancutt	Endothelial cell apoptosis following stereotactic radiation therapy in canine soft tissue sarcomas	ERHS
#87	Templin-Hladky	Quantification of Feline Immunodeficiency Virus Proviral Load in FIVpco subtype A infected Puma (Puma concolor) and Bobcat (Lynx rufus)	MIP
#88	Trout	Neuroprotective efficacy and pharmacokinetics of novel para-phenyl substituted diindolylmethanes in a model of Parkinson's disease	ERHS
#89	Ullmer	Effects of xylazine on normal and interleukin-1 conditioned equine articular cartilage explants in vitro	CS
#90	Van de Motter	Detection of Chronic Wasting Disease Prions in Cerebrospinal Fluid by In Vitro Amplification	MIP
#91	Venable	Pulse Toceranib plus Lomustine for the Treatment of Unresectable Canine Mast Cell Tumors	CS
#92	Venn	The effects of an oral recuperation fluid on the clinical recovery of dogs with parvoviral gastroenteritis	CS
#93	Walton	Treatment of Chronic Implant-Associated S. aureus Infections with Therapeutic Staphylococcal Protein A Vaccination	MIP
#94	Wilson	The effect of rotational positioning of the canine tibia on radiographic measurement of frontal plane angulation	CS
#95	Wolfe	Quantitative and Facile Analysis of the ATP-binding Proteome of Mycobacterium tuberculosis	MIP
#96	Wyckoff	Bioassay detection of chronic wasting disease prions in soil	MIP
#97	Zhang	The influence of CELF 1 on myogenin expression during differentiation of C2C12 myoblasts	MIP

Departmental Abbreviations

BMS: Biomedical Sciences
CMB: Cell and Molecular Biology Program
CS: Clinical Sciences
ERHS: Environmental and Radiological Health Sciences
MIP: Microbiology, Immunology, and Pathology
NIH: National Institute of Health
VRS: Veterinary Research Scholars Program

Congratulations Again to 2012 CVMBS Research Day Winners:

Oral Presentations

First Basic	Alexa M. Dickson
Second Basic	Brendan K. Podell
First Clinical	Kathleen M. Brandes
Second Clinical	David M. Wilson

Poster Presentations

First	Bridget A. Schuler
Second	Kimberly M. Tarvis
Third	Britta A. Wood

Golden Pipet Award – Department of Biomedical Sciences

2013 CVMBS Research Day Organizing Committee

Dawn Duval - Faculty Chair – Clinical Sciences
Brad Borlee – Assistant Faculty Chair – Microbiology, Immunology, and Pathology

KC Gates – Biomedical Sciences
Dawn Sessions Bresnahan – Biomedical Sciences
An Dang – Biomedical Sciences
Valerie Moorman – Clinical Sciences
Joe Neary – Clinical Sciences
Brock Sishc - Environmental and Radiological Health Sciences
Theo Gurol - Environmental and Radiological Health Sciences
Nicole Podnecky - Microbiology, Immunology, and Pathology
Brendan Podell - Microbiology, Immunology, and Pathology

Sue VandeWoude - CVMBS Associate Dean of Research
Aimee Oke – CVMBS Dean's Office

Veterinary Summer Scholars Program
College of Veterinary Medicine and Biomedical Sciences

The Veterinary Summer Scholars program was initially established through support from Merck-Merial to provide an opportunity for veterinary schools to expose students in their first and second years of veterinary medical school to biomedical research. With continued support from Merial, several other organizations, CVMBS and faculty mentors have contributed funds to provide summer stipends for program participants. The current Veterinary Student Scholars program gives veterinary students hands-on exposure to veterinary medical research to introduce them to potential research careers. CSU CVMBS recently received funds from the National Institutes of Health and will be able to further expand the very successful program next year.

Eighteen veterinary students from CSU and abroad participated in the 2012 CSU Veterinary Summer Scholar program. Students spent the summer working in research labs, attending weekly research seminars and field trips to CSU, federal and state research facilities. CSU hosted the 2012 Merial NIH Veterinary Scholar Symposium last August which featured Keynote Lecturer Dr. Elias Zerhouni, President of Sanofi, and former Director of the National Institutes of Health. Over 500 attendees from around the continent and world attended, making it the largest Veterinary Scholar Symposium to date. Many of the projects conducted by CSU students last summer are being presented today at the CVMBS Research Day.

2012 Summer Scholars Sponsors

Merial Limited

Morris Animal Foundation

Merial France

American Humane Association

American Society of Lab Animal Practioners

CSU College of Veterinary Medicine

To view the research of students funded in 2012 or to apply for the summer 2013 program, please visit the website at:

http://csu-cvmbs.colostate.edu/dvm-program/Pages/Veterinary-Scholars-Program.aspx

PVM Student Grant Program
Center for Companion Animal Studies
Department of Clinical Sciences

In 2006, the HESKA Corporation made a $20,000 donation to support research that involved PVM students. That year, the monies were used to support 5 excellent projects chosen from 9 that were submitted. With continued collaboration from the HESKA Corporation, the PVM student grant program was opened to other corporate and non-corporate donors. The amount of funding has continued to grow yearly. In 2012, $47,500 was raised and distributed to 25 different projects all of which involved a PVM student as a scientist. Many of those projects are being presented today at the CVMBS Research Day. Colorado State University offers thanks to all sponsors of this program and is looking forward to advancing the veterinary sciences with our partners in the years to come while concurrently involving PVM students in clinical research.

2012 PVM Student Grant Program Sponsors

Platinum Sponsor

Merial Limited

Gold Sponsors

Boehringer Ingelheim Vetmedica
HESKA Corporation
Hill's Pet Nutrition and SCAVMA
IDEXX Laboratories
Merck Animal Health
Nestle Purina PetCare
Pfizer Animal Health
Veterinary Centers of America

Silver Sponsors

Bayer Animal Health

Bronze Sponsor

International Veterinary Seminars

To view the grants funded in 2012 or to make a donation, please visit the Center for Companion Animal Studies website at:

http://csuvth.colostate.edu/veterinarians/research/companion_animals/student_projects.aspx

Oral Presentations

Session I ~ Salon 1
1:00-5:00PM

CLINICAL SCIENCE

Effects of Adipose-Derived Mesenchymal Stromal Cells on Osteosarcoma Growth and Metastasis

Megan E. Aanstoos-Ewen, Nicole Ehrhart

Osteosarcoma, a malignant cancer primarily of the appendicular skeleton, affects 600-800 humans and 8,000-10,000 canines per year in the United States. Prognosis for long term survival is 55-75 percent at five years in humans under 30 years of age without metastatic disease at diagnosis. This rate drops for elderly patients or those with metastatic disease. In canines, 25 percent survive to two years. The disease mainly affects children and adolescents, and thus treatment modalities that help sustain a long-term, high quality of life are necessary. Current surgical treatment usually consists of either amputation or limb salvage. While preservation of the limb is ideal, there are several issues with current methods with respect to bone healing and revision surgeries.

Multipotent stem cells such as mesenchymal stromal cells have proven useful for bone growth, healing of allograft-host bone interfaces, and to coat implants to improve bony integration. However, mesenchymal stromal cells have also been shown to increase metastatic disease rates and primary tumor size in patients with a primary osteosarcoma tumor present.

These concerns have led to three questions: what are the effects on metastatic occurrence of osteosarcoma when stem cells are given in a mouse immediately after removal of the primary tumor; what is the possibility of local recurrence of osteosarcoma when mesenchymal stromal cells are given in the resected area of the previous tumor immediately following excision; and what are the possible interactions between stem cells and chemotherapy when given within two hours of each other in a metastatic occurrence of osteosarcoma murine model. These questions will provide an important contribution to the broader subject of whether mesenchymal stromal cells are a safe tool for use in healing bone in patients with a history of osteosarcoma. This presentation will specifically address model development methods, materials, and results to date.

Association of Thoracic Radiographs and Severity of Pulmonary Arterial Hypertension (PAH) Diagnosed in 66 Dogs via Doppler Echocardiography

Dustin S. Adams, Alex Valdés-Martínez, Elissa K. Randall, Angela J. Marolf

Purpose: Thoracic radiographs to evaluate the heart and pulmonary vasculature/parenchyma often accompany echocardiographic exams. No current literature correlates radiographic findings to severity of PAH (via echocardiography). We hypothesize that the more severe the PAH, the greater the number and conspicuity of radiographic findings suggestive of hypertension.
Materials/Methods: Dogs with PAH and normal control dogs that had echocardiographic and radiographic exams within 24 hours were included. Three radiologists blinded to echocardiographic results scored radiographs for right ventricular (RV) and main pulmonary artery (MPA) enlargement and pulmonary lobar artery enlargement, tortuosity, and blunting. A “reverse D” appearance, elevation of the cardiac apex, and estimation of right (3/5) to left (2/5) heart ratio determined RV enlargement. A bulge at the 1-2 o’clock position of the heart determined MPA enlargement. Comparison of the lobar arteries to the 3rd, 4th, and 9th ribs determined lobar artery enlargement. Presence or absence of each finding was scored "1" or "0" for a cumulative score of 0-9. Scores were averaged for each grade of PAH severity.
Results: 77 dogs were included: 20 mild, 21 moderate, 25 severe, and 11 absent PAH. The following radiographic findings increased with PAH severity: Reverse D (mild 36%, moderate 39%, severe 49%, absent 0%); 3/5-2/5 ratio (mild 33%, moderate 42%, severe 51%, absent 6%); MPA enlargement (mild 26%, moderate 37%, severe 48%, absent 12%); Lobar artery enlargement by 3rd rib rule (mild 44%, moderate 51%, severe 59%, absent 9%). Mean scores for PAH grade: mild (1.91), moderate (2.27), severe (2.84), and absent (0.39).
Conclusions: Evidence of RV, MPA, and lobar artery enlargement increased with severity of PAH. Yet, even for severe PAH cases the presence of any finding only occurred in approximately one-half of cases, indicating single radiographic findings should not determine PAH severity.

Optimization of a technique to distend the digital flexor tendon sheath in horses and subsequent evaluation with ultrasound and MRI

Alexander J. Daniel, Britta Leise, Kurt Selburg

Purpose: The digital flexor tendon sheath (DFTS) is a frequent source of lameness in horses but ultrasound of this region can be unrewarding. The goal of the study was to optimize a technique to distend the DFTS and evaluate any improvement in ultrasonographic interpretation by comparing findings to MRI and tenoscopy. Methods: Cadaveric specimens were collected (12 forelimbs) and the DFTS distended through a standard approach. Imaging at pre-determined locations in the DFTS was performed with ultrasound and MRI before and after distension. Tenoscopy was performed post-imaging to verify intra-thecal anatomical/pathological changes. Image analysis was performed by measuring the thickness and cross sectional area (CSA) of: deep digital flexor tendon (DDFT); superficial digital flexor tendon (SDFT); straight distal sesamoidean ligament (SDSL); palmar annular ligaments. Statistical analysis: One way repeated measures ANOVA comparing before and after ultrasound measurements to themselves and against MRI. Results: Distension (mean volume instilled 33.6+/-2ml) did not interfere with ultrasound or MRI examination. Statistical analysis showed that distension did not alter the measurement of the DDFT or SDFT with either MRI or ultrasound. There was no statistical difference between MRI and ultrasound in any of the measurements at the pre-determined levels ($p>0.05$). There was variability in the SDSL with statistical difference: before and after ultrasound ($p=0.01$); ultrasound after distension with MRI before distension ($p<0.0001$) and after distension ($p=0.001$). Subjective analysis showed improved delineation with ultrasound of: DDFT after distension; abaxial to dorsal borders of the SDFT in all regions except where the palmar annular ligament contacted the DFTS. Normal attachments of the intra-thecal structures to the DFTS were described. Conclusion: The technique resulted in a greater ultrasonographic understanding of DFTS anatomy and pathological variation after distension.

Prognostic molecular markers and immunohistochemical characterization of canine renal cell carcinoma

Elijah F. Edmondson, Barb E. Powers, E. J. Ehrhart

Renal cell carcinoma (RCC) is the most common primary tumor of the canine kidney and is one of variable histologic appearance and clinical behavior. We have previously shown that histologic features of canine renal cell carcinoma can be used to construct a grading scheme that is strongly correlated with both survival and the development of metastases. Additionally, the Fuhrman nuclear grade, which is the most prognostic feature of human RCC after stage of disease, was shown to statistically correlate with both overall and tumor specific survival when applied to canine tumors. Immunohistochemistry is helpful in human RCCs to classify tumors according to cytologic subtype, which strongly correlates with survival. The most common cytologic subtypes in humans include clear cell RCC, chromophobe RCC, and papillary RCC with less common subtypes including collecting duct carcinoma and translocation carcinoma. The immunohistochemical classification of canine RCC is currently based on case reports and a single retrospective study with 13 dogs and the prognostic vale of immunohistochemistry has not been evaluated. In this retrospective study, 72 canine RCCs were classified histologically and immunohistochemically using vimentin, cKit, and cytokeratin AE1-AE3. Additionally, tumors were stained with Hale's colloidal iron method and 19% were positive. 87% of tumors showed cytoplasmic or membranous positivity for cKit, 52% for cytokeratin, 74% for vimentin, and 29% stained positively for both cytokeratin and vimentin. The incidence of papillary, chromophobe, and clear cell RCC in dogs has been defined based on histologic features and histochemical and immunohistochemical staining.

Differentiation between Healthy Cattle and Cattle Infected with Mycobacterium bovis using the Volatile Organic Compound Profiles Present in Breath

Christine K. Ellis, Randal Stahl, Pauline Nol, Ray Waters, Mitchell Palmer, Kurt VerCauteren, Jack Rhyan, Matthew McCollum

Bovine Tuberculosis (bTB) is a zoonotic disease of public health and international trade importance. Surveillance programs and milk pasteurization have decreased the incidence of bTB in developed countries; however, in developing countries disease prevalence in cattle may approach 10-14%. Antemortem testing is essential for bTB control, however; such tests do not detect every infected animal. The surveillance tests currently in used in the United States take days to produce results, are labor intensive, require special training, and may not be cost effective. Development of an accurate, economical, non-invasive test would greatly improve surveillance and disease detection. Our pilot study demonstrates that GCMS analysis of breath samples collected onto sorbent cartridges allows discrimination between bTB infected and non-infected cattle, cattle infected with different strains of Mycobacterium bovis, and rooms housing infected and non-infected groups of cattle. Raw chromatographic data was warp transformed and analyzed using principle components and least discriminate analysis, and could be used to correctly classify infected and healthy cattle. Like other studies, we identified unique VOCs; however, we also identified unique changes within the VOC profiles of infected cattle that we believe represent host-pathogen interactions and host homeostatic responses to infection. These findings represent a new analysis method approach to VOC research. Continued investigation may lead to development of diagnostic, and disease surveillance strategies that preclude individual animal handling. Advantages of such a system include decreased stress on individual animals, decreased cost, increased efficiency, ability to screen groups of animals, and potential applications to surveillance of wildlife reservoirs of zoonoses or diseases of agricultural importance.

Differentiating Nasal Chondrosarcoma From Nasal Adenocarcinoma On Computed Tomography

Matthew J. Enroth, Angela J. Marolf, Alex Valdes-Martinez, Elissa K. Randall

INTRODUCTION: In veterinary medicine, no definitive computed tomographic (CT) criteria have been identified on CT examination to differentiate nasal adenocarcinoma and nasal chondrosarcoma. The purposes of this retrospective study were to: 1) determine if nasal chondrosarcoma was more likely to have internal mineralization than adenocarcinoma 2) evaluate any other unique CT features to aid in tumor diagnosis. METHODS: Computed tomographic images of 43 dogs with either nasal chondrosarcoma (n=18) or adenocarcinoma (n=25) were reviewed. Seventeen criteria were evaluated, including: nasal cavity occlusion, sinus involvement, nasal septum lysis or deviation, nasal turbinate lysis, cribriform plate lysis, hard palate lysis, homogeneity of the mass, contrast enhancement, internal mineralization of the mass and lymph node involvement. A Fisher's exact test was performed. P-values of 0.05 or less were considered significant. RESULTS: In patients with bilateral nasal cavity involvement, type of nasal cavity occlusion was statistically significant (p=0.0125). Bilateral full nasal cavity occlusion was present in 58% (7/12) of chondrosarcoma cases and 11% (2/18) cases of adenocarcinoma. Those with one fully occluded or both partially occluded nasal cavity occurred in 42% (5/12) cases of chondrosarcoma and 89% (16/18) cases of adenocarcinoma. Internal mineralization was found to be statistically insignificant. Heterogeneous attenuation of the mass was found in 48% (12/25) of adenocarcinoma cases and 77.78% (14/18) of chondrosarcoma cases (p=0.0637). CONCLUSION: When comparing CT characteristics of nasal adenocarcinoma versus nasal chondrosarcoma, only weak statistically significant differences were identified. In patients with bilateral nasal cavity involvement, type of nasal cavity occlusion was statistically significant. Both tumor types need to be considered as possible differentials when nasal tumors are identified on CT examination.

Dry bean consumption modulates metabolic byproducts in overweight dogs undergoing weight reduction

Genevieve M. Forster, Cadie A. Ollila, Jenna H. Burton, Adam L. Heuberger, Corey D. Broeckling, Dale Hill, John E. Bauer, Ann M. Hess, Elizabeth P. Ryan

Dry bean (Phaseolus vulgaris L.,) consumption has been shown to promote weight loss, alter carbohydrate metabolism, improve gastrointestinal health, decrease inflammation, and regulate blood lipids in humans, dogs, and lab animals. We recently reported that dietary bean intake (25% w/w) is safe and digestible in normal weight dogs. A restrictively randomized, controlled dietary weight loss clinical trial in overweight/obese dogs was next conducted to assess the safety and digestibility as well to determine changes in hormonal, metabolic and inflammatory metabolites. Cooked navy bean or black bean powder (25% w/w) was compared to an isocaloric, macro and micronutrient matched control diet. Thirty client-owned, adult dogs of diverse breeds were randomized to 1 of 3 dietary study groups at the Colorado State University Veterinary Teaching Hospital. Bean diets were digestible and changes in metabolic profiles and lipid metabolism were observed in at least one of the bean groups compared to control. Significant changes detected in serum analytes of bean fed dogs compared to control included triglycerides, BUN, creatinine, and ALP. These analytes associated with weight loss after four weeks of dietary intervention prompted further evaluation of the fecal metabolome and adipokines. Adiponectin, amylin, ghrelin, gastric inhibitory polypeptide, glucagon-like peptide 1, glucagon, insulin, leptin, peptide YY, and pancreatic polypeptide will be evaluated to determine the role of dry bean intake on gut hormones.
Dry beans are safe and digestible in overweight dogs undergoing weight loss and overweight and obese dogs represent a novel translational model to assess dry bean induced changes in metabolic byproducts during weight loss.

Evaluation of a Novel Formulation of Propofol Containing 2% Benzyl Alcohol in Cats

Gregg Griffenhagen, Marlis L. Rezende, Khursheed R. Mama

Purpose: A new formulation of the routinely used anesthetic agent propofol containing 2% benzyl alcohol as a preservative (Propoflo28) has been recently released for use in dogs, but little is known about its safety and efficacy in cats. This study was designed to evaluate and compare the pharmacodynamics of a single anesthetic induction dose of propofol and Propoflo28 in cats. Materials/methods: Six healthy, adult cats, weighing 2.7 to 7.7 kg, were administered 8mg/kg of either propofol (P) or Propoflo28 (P28) IV over one minute via a preplaced cephalic catheter using a balanced crossover design with a minimum 10 day interval between treatments. Ability to intubate was noted and physiological parameters were recorded prior to, and at selected time intervals after, drug administration. All cats were supplemented with oxygen as needed. Induction, intubation, maintenance, and recovery scores were assigned using a 3 point scale (1-smooth, 3-poor) by a single blinded observer. Time to intubation, extubation, and selected induction and recovery parameters were recorded, as was the response to noxious stimulus. Data (mean ± SD) were analyzed using repeated measures ANOVA with significance set at $p = 0.05$. Pre-administration values were used as a covariate to adjust for differences in baseline measurements. Results: No significant differences in physiologic parameters were observed between groups with the exception of oxygen saturation at 2 minutes (99% group P and 94% in P28) and heart rate at 4 hours (207 bpm in group P and 166 bpm in P28). No significant differences were seen in response to noxious stimulation, induction and recovery times, or quality scores between groups. Four cats in group P (66%) and one cat in group P28 (17%) were unable to be intubated within 3 attempts. Conclusions: The addition of 2% benzyl alcohol as a preservative did not alter the pharmacodynamics of propofol in this group of cats when administered as a single induction dose.

Coccidioidomycosis at the Phoenix Zoo, 2006-2011

Matthew M. Hay-Roe

Coccidioidomycosis is a fungal infection endemic to Arizona. It affects both animals and people, especially the immunocompromised. It can cause a variety of symptoms, and can exacerbate ongoing health problems. Complications can be extremely serious, and are untenable in certain rare exotic animal species. Clinical records were examined to determine the effectiveness of diagnosis and treatment in exotic mammals at the Phoenix Zoo, and recommend possible treatment improvements. Records from six species (one native species serving as a control) from 2006 to 2011 were searched for any mention of coccidioidomycosis and antibody titers. Of those records examined, three primate species exhibited signs of cocci (elevated titer and symptoms), and three individuals had definite lesions visible on radiographs. All confirmed cases were treated with fluconazole, and antibody titers dropped as a result of drug treatment. Although treatment and diagnosis is not clinically perfect, it is effective at reducing the effects of coccidioidomycosis in host species. No significant improvement is possible in the treatment protocol with currently available techniques.

Evaluation of Serum Vitamin E and Cholesterol Levels in Alpacas

Andi S. Lear, Stacey R. Byers

Purpose: Vitamin E concentrations in alpaca serum vary greatly between diagnostic laboratories. In humans and cattle, vitamin E concentrations have been altered due to sample handling, cholesterol levels, and hemolysis of the samples. The purpose of this study was to determine clinically relevant variation between vitamin E concentrations with different serum handling techniques. The effects of hemolysis and cholesterol levels were also evaluated. Materials/Methods: Blood was collected from 2 apparently healthy male alpacas. The whole blood samples were processed under conditions of exposure to fluorescent room light, contact with the rubber tube stopper, contact duration, and temperature until serum separation. The effects of hemolysis on vitamin E analysis was evaluated by the addition of known quantities of red blood cells to prepared serum samples which were then subjected to 3 freeze-thaw cycles. The serum was then evaluated for vitamin E and hemolysis index. Cholesterol concentrations were measured for all serum samples. A standard ANOVA was used to assess the effect of processing conditions on vitamin E concentration. Results: Vitamin E concentrations variations due to tube position were found to be statistically significant, however, no other processing condition was significant. A negative correlation was seen between hemolysis and vitamin E concentrations as expected from other species models. Although no correlation was seen between cholesterol and vitamin E due to the single collection time, preliminary data from ongoing research has proven otherwise. Conclusions: In conclusion, decreasing hemolysis during sample collection and upright storage prior to analysis will obtain the most accurate vitamin E evaluation. Elevated levels of cholesterol should also be taken into consideration when evaluating vitamin E concentrations in individual animals.

Incorporation of FDG-PET/CT into Radiation Therapy Planning to Improve Treatment of Canine Nasal Tumors

Samantha Loeber, Jamie Custis, Elissa Randall, Susan Kraft

Nasal tumors in dogs are often malignant with a high rate of tumor recurrence and poor long-term survival. Metabolic imaging with 18-fluorodeoxyglucose-positron emission tomography–computed tomography (FDG-PET/CT) is a non-invasive means of quantifying tumor metabolic activity in the context of anatomic location. We hypothesize that FDG-PET/CT will allow us to better identify nasal tumor extent and highly metabolic, aggressive areas of the tumor compared to CT alone.

FDG-PET/CT scans were done in place of conventional radiotherapy planning CT on 4 dogs with probable nasal cancer that were admitted to the CSU Veterinary Teaching Hospital for radiotherapy. Tumor volumes and standardized uptake values (SUV, index of glucose metabolic activity) were compared from post-contrast CT, PET and fused PET/CT scans using 3D-region-of-interest (ROI) analysis on the Philips Extended Brilliance Workstation (EBW).

Nasal histopathologies included squamous cell carcinoma (n=1), adenocarcinoma (n=2) and lymphocytic-plasmacytic rhinitis (n=1) (presumed to have missed true tumor regions in the mass). The carcinomas were intensely hypermetabolic (11.8, 20.9 and 25.91 max SUV) whereas the presumed, unconfirmed neoplasm was mildly hypermetabolic (2.3 max SUV). In 2/4 dogs, the contrast-enhanced CT volume was 7– 63% > PET volume, possibly because of enhancing peritumor reaction. The PET volume in the other 2 dogs was 35-56% > CT volume indicating that some hypermetabolic infiltrate detected on PET was normal on CT. In all 4 dogs, the PET scan showed additional hypermetabolic regions of potential tumor not detected by CT. The combination of PET/CT has the best chance of identifying potential areas of tumor to target with radiotherapy, although peritumor reaction will also be included. Enrollment of additional patients is still underway, with the goal of 6 for the study.

Research supported by Merial and the PVM Student Grant Program in the Center for Companion Animal Studies at CSU.

Validation of molecular techniques for rapid detection of tuberculosis in elephants

Roberta J. Magnuson, Lyndsey Linke, M.D. Salman

Elephants and many other animal species, including humans and primates, can be infected with Mycobacterium tuberculosis. Tuberculosis is a highly infectious disease and elephants have the potential to spread the disease not only to other elephants, but to humans. Culture is currently considered the “gold standard” for diagnosis of elephant TB. The practice of relying on culture for TB diagnosis, however, results in delays of up to 8 weeks and has low analytical sensitivity, requiring >100 organisms/ml for detection. Consequently, the infection can be spread to many other animals or humans during this delay, potentially escalating morbidity and mortality. As such, there is an unmet need to develop and validate rapid and reliable screening tests that allow for early diagnosis of TB in elephants, to greatly improve the control of the disease. Preliminarily, negative elephant trunk wash material was spiked with known numbers of M. bovis cells. DNA was extracted using several sample treatment and extraction protocols and detected by IS6110-targeted PCRs. These molecular methods detected as low as 1-50 M. bovis cells per 1.5ml trunk wash, in the presence of up to 500mg of soil. Application of these methods to species of non-tuberculous mycobacteria demonstrated analytical specificity of 100%. Clinical samples from culture-positive and culture-negative Asian elephants trunk washes are being utilized in the current study to validate the molecular detection techniques. We hypothesize that the molecular detection techniques will yield a reliable and acceptable diagnostic sensitivity and specificity as compared to the current gold standard of culture. Validation is a necessary step toward accomplishing our long term goal of implementing the molecular detection techniques for international use in wild and companion elephants as well as into the USDA guidelines as tests for annual screening and early diagnosis of TB in captive elephants.

Multimodal diagnostic approach to stifle disease in Quarter horses

Brad B. Nelson, Chris E. Kawcak, Laurie R. Goodrich, Natasha M. Werpy, Alejandro Valdés-Martínez, C. Wayne McIlwraith

Stifle disease is a common cause of lameness in Quarter Horses. Although radiography, ultrasound, and arthroscopy have been utilized to diagnose stifle lameness, this joint is complex and many times the cause of pain goes undefined. This study was designed to evaluate computed tomographic arthrography (CTR) of stifle joints in addition to radiography, ultrasound, and arthroscopy to better identify lesions within the stifle.

Twenty four horses were enrolled in the study. A requirement for inclusion was significant improvement of lameness following local intraarticular anesthesia of the stifle, medial and lateral femorotibial and femoropatellar joint. All horses underwent radiography, ultrasound, CTR, and arthroscopy of the affected joints. Lesions in each horse were recorded, graded and compared between diagnostic methods.

Meniscal lesions were well visualized with CTR 6/8 (75%) and were comparable to ultrasound. A spearman correlation revealed a moderate association between arthroscopy and CTR. Cranial meniscotibial ligament pathology was more commonly diagnosed with CTR 8/12 (67%) than on ultrasound 2/12 (17%), but arthroscopy was the most sensitive. Cartilage lesions were visible on CTR, but insensitive and no correlations were demonstrated. Only eight of 21 (38%) joints with cartilage damage were visible with CTR and vastly underestimated the degree of damage.

Although radiography and ultrasonography are commonly used to determine the source of stifle lameness prior to arthroscopic exploration, they are relatively insensitive methods for diagnosing certain lesions. In this study, lesions involving cranial meniscal ligaments, cartilage and certain meniscal tears were better diagnosed with CTR than other imaging. Due to joint complexity, CTR should be considered an important diagnostic tool and used in conjunction with radiographs and utrasoud in determining the source of stifle lameness in horses.

The alveolar-arterial oxygen gradient of primiparous dairy heifers is associated with total milk production

Hallie G. Noland, Joseph M. Neary, Franklyn B. Garry

Purpose: The modern dairy cow is physiologically challenged: oxygen demand is close to the oxygen uptake capacity of the cardiopulmonary system. Previous work has shown that a calf that has bovine respiratory disease before 3 months of age has a reduced rate of weight gain and a reduction in future milk production: on average, 150kg less during the first lactation than herdmates without a history of respiratory disease. Residual pathology may reduce the efficiency of oxygen uptake to reduce a calf's future performance within the dairy herd. Oxygen uptake ability is estimated by calculating the alveolar-arterial oxygen gradient. An increasing A-a gradient indicates poor transfer of oxygen from the alveoli to the blood. We hypothesized that a cow's milk production performance is negatively associated with the alveolar-arterial oxygen gradient. Materials/Methods: A cohort of 42 first lactation heifers was sampled on one dairy in northern Colorado. Heifers were sampled on 3 occasions: -34.7 (2.7 SE), +5.2 (0.7 SE) and +49.9 (1.1 SE) days relative to calving. These 3 occasions represent pre-calving, post-calving and peak lactation, respectively. We evaluated the relationship between A-a gradient and total milk production within the first 50 days of lactation. Milk production within the first 50 days is predictive of total milk production for the lactation. Samples taken from the coccygeal artery were immediately analyzed on a portable iSTAT machine. Results: Alveolar-arterial oxygen gradients were negatively associated with milk production when measured at all 3 time points, but only pre-calving values were statistically significant ($p=0.04$). For every 1 mmHg increase in the alveolar-arterial oxygen gradient milk production decreased, on average, by 36.0 lbs (14.6 SE) over 50 days in milk. Conclusions: This study highlights the importance of oxygen uptake ability on milk production performance of dairy heifers.

Pen-level associations between antimicrobial use and resistance in feedlot cattle

Noelle R. Noyes, Kathy M. Benedict, Sheryl P. Gow, Richard J. Reid-Smith, Calvin W. Booker, Tim A. McAllister, Sherry J. Hannon, Cheryl L. Waldner, Sylvia L. Checkley, Paul S. Morley

Purpose: The goals of this analysis were to estimate pen-level prevalence of antimicrobial resistance (AMR) and the impact of antimicrobial use (AMU) on this resistance in a feedlot population. Materials/Methods: Composite fecal samples were obtained from 310 randomly enrolled pens in four feedlots, over a period of three years. Samples were cultured for non-specific type Escherichia coli and tested for susceptibility to 19 antimicrobials. Computerized treatment records were maintained for all pens. Adjusted AMR prevalence estimates were calculated from generalized estimating equations (GEE). Associations between AMU and AMR were identified using GEE, GEE with alternating logistic regression (ALR) and generalized linear mixed modeling (GLMM). Antimicrobial exposures were modeled as both continuous and categorical variables.

Results: Crude resistance prevalence rates were below 2% for 13 of the 19 drugs tested; of the remaining six drugs, tetracycline exhibited the highest adjusted prevalence at 76%. Three AMU-AMR associations were statistically significant across all models: recent exposure to parenteral tetracycline increased the odds of tetracycline resistance; recent parenteral sulfisoxazole use increased the odds of sulfonamide resistance; and recent injections of macrolide decreased the odds of ampicillin resistance. Beyond these three associations, modeling technique (GEE vs. GEE/ALR vs. GLMM) and quantification of drug exposures (categorical vs. continuous) led to major differences in final multivariable model results.

Conclusions: Recent exposure to tetracycline, sulfisoxazole and macrolide clearly impacts pen-level resistance to tetracycline, sulfonamide and ampicillin, respectively; the practical implications of these associations are less clear. Modeling decisions greatly impact model results; therefore researchers in this field should explore and present all valid models in order to provide the most comprehensive answer to the AMU-AMR question.

Oral Presentations

Session II ~ Salon V
1:00-5:00PM

BASIC SCIENCE

The Commandeering of the HuR Protein by Alphaviruses Affects Cellular Post Transcriptional Gene Regulation

Michael D. Barnhart, John R. Anderson, Carol J. Wilusz and Jeffrey Wilusz

Purpose: To uncover novel pathways of viral pathogenesis due to the interface between alphaviruses and the cellular mRNA decay machinery.
Materials/Methods: Sindbis virus infections were performed in tissue culture cells and analyzed by a variety of methods including immunofluorescence, western blotting, qRT-PCR and electrophoretic mobility shift assays.
Results: Studies have led to four major observations regarding implications of the interaction between alphaviruses and HuR, a cellular protein primarily involved in regulating RNA stability. First, we demonstrated that cellular HuR protein can interact with the RNA of two alphaviruses (Ross River and Chikungunya) that possess unconventional 3' UTRs, strongly suggesting that all members of the virus family use HuR protein in their life cycles. Second, transfection studies with isolated viral RNA fragments indicated that the mechanism of induction of HuR relocalization to the cytoplasm in infected cells is due to the viral RNA acting as a sponge. Third, HuR interaction with numerous cellular mRNAs was found to be drastically decreased during SinV infection and was associated with dramatic destabilization of the cellular transcripts as determined by mRNA half-life analysis. Finally, we observed a novel effect of Sindbis virus infection on alternative polyadenylation of cellular transcripts. This is likely a direct result of sequestration of the HuR protein in the cytoplasm by the virus.
Conclusions: Collectively, these data indicate that in the process of usurping the cellular HuR protein for its own use, alphaviruses are also effectively destabilizing numerous cellular mRNAs. Interestingly, many cellular mRNAs affected by alphaviruses play key roles in inflammation, innate immune responses and other fundamental cellular processes. Thus alphaviral-induced alterations in cellular mRNA stability and polyadenylation may play a very important but heretofore underappreciated role in pathogenesis.

Autophagy functions in a pro-viral manner during West Nile virus infection of mosquitoes

Doug E. Brackney, Gregory D. Ebel

Purpose: Autophagy is an highly conserved process that mediates the transfer of cytoplasmic materials to lysosomes for degradation. This pathway serves an important role in maintaining cellular homeostasis and cell survival. In addition, autophagy functions as an innate immune defense against intracellular pathogens. Interestingly, the role of autophagy during viral infections has been implicated as having both pro- and antiviral activity. Surprisingly, the role of autophagy during arbovirus infection of vector mosquitoes is unknown. Therefore, we investigated the role of autophagy during West Nile virus (WNV) infection of C6/36 mosquito cells and hypothesized that autophagy functions in a pro-viral capacity during WNV infection of mosquito cells and mosquitoes.
Materials/ Methods: Cells were treated with a non-specific siRNA pool, Atg-12 siRNA, the autophagy inhibitor 3-methyladenine, the autophagy inducer rapamycin or untreated. Subsequently, cells were infected at a multiplicity of infection of 0.1 for one hour and at 36 hours post infection WNV titers were determined and cells prepared for confocal microscopy. For the in vivo studies female mosquitoes were inoculated with 150 ng of double-stranded RNA (dsRNA) specific for either Atg-5, Atg-12, or EGFP. Two days post inoculation mosquitoes were infected with WNV per os. Engorged females were collected and housed in the insectaries for 4 or 7 days post infection. At each time point midguts and carcasses were collected from 10 mosquitoes in each group.
Results: We found that WNV induces autophagy and that autophagy is required for efficient WNV replication in C6/36 cells. Further, we determined that suppression of key components of the autophagy pathway in the mosquito results in reduced WNV infectivity of Culex quinquefasciatus mosquitoes.
Conclusions: These data indicate that autophagy is fundamentally important to the success of WNV replication in mosquito cells and the infectivity of mosquitoes.

Effects of NOD2 on the Immunogenicity of Lactobacillus as a Mucosal Vaccine Vector

Sara A. Bumgardner, Akinobu Kajikawa, Lin Zhang, Chad B. Frank, Alora S. LaVoy, Yvonne D'Monte, Gregg A. Dean

Purpose: HIV-1 is typically transmitted at mucosal surfaces. Thus, successful vaccination should induce anti-viral mucosal immune responses. Using BALB/c mice we have shown Lactobacillus acidophilus (LA) expressing HIV Gag has this potential as an oral vaccine. Presently, we investigated whether ablating the innate immune receptor NOD2 (nucleotide oligomerization domain 2) would enhance the humoral or cell-mediated response achieved with the Gag expressing LA. Materials/methods: Wild-type C57BL/6 and NOD2-/- mice were gavaged with 3 daily doses of LA expressing Gag, LA expressing Gag plus the TLR5 ligand, FliC, or appropriate controls at week 0, 2, and 4. Mucosa associated and systemic lymphoid tissues were collected at week 6 for B cell phenotyping, HIV specific and total IgA determination and IFNgamma ELISpot. Serum and cecal contents were analyzed for anti-Gag and anti-LA IgG or IgA. Additionally, intestinal inflammation was assessed histologically and intestinal cytokine production was measured in ex vivo cultures. Results: LA-Gag immunized NOD2-/- mice had increased total IgA and plasma cells in the colon and a minor but significant increase in systemic HIV-specific IFNgamma. LA specific IgA and serum IgG was significantly enhanced over controls in NOD2-/- mice inoculated with LA-Gag plus FliC. While no HIV-specific IgA response was detected, LA-Gag did elicit both a significant increase in HIV-specific serum IgG and in local IL-1beta production from C57BL/6 mice that was absent in the NOD2-/- mice. Mild enteritis was observed in some animals but did not correlate with immunological results. Conclusions: These results suggest NOD2 and IL-1beta are crucial for the development of HIV-specific IgG in our model. The lack of corroborating anti-Gag mucosal IgA in C57BL/6 versus BALB/c mice makes assessing the role of NOD2 difficult in this regard. We are currently evaluating the contribution of mouse genetic background and gut microflora to this mechanism.

Exosomal miRNAs regulate TGFß family members during equine ovarian follicular development

Juliano C. da Silveira, Elaine M. Carnevale, Julhiano B. Rossini, Jacobo S. Rodriguez, Werner Giehl Glanzner, Quinton A. Winger, Gerrit J. Bouma

Exosomes are cell-secreted vesicles between 40-100nm in size, and contain bioactive materials such as miRNAs and proteins. Exosomes can be taken up by target cells through different endocytotic pathways. Recently, we described the presence of exosomes in follicular fluid that can be taken up by granulosa cells. During ovarian follicular development, cell communication is a crucial and well-regulated event, culminating with follicular ovulation or atresia. These events are dependent on endocrine, paracrine and autocrine signaling. TGFß signaling is key in follicular development and consequently ovulation and oocyte competence. Our hypothesis is that exosomes secreted in ovarian follicular fluid can regulate members of the TGFß family in granulosa cells during follicle development. In order to test this hypothesis granulosa cells and follicular fluid were collected from ovarian follicles (35mm size; immature, n=4) and 34h after GnRH/LH stimulation (mature, n=4). Real-time PCR was used to investigate 18 members of the TGFß family in freshly collected granulosa cells and granulosa cells in culture or treated for 24h in culture to exosomes (EXO). Initial gene expression analysis revealed 10 TGFß members were present at higher levels in cultured granulosa cells compared to 7 in freshly collected granulosa cells. ID2 was significant higher in freshly collected immature compared to mature granulosa cells. ACVR1 ($p<0.05$) and ACVR2B ($p<0.05$) levels were decreased by EXO treatments compared to no treatment. SMAD target genes CDKN2B ($p<0.03$) levels were increased following EXO treatments, while ID1 ($p<0.02$) levels were decreased by treatments. ID2 ($p<0.02$) levels were decreased by treatment with EXO from immature follicles. In conclusion EXO treatments can alter levels of TGFß family members in granulosa cells. We currently are investigating the presence of miRNAs in EXO isolations in order to identify exactly the miRNAs involved in regulating TGFß members levels.

Comparative analysis of MAPK and PI3K/AKT pathway activation and inhibition in human and canine melanoma

Jared S. Fowles, Cathrine L. Denton, Daniel L. Gustafson

Purpose: Human melanoma (HM) has historically been resistant to therapy, but new drugs targeting mitogen activated protein kinase (MAPK) and AKT pathways have improved survival. Resistance to these therapies is emerging, however, indicating better preclinical models are needed to improve combination strategies. Dogs with cancer provide an advanced model with many advantages for human research. Studies report upregulation of these pathways exist in canine melanoma (CM) as well. Our purpose is to compare activation and effects of inhibiton of the MAPK and AKT pathways in both HM and CM.
Materials/Methods: Pathway activation of HM and CM tumors and cells was investigated through gene expression analysis using linear models for microarray data analysis and IPA software, mutational analysis of v-Raf murine sarcoma viral oncogene homolog B1 (BRAF) and neuroblastoma RAS viral oncogene homolog (NRAS) through DNA sequencing, and activation of extracellular-regulated kinase (ERK) and AKT in absence of serum. Inhibitors to MAPK and AKT pathways AZD6244 and rapamycin (RAP) were used alone and in combination in cell viability assays and in cell cycle analysis and drug synergy was assessed.
Results: HM and CM share similar differential gene expression patterns in MAPK and AKT pathways. Of 7 HM cell lines studied 2 had mutations in NRAS, 3 in BRAF, and 2 were wildtype (WT). From 20 CM tumors and cell lines, most were WT except 2 samples with NRAS mutations, 1 activating and 1 silent. Starved HM and CM cells have constitutive activation of MAPK and AKT pathways. HM and CM cells are similarly sensitive to AZD6244 (IC50 = 5.7-391nM) and RAP (IC50=0.027-12nM) with the combination synergistic in both species. AZD6244 and/or RAP caused G1 arrest in HM and CM cells.
Conclusions: HM and CM share activation of MAPK and AKT pathways, although probably through different mechanisms. Targeting both MAPK and AKT pathways is advantageous in both species, validating CM as a model for HM.

Prenatal dexamethasone impacts the blood vessels within the paraventricular nucleus of the hypothalamus

Krystle A. Frahm, Stuart A. Tobet

The Paraventricular Nucleus of the Hypothalamus (PVN) is a dense collection of neurons that play key roles in maintaining homeostasis and initiating stress responses. It is also characterized by a dense matrix of blood vessels compared to surrounding brain regions. The PVN has been implicated in mood disorders such as depression in which there is disruption of the hypothalamic-pituitary-adrenal axis known to be important in stress responses. Glucocorticoids have shown to alter the neural circuitry within the PVN therefore, we investigated whether glucocorticoid signaling might also regulate the unique vasculature within the PVN. We have recently shown that the blood vessel pattern in the PVN has a postnatal development. Therefore, on P20, blood and pericytes as key components of the blood-brain barrier (BBB) were visualized. For blood vessel density, results showed significant decreases in blood vessel length and total immunoreactivity in dex- compared to vehicle-treated mice across the entire PVN ($p < 0.05$) and in the rostral and mid PVN regions particularly ($p < 0.01$). To investigate BBB competency, leakage of FITC from perfused blood vessels was determined. We found PVN-specific increased leakage in dex-treated mice compared to vehicle-treated ($p < 0.05$). We also found a change in the cellular composition in the PVN with dex-treated mice having increased desmin-immunoreactivity compared to vehicle-treated mice ($p < 0.05$), which has been shown to indicate vascular dysfunction. These results show that the overall blood vessel pattern and composition differs in dex-treated compared to vehicle-treated mice. Collectively these changes provide insight into the long-term functional consequences observed after prenatal dex-exposure. Overall, altered vascularity within the PVN may impair its neurons' ability to provide proper responses or feedback resulting in dysfunction.

The Effect of Sample Storage Media, Refrigeration, and Time on Urine Culture Accuracy in Canine Urine Experimentally Inoculated With Known Bacterial Quantities

Coreen Frawley, Kimberly Yore, Valerie Johnson, Kristy Dowers

Purpose: Bacterial culture of refrigerated urine samples is most accurate when performed within 24 hours. Reports comparing urine cultured immediately and urine stored under refrigeration or at room temperature beyond 24 hours are lacking. Other transport media have not been investigated for urine culture despite evidence that these media provide accurate culture results for conjunctival scrapings and group B streptococcus isolates. This study evaluates culture reliability of sterile urine inoculated with bacteria from clinical isolates of canine urinary tract pathogens at known concentrations and stored under various conditions for up to 7 days.
Materials/methods: A 66 mL urine sample was obtained via cystocentesis from a healthy research dog. Urinalysis and immediate aerobic culture on Columbia blood agar and MacConkey were performed to rule out infection and sample contamination. The remaining urine was divided into 4 samples and inoculated with either Escherichia coli or Staphylococcus psuedointermedius at concentrations of 1,000 or 100,000 cfu/ml. Each portion was further divided and stored in plain sterile tubes under refrigeration (PST-FR) and at room temperature (PST-RT) or Amies transport medium without charcoal (ATM). All samples were run in triplicate at 0, 24, 48, 72, and 168 hours. ANOVA was used to determine the effect of time, refrigeration, and storage media on bacterial counts. Mean number positive cultures were calculated for time point and storage method.
Results: An interaction between storage method and time was found to significantly affect bacterial counts ($p<0.05$) for both bacteria. Storage beyond 24 hours resulted in decreased positive cultures for PST-FR and PST-RT. Incubation for at least 24 hours in ATM resulted in superior bacterial recovery under typical aerobic culture conditions.
Conclusions: The findings suggest that ATM may be a preferred storage method when delayed urine culture or low bacterial concentrations are anticipated.

μ-opioid receptor mediated modulation of intrinsically photosensitive retinal ganglion cells

Shannon K. Gallagher, Andrew T. Hartwick, Jozsef Vigh

Purpose: Since their discovery, mechanisms for modulation of intrinsically photosensitive retinal ganglion cells (ipRGCs) have been elusive. Neuromodulatory processes that are capable of altering ipRGC activity are likely to have profound consequences on light-mediated behavior and/or disease. Recently, we have identified the presence of the endogenous opioid system (ß-endorphin and its preferred receptor) in the mammalian retina. In this study we investigated whether the ipRGCs are subject to opioid modulation.
Methods: Standard immunohistochemical procedures were utilized for melanopsin and μ-opioid receptor (MOR) colocalization experiments. Light-evoked spiking of ipRGCs was recorded from flat-mount retinas isolated from young (postnatal days 6-11) and adult (>3 months) Sprague Dawley rats of either sex using a multielectrode array (MEA). Retinas were continuously superfused with oxygenated Ames medium at 37degC. Following dark adaptation, ipRGC spiking was recorded in response to 20 s light pulses (470nm; 7.5 x 10^14 photons/cm2/s). In all experiments, ipRGCs were pharmacologically isolated using a cocktail of synaptic blockers. The MOR selective agonist DAMGO was applied at various concentrations (1nM to 10 μM) for 10 min before light stimulation with/without MOR antagonist CTOP (1 μM).
Results: Double labeling studies showed colocalization of MOR-ir puncta on the dendritic processes of melanopsin-ir cells in the rat retina. Consistent with this finding, DAMGO dramatically reduces both the duration and firing rate of ipRGCs light responses in retinas from young (postnatal days 6-11) rats in a dose dependent manner. CTOP reversed the DAMGO effect. DAMGO affected ipRGCs similar in adult retinas.
Conclusions: This study is the first to demonstrate a direct MOR mediated neuromodulation of ipRGCs. With this evidence, the retinal MOR system is an attractive target for directed therapeutic interventions of diseases and disorders involving ipRGC function.

Correlation of Mast Cell Tumor Aggressiveness with Degree of Cutaneous Mucinosis in Chinese Shar-Pei Dogs

Alana Garner, James Perry, Randall Basaraba, Douglas Thamm, Anne Avery

Purpose: Cutaneous mucinosis in Shar-Pei dogs is the result of excessive dermal hyaluronan, a protein associated with angiogenesis and tumor cell motility in multiple human and canine neoplasms. Cutaneous mucinosis in Shar-Pei has been associated with a gene duplication upstream of the hyaluronic acid synthase 2 gene (HAS2). The objective of this study was to evaluate the relationship between HAS2, cutaneous mucinosis, and features of mast cell tumor (MCT) aggressiveness in Shar-Pei dogs. Materials/Methods: Biopsies of cutaneous MCTs from 149 Shar-Pei and 100 non-Shar-Pei were graded according to the Patnaik (1984) and Kiupel (2011) systems for canine cutaneous MCTs. Biopsies of the Shar-Pei MCTs were also evaluated for degree of cutaneous mucinosis, depth of invasion, and microvessel density (MVD). Shar-Pei and non-Shar-Pei MCTs were evaluated via qPCR for relative copy number of the gene duplication upstream of HAS2. Results: The proportion of grade III tumors was significantly higher in Shar-Pei than the general canine population (Fisher's exact test, p=1.044e-11). Shar-Pei biopsies had significantly higher copy numbers than non-Shar-Pei biopsies (Wilcoxon rank sum test, p=1.128e-11). The relative copy number was significantly less in biopsies without mucinosis (Kruskal-Wallis rank sum test with pairwise Wilcoxon, p=0.027). Higher copy number was not associated with a higher grade or deeper invasion of MCTs, but did have a moderate positive correlation with mitotic index and a strong positive correlation with MVD (Pearson r correlation, p<0.05). MVD was also higher in high-grade MCTs than low-grade MCTs (Wilcoxon rank sum test, p=0.01154). Conclusions: Our data suggest a relationship between HAS2 gene duplications and features of MCT aggressiveness in Shar-Pei dogs. Ongoing research will contribute to improved diagnostic tests to determine a more accurate prognosis for future patients and give insight into the mechanisms behind MCT aggressiveness.

Highly Sensitive In Vitro Evaluation of Cervid Field Samples for Chronic Wasting Disease Infection

Laura L. Hoon-Hanks, Nicholas J. Haley, Davin Henderson, Glenn C. Telling, Edward A. Hoover

Purpose: Chronic wasting disease (CWD), a transmissible spongiform encephalopathy (TSE), is caused by an infectious prion affecting cervids (e.g. deer, elk, and moose). Since its initial description in 1967, CWD has been documented in wild and captive cervid populations in 22 states, three of which had never detected CWD prior to 2012. With the movement of elk and deer populations throughout the U.S., surveillance is essential in the prevention of disease spread. Conventional CWD detection methods, such as immunohistochemistry (IHC), western blotting, and enzyme-linked immunosorbant assay (ELISA), require harsh pre-treatments to eliminate normal cellular prion protein (PrPC); a practice that may reduce the levels of infectious PrP (PrPCWD) and decrease the sensitivity of the assay. As a sensitivity comparison study, we evaluated lymphoid tissue from deer and elk - previously analyzed by conventional methods - using two sensitive amplification assays: serial protein misfolding cyclic amplification (sPMCA) and real-time quaking-induced conversion (RT-QuIC). Materials/Methods: Cervid samples (n=254) from West Virginia, Colorado, and New York were analyzed by sPMCA (3 rounds run in duplicate, evaluated by western blot) and RT-QuIC (140 fifteen-minute cycles run in triplicate). Each sample was then compared to the ELISA/IHC results provided by state agencies. Results: Of 11 samples testing positive by ELISA or IHC, sPMCA correctly identified 7 of 11, while RT-QuIC detected PrPCWD in 11 out of 11. RT-QuIC additionally detected two positive samples not identified by ELISA or IHC. All remaining samples were negative by all assays. Conclusions: RT-QuIC appears to be at least as sensitive as ELISA and IHC, if not more so, and is likely to be more sensitive than sPMCA. Through further testing of 750+ samples, we hope to determine if there is a statistically significant difference in sensitivity between RT-QuIC and ELISA/IHC.

Mosquitoes and Mycobacteria: A forbidden love

J. Charles Hoxmeier, Brice Thompson, Brian Foy, Karen Dobos

Buruli Ulcer disease is a severe, ulcerative disease of the skin resulting from infection with Mycobacterium ulcerans. Considered a neglected tropical disease, Buruli Ulcer disease is increasing in incidence and prevalence while basic questions remain regarding its route of transmission and environmental maintenance. This study evaluated the interaction between Anopheles gambiae mosquitoes and M. ulcerans bacilli to determine if this species could play a role as a vector or as a reservoir for this disease. Mosquitoes were raised in water inoculated with live, virulent M. ulcerans, gamma-irradiated M. ulcerans (whole, dead), or no supplemental bacteria, over a period of 8-10 days at 28C and 70% humidity. The subsequent development of the mosquitoes was monitored on a daily basis. A Kaplan-Meier survival curve was generated and indicated a significant difference ($p=0.001$) in survival to adulthood between mosquitoes raised with live M. ulcerans compared to irradiated M. ulcerans. PCR was used for detection of M. ulcerans DNA, and immunofluorescence (IF) imaging to localize and visualize M. ulcerans on the mosquito. Mosquitoes from both the live and dead M. ulcerans-fed groups demonstrated positive PCR signals. IF analysis demonstrated different M. ulcerans contamination patterns on the external tissues of the proboscis between treatment groups. Finally, we initiated metabolomics profiling and bacterial culture of adult mosquitoes from all treatment groups, in an effort to begin to understand the differences observed in developmental delay due to the impact of water and insect contamination with live M. ulcerans. Many mosquito species, including A. gambiae, are common in regions in which Buruli Ulcer disease is endemic, and the most prominent risk factor for development of disease is an association with standing water. A relationship between mosquitoes and M. ulcerans may play a role in the transmission and environmental maintenance of Buruli Ulcer disease.

A novel RNAi delivery system engineered to target epithelial cells and prevent avian influenza replication

Lyndsey Linke, Johannes Fruehauf, Gabriele Landolt, Roberta Magnuson, Jeff Wilusz, Mo Salman

Purpose: Outbreaks of avian influenza virus (AIV) have severe economic consequences to the poultry industry and increase the risk for transmission to humans. Current vaccination strategies are limited and clinical application of RNAi needs to be demonstrated. Transkingdom RNAi (tkRNAi), a unique delivery platform, uses nonpathogenic bacteria to generate and deliver siRNAs to target tissues. These novel tkRNAi vectors could be the key to attaining clinical application and our long term goal of using RNAi to develop a novel alternative to the AIV vaccine for commercial use in poultry. The objective is to provide proof of concept for inhibiting AIV using the novel tkRNAi platform to develop an anti-AIV vector to deliver siRNAs to chicken epithelial cells, as a preliminary avian tissue model for future work in chickens. These novel vectors were constructed and two specific aims are being pursued: 1) Test vector uptake and invasion of chicken epithelial cells using a fluorescent marker; and 2) evaluate the anti-AIV vectors for their ability to inhibit AIV replication in chicken epithelial cells. Materials/methods: Assessment of vector uptake and invasion, AIV replication, and the production of infectious viral particles are being determined via flow cytometry, RT-qPCR based on the AI matrix gene, and TCID50, respectively. Results: These vectors can be efficiently delivered to chicken epithelial cells, with minimal CPE. Work is currently underway to determine if these vectors show potential to inhibit AIV replication in vitro. Conclusions: Demonstrating the value of this novel approach could translate into an effective antiviral technology that limits outbreaks in poultry, and could represent a transformative approach to controlling influenza with great potential to have a sustained and significant impact on human disease. Applying the tkRNAi delivery approach is innovative and is the first instance of such a delivery mechanism to inhibit influenza replication.

Viral excretion and tissue tropism of feline immunodeficiency virus in saliva and oral tissues

Craig Miller, Karen Boegler, Susan VandeWoude

Purpose: To characterize the excretion and tropism of feline immunodeficiency virus (FIV) in saliva and oral tissues to hypothesize mechanisms associated with oral shedding and transmission of FIV. FIV is believed to be transmitted in saliva primarily by bite wounds, although mechanisms associated with salivary transmission have not been well studied. Human immunodeficiency virus (HIV) is also known to be present in the saliva of infected individuals and has been shown to be genetically, structurally, and biochemically similar to FIV. Studies involving HIV salivary pathogenesis have increased the prospect of alternative antiviral therapies and diagnostic methodologies in endemic areas. Therefore, further elucidation of lentiviral salivary excretion and transmission mechanisms may have significant implications in both human and veterinary medicine. Materials/methods: To evaluate viral kinetics and salivary shedding, 18 cats were intravenously inoculated with a well-characterized, highly virulent strain of FIV. Viral RNA and DNA present in saliva and oral mucosal and lymphoid tissues were quantified using RT-PCR analysis. Histologic evaluation of oral tissues was retrospectively performed by light microscope. Results: We demonstrate that saliva contains significant amounts of both viral RNA and proviral DNA, and that viral and proviral loads in oral lymphoid tissues (tonsil, retropharyngeal lymph node) were significantly higher than oral mucosal tissues (tongue, buccal mucosa, salivary gland). Histologic evaluation of oral tissues reveal mild to moderate reactivity of the retropharyngeal lymph node and tonsil, as well as mild to moderate, subepithelial, lymphoplasmacytic, histiocytic, and mastocytic infiltration of the tongue and buccal mucosa. Conclusions: Results suggest multi-organ involvement in viral shedding and infectivity that appears to predominate in oral lymphoid tissues.

Evaluation of artemisinin analogs in canine and human tumor cell lines

Michelle A. Morges, David M. Rubush, Barbara J. Rose, Tomislav Rovis, Douglas H. Thamm

Introduction: Artemisinin, a bioactive extract derived from a Chinese plant, is most known for its antimalarial properties. More recently, artemisinin and its derivatives have been investigated for cancer treatment. Artemisinin itself is unstable and has poor bioavailability, thus leading to the development of synthetic derivatives. The purpose of this study was to evaluate multiple artemisinin derivatives in a variety of cancer cell lines. Methods: The growth inhibitory effects of artemisinin, dihydroartemisinin (DHA), and multiple novel derivatives were evaluated against the canine osteosarcoma cell line D17 using a bioreductive fluorometric assay. Artemisinin and three analogs were then tested via the same method in several human cancer cell lines (prostate, lung, breast, melanoma). DMR1-G, the most active analog, was then evaluated against a panel of canine tumor-derived cell lines. Finally, DMR1-G growth inhibition was compared to DHA. Results: Multiple artemisinin analogs had superior antiproliferative activity against D17 compared to artemisinin or DHA, with IC50's ranging from 3.6 ->100 uM. Activity was also observed in multiple human cell lines. DMR1-G was deemed the most potent and was evaluated in a variety of canine cell lines, with IC50's ranging from 18.5-395 uM. Hematopoietic and mesenchymal derived cells were generally more sensitive than epithelial or melanocytic derived cells. Overall, DMR1-G had superior activity when compared to DHA. Conclusions: DMR1-G inhibited the growth of a variety of human canine and human cancer cell lines, while DHA had limited activity. DMR-1G is promising as a molecule for additional evaluation, and as a scaffold for additional structural elaboration.

Metnase Regulation of DNA Integration

Jingyi Nie, Jac Nickoloff

Metnase is a fusion protein that is present only in higher primates. It has a nuclease domain from mariner transposase, and a methyltransferase domain that methylates histone H3 at DNA double-strand breaks (DSBs) and Metnase itself. Metnase is involved in multiple cell functions including DSB repair by non-homologous end joining (NHEJ), DNA integration, topoisomerase II catalyzed chromosome decatenation, and replication stress responses including fork restart and checkpoint activation. The aim of this project is to examine the role of Metnase during DNA integration. Metnase promotes NHEJ of plasmid and chromosomal DSBs, and DNA integration. During plasmid NHEJ, Metnase protects plasmid DNA ends from degradation. Here we test if Metnase similarly protects ends of integrating plasmid DNA, as well as host DNA, during integration. Linearized plasmid vector encoding a puromycin resistance marker was transfected into 293T cells that do not express Metnase, or co-transfected with a Metnase overexpression vector. Integration products were isolated and plasmid-genome DNA junctions were isolated using a rapid amplification of genomic ends assay. As reported previously, usage of microhomology or base addition is common at integration junctions. We found that the length of microhomology between plasmid and genome DNA is shorter when Metnase is overexpressed. Unexpectedly, our data shows that Metnase does not prevent large deletions of plasmid ends or reduce non-templated insertions at plasmid-DNA junctions. We also observed that Metnase promotes integration more frequently in coding sequences, suggesting that Metnase may promote gene inactivation, for example, during horizontal gene transfer from tumor cells dying by apoptosis or other death pathways. Because Metnase is overexpressed in several types of tumors and confers resistance to replication stress agents, it is a potential target to modulate in cancer cells or surrounding normal tissue to improve cancer therapy.

Oral Presentations

Session III ~ Salon II
1:00-5:00PM

CLINICAL/BASIC SCIENCE

Assessment of diagnostic tests for identification of Giardia spp. and Cyptosporidium spp. detection in dogs and cats, in the absence of gold standard: A Bayesian approach

Jairo E. Palomares, Lora R. Ballweber, Mo D. Salman

Giardia spp. and Cryptosporidium spp. are important protozoa affecting cats and dogs. The primary clinical signs include; diarrhea, vomiting, abdominal cramping, and mild fever. The sensitivity and specificity of a diagnostic test can be determined by comparing with a reference test (gold standard), which represents the true disease state of the population of interest, however, the true disease state is rarely known in practice, because perfect test results may be difficult or impossible to obtain. The Bayesian Approach (Gibbs sampling implementation) is a novel method used in this situations. The aim of this study is to estimate the relative sensitivity and specificity of four diagnostic tests in the absence of a reference test (gold standard) using the Bayesian approach. This study is still in development. All fecal samples from dogs and cats that were submitted to the parasitology laboratory between June and August, 2012 were concentrated and frozen. Four diagnostic tests were performed according with the fabricant directions: Merifluor Cryptosporidium/Giardia IFA kit; Meridian Bioscience Inc., Cincinnati OH., Safepath (IVD) Cryptosporidium/Giardia Fecal DFA detection kit and Giardia Antigen Detection Microwell ELISA; IDV Research Inc., Carlsbad, CA., and Snap Giardia; IDEXX Laboratories Inc., Westbrook, ME. Other data from the clinical history and characteristics of the sample were also recorded in order to define different populations, necessary for the statistical analysis. Cross tabulations, stratified comparison of proportions, and pair-wise agreement Kappa are the first approximation to the data analysis. For the estimation of the relative sensitivity and relative specificity of the diagnostic tests without a reference test the Bayesian approach for the Hui-Walter model will be used. Relative sensitivity and specificity of each of the assessed tests will be presented with their practical clinical applications.

Changes in alveolar-arterial oxygen gradient in dairy calves from one week to one month of age

Sarah M. Raabis, Joseph M. Neary, Franklyn B. Garry

Purpose: To document the changes in alveolar-arterial (A-a) oxygen gradient in dairy calves from one week to one month of age. An increase in the A-a gradient indicates poor transfer of oxygen from the alveoli into the arterial blood. We hypothesized: 1) the A-a gradient would decrease in dairy calves from one week to one month of age due to increasing functional maturity of the lung and 2) clinical signs of respiratory disease would be associated with an increase in the A-a gradient. An A-a gradient over 10mmHg indicates poor gaseous exchange to the arterial blood.
Materials/methods: 62 heifer calves born on one dairy in northern Colorado were sampled at one week and one month of age. Samples included: 1ml of blood from the coccygeal artery for blood-gas analysis on a portable iSTAT machine, body mass and rectal temperature. Calves were evaluated for signs of respiratory disease and a score given according to the type and amount of nasal discharge and evidence of coughing. Passive transfer of colostral antibodies was adequate in all calves enrolled in this study. Generalized estimate equations were used to account for repeated measures in this study. A backwards elimination model was performed.
Results: The A-a gradient decreased with increasing age as hypothesized (p=0.006). The mean A-a gradient at one week of age was 20.75 mmHg (+/- 2.05). At one month, the A-a gradient was 17.72 mmHg (+/- 1.56). For every one day increase in age, the A-a gradient decreased by 0.14 mmHg (+/- 0.05). Multiple-induced or spontaneous coughing was significantly associated with increasing A-a gradient, when controlling for age (p=0.03). The occurrence of multiple-induced or spontaneous coughing was associated with 6.2 mmHg (+/- 2.8) increase in the A-a gradient.
Conclusions: The A-a gradient decreases with age as hypothesized but evidence of respiratory disease is associated with an increased gradient. An increase in the A-a gradient may have long-term health consequences.

Computed Tomography evaluation of metastatic lymph nodes from head or neck cancers of canine and feline patients and the initial development of indirect CT lymphography.

Lisel Ruterbories, Elissa K. Randall, Susan L. Kraft

Computed Tomography (CT) imaging is a non-invasive means of achieving a more accurate picture of lymph nodes (LNs) than radiography. Regional LNs are assessed on CT images of patients with head and neck cancer. Detection of metastasis affects treatment and prognosis. Absolute LN size and contrast enhancement patterns can help determine metastatic status. Central necrosis of human LNs has also been shown to correlate with metastasis. However, specific criteria regarding CT imaging characteristics of metastatic versus reactive LNs have not been well established for veterinary patients. This is a retrospective study of head and neck CT scans of small animal patients with known LN cytology or histopathology. LNs were evaluated using criteria including size, shape, contrast enhancement pattern and central lucency. These findings were compared to cytology and histopathology for predictive factors of malignancy. Head and neck LNs are currently being evaluated from patients with the following:
Carcinoma (n=24), Soft Tissue Sarcoma (n=9), Osteosarcoma (n=7), Chondrosarcoma (n=1), Plasma Cell Tumor (n=2), Lymphosarcoma (n=1), Melanoma (n=4), Acanthomatous Ameloblastoma (n=1), brain and nasal tumors without histopathology (n=2), and non-neoplastic disease (n=4) from 55 total scans. At this point, average LN short-axis diameter is 6.27mm +/- 2.88 for reactive nodes, 12.68mm +/- 9.14 for the metastatic nodes, and 7.13mm +/- 1.53 for no abnormalities. The findings to date confirm larger LN size is associated with metastatic disease but there is a wide overlap in size between reactive and metastatic nodes with a trend for metastatic nodes to be larger, abnormally shaped and heterogeneously enhancing. All groups include LNs with central lucency. These established criteria may guide the ability to distinguish reactive from metastatic LNs; however, the specificity and sensitivity of conventional CT for detecting nodal metastasis remains suboptimal.

Environmental infectivity of Equid Herpesvirus type 1

Nadia T. Saklou, Brandy Burgess, Paul W. Morley, Lutz S. Goehring

Equid Herpesvirus type 1 (EHV-1) is a highly contagious agent for horses, able to cause outbreaks of primary respiratory disease, retinopathy, myelopathy and/or abortion. Horizontal transmission is directly through nasopharyngeal droplet transmission, or, indirectly, through fomite transmission. Once expelled into the environment viral maintenance of infectivity will depend on a variety of factors such as surface tension forces, temperature fluctuations and UV-light exposure. We hypothesized that viral survival will be different if in contact with various surfaces or materials, and when in different environments. An EHV-1 suspension was placed on surfaces/ materials: plastic, fabric, leather, bedding materials shavings and straw. Materials were placed in different environments: constant 4ºC, 'barn' and 'outdoor' environment'. Samples of each material and environment were collected at time points 0, 3, 12, 24, 36 and 48 hrs. In the laboratory supernatants of materials immersed in virus culture medium were collected and stored frozen. Collectively, samples were thawed and viral titration was done using a plaque assay. Statistical analysis used generalized linear models with random effects mixed models controlling for repeated measures. Statistical significance was assumed when $p<0.05$.
Results showed significant differences upon first contact (t=0) of the virus with different materials, most noticeable with shavings and leather. Both environmental conditions showed a rapid decrease in viral survival, especially during the first 3 hrs. While results show significant reduction on some surfaces and materials over others, it is important to realize that viral maintenance of infectivity was still significant under simulated 'barn conditions' following the 3 hrs time point. These results emphasize the importance of following diligent hygiene and biosecurity protocols when mitigating an EHV-1 outbreak.

Oncologic outcome and prognostic factors in 1134 dogs with appendicular osteosarcoma treated at a single institution

Laura E. Selmic, Stewart D. Ryan, Nicole P. Ehrhart, Deanna R. Worley, Jens Eickhoff, Stephen J. Withrow

Purpose: The purpose of the study was twofold, to report the outcome following treatment in a large population of dogs with appendicular osteosarcoma (OSA) and to evaluate for prognostic factors in the cohort of dogs that received amputation and chemotherapy.
Materials and methods: Retrospective review of medical records at CSU identified 1134 dogs that received treatment for appendicular OSA between 1997 and 2010. Treatment and follow-up information was abstracted from the records. The Kaplan-Meier method was used for calculation of median survival time. Univariate and multivariate survival analysis was performed.
Results: Palliative-intent treatments were administered in 377 dogs (33.2%): analgesic medications alone (n=41, Median survival time (MST)=66 days), palliative radiation treatment ± bisphosphonates (n=177, MST=122 days), amputation only (n=147) and limb-spare only (n=12). Curative-intent treatments were administered in 757 dogs (66.8%): curative-intent radiation therapy and chemotherapy (n=44, MST=243 days), amputation and chemotherapy (n=488, MST=255 days) and limb-spare and chemotherapy (n=225, MST=389 days). Univariate analysis revealed that factors associated with a poorer survival included ALP > 142 IU/L ($p<0.03$), weight = 40Kg ($p<0.006$), proximal vs. distal bone location ($p<0.005$) and humerus vs. all other sites ($p<0.001$). In the multivariate analysis, following adjustment for ALP, stage, weight and proximal vs. distal bone location, dogs with a proximal humeral OSA location were found to have a significantly worse survival compared to dogs with radial OSA location ($p<0.03$).
Conclusions: Treatment outcomes in a large population of dogs with appendicular osteosarcoma are similar to those previously reported. Location may be a more important prognostic indicator than previously recognized.

Correlation of Nodal Mast Cell Infiltration Pattern with Clinical Outcome in Dogs with Mast Cell Tumors

Kristen M. Weishaar, Douglas H. Thamm, Debra A. Kamstock

Purpose: The primary objective of this study was to determine if different histological features of mast cell-infiltrated lymph nodes (LNN) correlated with clinical outcome in dogs with mast cell tumors (MCT). A secondary goal was to propose a classification system for histologic evaluation of LN metastasis.
Materials/methods: The CSU Diagnostic Medicine Center database was searched for cases of canine MCT with reported LN metastasis. Additional cases were drawn from a clinical trial involving sentinel lymph node mapping. Lymph nodes and primary tumors (when available) were reviewed by a single pathologist. The pattern of nodal mast cells was classified according to a novel classification system. Cases where LN metastasis was diagnosed at necropsy or where treatment was pursued in the setting of gross disease were excluded from outcome analysis. Demographic data, treatment, and clinical outcome were collected for each case. Results: Thirty-seven cases met the defined criteria. Primary tumors consisted of one grade I, 24 grade II, and 15 grade III tumors. LN specimens for each case were evaluated and classified as: HN0 (non-metastatic; n =3), HN1 (pre-metastatic; n = 13), HN2 (early metastasis; n = 6), HN3 (overt metastasis; n = 15). The 2yr % disease-free for HN0/1 and HN2/3 nodes was 86% and 49% respectively ($p = 0.017$) and 2yr % survival was 87% and 55% ($p = 0.026$) respectively.
Conclusions: Characteristics of mast cell infiltration in LNN correlate with clinical outcome. The proposed classification system is prognostic for clinical outcome in dogs with MCT (shorter disease-free interval and survival time associated with HN2/3). Additional studies are warranted.

Comparing Radiation-Induced DNA Damage Response in Lung Tissues of Recombinant Congenic Strains of Mice

Donasian O. Ochola, Christina M. Fallgren, Chris A. Hauss, Paula C. Genik, Joel S. Bedford, Michael M. Weil

A potential adverse consequence of radiotherapy for cancer is the induction of secondary tumor and it is possible that some cancer patients are more susceptible than others to radiation-induced (RI) second malignancies. However the genes involved, how they function and their interactions are unknown. We are exploring the possibility of a link between heritable differences in DNA double strand break (DSB) repair efficiency, which is influenced by many factors, and susceptibility to RI lung cancer in a mouse model. Previous experiments with 20 different recombinant congenic strains (RCS) of mice derived from BALB/c x STS progenitors showed wide inter-strain variations in susceptibility to RI lung tumor development. We hypothesize that the strains that had high incidence of lung tumor are less efficient in repairing RI DNA DSB compared to strains with low tumor incidence. We optimized the assay for determining DNA DSB response in lung tissues of RCS mice by measuring the number of residual y-H2AX foci that represent unrepaired DNA DSB. We irradiated mice with y-rays from a 137Cs source at a low-dose rate of 10cGy/hr for 24hrs followed by CO2 euthanasia. Lungs were used to prepare formalin-fixed, paraffin-embedded sections for immunofluorescence. Anti-y-H2AX (1st) and Alexa Fluor 594-conjugated (2nd) antibodies were used to visualize y-H2AX foci. Fluorescence microscopy, MetaMorph software and a CCD camera were used to obtain images that were analyzed for foci number, characteristics and location. Proper perfusion to eliminate RBC and H2O2 or sodium borohydride treatment are essential to reduce background. Low-dose rate irradiation gave foci easier to enumerate than acute dose irradiation. Foci appear to coalesce, were mainly excluded from heterochromatin regions and varied in number among strains from 8.3±3.1 to 24±5.3. Preliminary results show correlation between foci number and the observed strain-dependent susceptibility to radiation-induced lung tumors.

Establishing a Reference Interval for Fibrinogen in Box Turtles (Terrepene ornata ornata)

Lily Parkinson and Matt Johnston

The number of turtle-owning households in the United States is on the rise. Providing veterinary care for this growing population of pet turtles can be a challenge, as many diagnostic tools available in other domestic species are not well researched in chelonians. Even turtle blood chemistry panels require a great deal of further study, making the interpretation of any results from a blood draw challenging for veterinarians. To begin to glean useful information from blood draws in pet chelonians, reference values for blood parameters in pet turtle species must be established. It has been suggested that fibrinogen may be a useful blood component to quantify in turtles with infections. This study seeks to establish a reference interval for fibrinogen in ornate box turtles (Terrepene ornata ornata). Initial data from 24 turtles suggest two possible interpretations and reinforce the need for more data from additional turtles. The first possible interpretation hints at a relatively narrow fibrinogen reference interval with a few outliers. These outliers fell outside the range due to health reasons not immediately evident from the study's initial health screening. A second interpretation may be that all turtles that passed the study's initial health screening have a normal fibrinogen level, and, with future data, those turtles on the high end of the normal range will not appear to be outliers. This ambiguity highlights the need for further research in this area leading to a normal reference interval for fibrinogen to benefit the box turtles and their caretakers.

Tuberculosis in elephants in the United States: an assessment of risk factors, diagnostic test performance and treatment outcomes.

Desiree Parks, Michele Miller, Ramiro Isaza, Dennis Schmitt, Sharon Lynn Deem, Francisco Olea-Popelka

Purpose: Elephant tuberculosis is a recognized disease problem in captive U.S. elephants and is poorly understood. Exposure, risks of transmission, methods for determining TB infection, and TB treatment outcomes are not clearly defined, leading to confusion among the elephant community. The purpose of this study is to identify risk factors for elephant TB, assess the current available diagnostic methods, and evaluate TB treatment outcomes among U.S. elephants to provide information for evidence-based recommendations.
Materials and Methods: The project design is based on a retrospective review of all elephant facilities in the US including current facility/management information, TB diagnostic test results and treatment outcome, collected through a questionnaire.
Results: We have generated a questionnaire that has been discussed with the major stakeholders at the 2nd Annual TB stakeholders meeting at the Tulsa Zoo, Oklahoma on July 9-10, 2012. This survey was pre-tested with Zoo veterinarians and managers, and approved by the international elephant foundation (IEF). The questionnaire includes questions on signalment and origin of the elephant, the facility, management and its staff, and the diagnosis and treatment of TB for elephants in that facility. Confidentiality agreements were also reached regarding the information collected on this survey. An electronic data entry frame was generated and currently an online format is being developed to enhance participation. Data analysis is expected to be conducted during spring and summer 2013.
Conclusions: This study will provide relevant information to improve interpretation of diagnostic tests, identification of risk factors associated with infection, and assessment of the infection status of the U.S. elephant population. This will facilitate decision-making by elephant managers, veterinarians, and regulatory officials regarding movement, treatment, and management of elephants to prevent TB infection.

Losartan Repurposed as Novel Monocyte Migration Inhibitor for Treatment of Cancer Metastasis

Daniel P. Regan, Amanda M. Guth, Jordon Dunham, Michelina Petri, Robyn E. Elmslie, Steven W. Dow

Purpose. Inflammatory monocytes have been shown to play key roles in the pre-metastatic and metastatic niche through promotion of tumor cell extravasation, seeding, growth, and angiogenesis, as well as suppression of anti-tumor immunity. Migration of inflammatory monocytes to sites of inflammation or tumor metastasis is predominately mediated primarily via the action of the CCL2-CCR2 chemotactic axis. Thus, disruption of this axis through receptor or ligand blockade represents an attractive therapeutic target for the treatment of metastatic disease.
Materials/Methods. Losartan, an anti-hypertension drug, has also been reported to have anti-inflammatory activity and to block monocyte migration by binding to CCR2. Therefore, we conducted studies to assess the monocyte migration inhibiting activity of losartan for mouse, human, and dog monocytes. In addition, the effectiveness of losartan as an anti-metastatic agent was evaluated in mouse metastasis models.
Results. Losartan effectively blocked human and canine monocyte migration in vitro, and effectively inhibited mouse monocyte migration in a murine inflammation model. Furthermore, losartan significantly reduced mammary carcinoma pulmonary metastases in a mouse breast cancer metastasis model.
Conclusions. Losartan is an effective monocyte migration inhibitor both in vitro and in vivo in mice and in dogs. Sustained administration of losartan resulted in a significant reduction in tumor metastases in a mouse mammary carcinoma model. Studies are currently underway to assess the mechanism of action of losartan for tumor metastasis inhibition.

Survivin Inhibition in Canine Lymphoma and Osteosarcoma cell lines via EZN-3042

Jenette K. Shoeneman, E.J. Ehrhart III, J.B. Charles, B.E. Powers, Douglas H. Thamm

Canine lymphoma (LSA) and osteosarcoma (OSA) are diseases with extremely high mortality rates. While current therapies can slow progression of these diseases, new approaches to therapy are needed. Survivin is a protein with both anti-apoptotic and proproliferative activity; it is commonly elevated in human cancer. Survivin expression is a negative prognostic factor in dogs with LSA and OSA, and both canine LSA and OSA cell lines express high levels of survivin. We hypothesized that inhibition of survivin via locked nucleic acid (LNA) antisense oligonucleotide (EZN-3042) in canine LSA and OSA cell lines would increase apoptosis and chemotherapy sensitivity. We additionally hypothesized that we would see inhibition of survivin in a murine intra-tibial OSA model treated with EZN-3042. Survivin knockdown via EZN-3042 in LSA and OSA cells resulted in a 2-4 fold decrease in survivin mRNA and protein expression. Cell growth assays demonstrated up to 50% growth inhibition in EZN-3042 treated cells in both cell lines. Caspase-3/7 assays demonstrate significantly increased apoptosis in EZN-3042 treated OSA cell lines. EZN-3042 treatment enhanced OSA sensitivity to serum starvation and doxorubicin. Survivin expression was also decreased in a murine intra-tibial OSA model treated with EZN-3042. Our results demonstrate that survivin inhibition increases apoptosis and chemosensitivity in LSA and OSA cell lines, and that EZN-3042 is capable of inhibiting survivin expression in vivo. Thus, survivin may be a viable therapeutic target for the treatment of canine LSA and OSA.

Roles of caspase 3 and telomerase in the radiation induced reprogramming of non-cancer stem cells into cancer stem-like cells

Brock J. Sishc, Christine L.R. Battaglia, Miles Mckenna, Andrea Hernadon, Susan M. Bailey

The accelerated repopulation of solid tumors following radiation therapy has long been a concern for radiation oncologists seeking curative outcomes. Tumor repopulation is thought to arise from the mobilization of surviving, radio-resistant Cancer Stem Cells (CSC's) existing within the tumor bed. However, recent evidence suggests that exposure to ionizing radiation triggers non-stem cancer cells (NSCC's) to reprogram themselves into radio-resistant CSC's, the mechanism of which remains undefined. Here, we propose that cellular reprogramming following exposure to ionizing radiation is dependent upon the previously defined, caspase 3 dependent "Phoenix Rising" pathway, telomerase activity, and bystander signaling. Using the MCF-7 mammary carcinoma cell line, we demonstrate increases in telomerase activity (a marker of stem cell activity) following both direct and indirect exposures to ionizing radiation in a manner dependent on caspase 3. Furthermore, the activity of caspase 3 increased clonogenic cell survival and cell division following exposures to ionizing radiation. Flow Cytometry was utilized to evaluate the presence of CD44 +/CD 24 low mammary carcinoma stem cell populations following direct and indirect exposures to ionizing radiation. Our findings lead us to conclude that caspase 3 and "Phoenix Rising" signaling plays a critical role in the reprogramming of non-cancer stem cells in a manner that is also dependent on telomerase activity. Future studies will employ selective, small molecule inhibitors of telomerase and "Phoenix Rising" in an attempt to block ionizing radiation induced reprogramming and improve clinical outcome. Support for this research from NASA (NNJ04HD83G and NNX08AB65G) is gratefully acknowledged.

Endogenously-generated lipid peroxidation products dilate rat cerebral arteries by activating TRPA1 channels in the endothelium

Michelle N. Sullivan, Allison Bruhl, Scott Earley

Purpose: The Ca2+-permeable ankyrin (A) transient receptor potential (TRP) channel TRPA1 is present in the cerebral vascular endothelium localized to myoendothelial junctions (MEJ). Upon activation, TRPA1 evokes a vasodilatory response. TRPA1 is activated by exogenous, electrophilic compounds, but endogenous agonists of the channel in this tissue remain elusive. We hypothesized that TRPA1 is activated by lipid peroxidation products (LPP) generated from NADPH oxidase (NOX) activity within MEJ of cerebral arteries.
Materials/Methods: Immunohistochemistry was used to determine the location of TRPA1 and NOX1, 2, & 4 in rat cerebral arteries. Total internal reflection fluorescence (TIRF) microscopy was used to record TRPA1 Ca2+ sparklets in primary cerebral artery endothelial cells (EC); one-way analysis of variance followed by a Student-Newman-Keuls post hoc test was used to detect differences in TRPA1 Ca2+ sparklet frequency between groups. Isolated vessel pressure myography experiments were performed at physiologic pressure (80mmHg) to determine the effects of TRPA1 agonists/antagonists on arterial diameter; unpaired t-tests detected differences in % dilation between groups. All data are means±SE; values of n are the number of cells or vessels per experiment.
Results: NADPH, a NOX substrate, increased TRPA1 Ca2+ influx frequency in EC (0.04±0.02Hz before vs. 0.28±0.08Hz after, n=20-30). NADPH also dilated arteries in a concentration-dependent manner (EC50=1.2uM) that was diminished by the selective TRPA1 inhibitor HC030031 (HC) (61.3±21.6% dilation (NADPH) vs. 8.7±16.2% dilation (HC + NADPH), n=3). The LPP 4-hydroxynonenal (4-HNE) also caused vasodilation (EC50=8.4uM) that was abolished by HC (51.4±7.8% dilation (4-HNE) vs. 0.0±11.6% (HC + 4-HNE), n=5). Immunolabeling of cerebral arteries revealed co-localization of TRPA1, NOX2, and 4-HNE in MEJ.
Conclusion: Together our findings suggest that NOX-derived LPP generation dilates cerebral arteries by activating TRPA1.

The retinal ganglion cell distribution and visual acuity in alpacas

Hsiao-Hui (Joyce) Wang, Stacey Byers, Juliet Gionfriddo, James Mad, Jozsef Vigh

Purpose: Retinal ganglion cell (RGC) distribution is associated with the visual pattern of animals and is also related to their visual acuity. In general, animals with laterally-placed eyes possess a horizontal visual streak having the highest RGC density at the temporal end of the streak. This provides panoramic visual field assisting them to avoid predators. However, a study showed that dromedary camels have a usual retinal specialization compared to other grazing animals. The purpose of our study is to investigate the RGC distribution in alpacas, which are closely related to camels, and thus to determine their visual acuity.
Materials/Method: Three healthy eyes were collected from three different alpacas after euthanasia and the eye cups were fixed in 4% paraformaldehyde for an hour. The retinas were labeled for immunohistochemistry with goat Brn3a (C-20) antibody, a RGC marker, and donkey anti-goat Alexa Fluor-488 antibody. After labeling, the entire retinas were whole-mounted on the slides and the images were acquired with a fluorescence microscope (Carl Zeiss). The sampling area of imaging was approximately 25% in all samples.
Results: The reconstructed retinal map from Brn3a antibody labeling showed a horizontal streak slightly above the optic disc. The areas of the highest RGC count were at temporal region of the visual streak. The mean of total RGC counts and the highest RGC count were 685,050 cells per retina (range: 572,527 – 836,803) and 3,921 cells per millimeter square (range: 3,560 – 4,143), respectively. The average of the imaging sampling area was 23% (range: 21-24%).
Conclusion: According to the result of Brn3a antibody labeling, alpacas have a horizontal streak with the highest RGC density at the temporal streak as do other grazing animals, such as horses, cattle and sheep.

Determination of the Flea Species Infesting Dogs in Florida and Bartonella spp. Prevalence Rates

Kimberly Yore, Brian DiGangi, Melissa Brewer, Michael Lappin

Purpose: Bartonella spp. are bacteria that cause lifelong intraerythrocytic infections in their mammalian adapted hosts and cause disease in nonhost adapted species. Bartonellas for which main vectors and reservoirs remain unproven are Bartonella vinsonii subsp. berkhoffii and Bartonella clarridgeiae. To help elucidate the role of dogs and their fleas in bartonellosis, this study stratified Bartonella spp. amplified from healthy dogs and their fleas by genera of the fleas associated with the infestations.
Materials/methods: Blood (EDTA), serum, and fleas were collected from 80 healthy dogs on admittance to a shelter in Florida. Fleas of 43 dogs were individually examined and the genera determined based on key distinguishing features. Fleas were grouped (maximum 5 fleas) by genera, total DNA was extracted from each flea group and the blood of the corresponding dogs, and the DNA were assayed in a previously reported conventional PCR assay that amplifies the DNA of Bartonella spp.. Positive amplicons were sequenced to confirm the Bartonella species.
Results: Of the 43 dogs for which the flea genera was determined, infestations occurred with C. felis alone (28 dogs; 65.1%), Pulex spp. alone (8 dogs; 18.6%), and both fleas (7 dogs; 16.3%). Bartonella spp. DNA was amplified from 14 of 80 dogs (17.5%) and from at least one flea group from 12 dogs (15.0%) giving a total of 20 positive (dog, fleas, or both) sample pairs. Bartonella vinsonii subsp. berkhoffii DNA was amplified most frequently.
Conclusions: The study documents Bartonella vinsonii subsp. berkhoffii can be amplified from Pulex spp. infesting domestic dogs, DNA of B. clarridgeiae can be amplified from both flea genera, and provides evidence that dogs may serve as a reservoir for both Bartonella spp.. The detection of Pulex spp. in dogs suggests shared direct or environmental contact with infested foxes or humans. This is the first report of Bartonella vinsonii subsp. berkhoffii in Pulex spp. fleas from a dog.

Poster Presentations

Single-particle tracking of Nav1.6 suggests a novel anchoring mechanism and demonstrates direct trafficking to the AIS

Elizabeth J. Akin, Aubrey V. Weigel, Diego Krapf, Michael M. Tamkun

Voltage-gated sodium channels are responsible for the initiation of action potentials in excitable cells. These channels are highly concentrated at the axon initial segment (AIS) of neurons due to their interactions with ankyrin-G. This interaction is mediated by a 9 amino acid sequence, termed the Ankyrin Binding Motif (ABM) present on the II-III linker. In order to study the dynamics of sodium channels in living neurons in real time, we created a fluorescently labeled Nav1.6 protein with an extracellular tag (biotin acceptor domain). We used single-particle tracking of channels labeled with streptavidin conjugated quantum dots (QDs) and/or Alexa594 (A594) to directly compare the mobility of Nav1.6 channels localized to the AIS and somatodendritic compartments of 8DIV hippocampal neurons. We observed two populations of Nav1.6 channels, a small mobile population and a much larger immobile population. To determine the role of ankyrin-G binding in the diffusion of the full-length sodium channel, we deleted the ABM from the Nav1.6 construct. As expected, this mutant channel did not concentrate at the AIS and instead was localized throughout the soma and processes, based on both GFP fluorescence and labeling of surface channels using A594. Single-particle tracking of the mutant channels revealed that the majority of these channels are also immobile in the plasma membrane of the soma and dendrites. This suggests that although binding to ankyrin-G is necessary and sufficient for Nav1.6 to localize to the AIS, a different mechanism is responsible for the localization and membrane dynamics in the somatodendritic region of hippocampal neurons. Using A594 to label newly inserted channels, we observe that channels localize to the AIS via direct trafficking, rather than diffusion trapping. This is consistent with the idea that the majority of channels on the neuronal surface have low mobility.

Quantitative measurement of NF-kB and IRF3 nuclear translocation in individuals with a hypomorphic NEMO mutation

Celeste Allaband, Eric Hanson

NF-κB is an important component in the pathophysiology underlying many important pathogens including Foot and Mouth Disease (FMD) and Anthrax. By studying naturally occurring human mutations in the NF-κB essential modulator (NEMO) we hope to learn ways of therapeutically modifying detrimental host responses to FMD and related pathogens. Hypomorphic mutations in NEMO result in the rare syndrome of hypohydrotic ectodermal dysplasia with immunodeficiency (HED-ID or “NEMO Syndrome”). Affected individuals show variably impaired B-cell costimulation, TNF receptor, Antigen-receptor, or TLR signaling. This results in increased susceptibility to mycobacteria, encapsulated bacteria, herpesviruses, and opportunistic organisms. Normally, stimulation of cells with TNF induces NEMO-dependent IKK activation and subsequent translocation of the NF-κB transcription factor family member p65 into the nucleus. IRF3 is a transcription factor that activates NEMO in response to viral infection. The ability to induce p65 or IRF3 nuclear translocation is an important function in individuals with immune system defects of unknown etiology. We developed a method of quantitative immunofluorescence microscopy to detect TNF induced p65 and IRF3 nuclear translocation in skin fibroblasts from patients with known NEMO mutation, primary immunodeficiency of unknown etiology, or control individuals. Stimulation of dermal fibroblasts from a patient with a NEMO mutation which leads to reduced protein expression resulted in impaired p65 nuclear translocation. Interestingly, fibroblasts from an individual with perinatal cytomegalovirus infection and inflammatory eye and skin disease resulted in altered IRF3 nuclear translocation kinetics. These results illustrate the utility of measuring nuclear translocation of key transcription factors in screening patients with suspected signaling defects. Following these results, further work is being done to understand the molecular mechanism these differences.

The Effect of Autophagy Inhibition on Anchorage Independent Growth

Rebecca Barnard, Paola Maycotte, Ryan J. Hansen, Daniel L. Gustafson, Andrew Thorburn

Purpose: Autophagy has been shown to play a role in metastasis progression, albeit, poorly understood. Some evidence suggests that autophagy is induced after detachment and facilitates anchorage independent growth. Therefore, we studied the effect of autophagy inhibition on anchorage independent growth using multiple cancer models both in vitro and in vivo.
Material and Methods: Murine cell lines used were 4T1, mammary carcinoma, B16-F10, melanoma, and DLM8, osteosarcoma. Autophagy was inhibited pharmacologically with chloroquine (CQ) or bafilomycin a1 (BafA1) and genetically by knockdown of Beclin-1 (Bcn-1) or Atg7. Proliferation of cells in the presence or absence of active autophagy was assessed using an Alamar Blue assay. PolyHEMA coated plates were used to prevent attachment. For in vivo models, mice were pretreated with CQ for 72h at 60mg/kg daily IP and treated until end of study. 4T1 luciferase cells, or B16-F10 cells were tail vein injected into syngeneic Balb/c or C57Bl/6J mice. Mice were monitored thrice weekly until the development of luciferase positive metastases or 10% weight loss. Significance was determined by t-test or log rank analysis in Prism.
Results: Pharmacologic inhibition had no significant effect on 4T1 proliferation either in vitro or in vivo. However, CQ did inhibit proliferation for B16-F10 and DLM8 cells, and inhibition was more pronounced in suspended B16-F10 cells. In addition, the development of metastases was significantly delayed in CQ treated, B16-F10 challenged mice. Conversely, Bcn-1 knockdown was able to significantly inhibit proliferation for all cell types and under all culture conditions. Further study with the Atg7 cells and BafA1 will reveal if this effect is merely an off target effect of Bcn-1 or truly autophagy inhibition. Conclusion: These studies suggest that the role of autophagy in anchorage independent growth and survival is likely context dependent and may depend on how autophagy is inhibited.

Determining the Efficacy and Treatment Regimen of an siRNA Therapeutic for Prion Disease

Heather Bender, Noelle Noyes, Mark Zabel

Prion diseases, or Transmissible Spongiform Encephalopathies (TSEs), primarily affect sheep, cattle, cervids, and humans. The prion hypothesis suggests that these diseases are caused by the conversion of a native protein, PrPC, into a misfolded protease resistant isomer called PrPRes. Prion diseases cause substantial neurodegeneration, which always results in death. Currently, there are no treatments for these diseases. However, a potential therapeutic target is the downregulation or ablation of PrPC, so that it cannot be converted to the infectious isomer PrPRes. Previously, our lab identified a novel siRNA therapeutic that targets PrPC, and is able to cure mouse adapted scrapie (RML-5) infected cells and chronic wasting disease (CWD) infected cells in vitro. To determine the in vivo efficacy of the siRNA therapeutic, we infected mice with RML-5 and treated them with the siRNA therapeutic after inoculation. Preliminary data shows that the siRNA therapeutic delays the onset of clinical signs of prion disease, and increases the lifespan of RML-5 infected mice by about 25%. In a separate in vivo study, we observed a decline in behavioral and cognitive activity of mice infected with RML-5 and CWD 60-70 days post inoculation. This timepoint is about 60 days before clinical signs in CWD infected mice and about 80 days before clinical signs in RML-5 infected mice. Together, the results of these studies suggest that a) siRNA treatment may be a possible therapeutic for prion diseases, and b) behavioral and cognitive tests may help determine an siRNA therapeutic regimen, and may be a useful indicator for pre-clinical prion disease diagnosis.

RV-cyclin and CDK8: the interaction and implication

Claire Birkenheuer, Sandra L. Quackenbush, and Joel Rovnak

Walleye dermal sarcoma virus (WDSV) infection provides an accessible model for studying tumor development. Retroviral cyclin (RV-cyclin), a protein encoded by WDSV, interacts with and enhances the kinase activity of cyclin dependent kinase 8 (CDK8). Here we show that RV-cyclin up-regulates expression of a certain set of CDK8 regulated genes—the serum-response genes. Not only does this enhancement occur through transient transfection of HeLa cells with RV-cyclin, but can also be observed upon serum-stimulation of an HCT116 cell line stably expressing RV-cyclin. Additionally, we show that RV-cyclin's enhancement of the serum-response genes is dependent on activation of the mitogen-activated-protein kinase (MAPK) pathway. These data, along with chromatin-immunoprecipitation (ChIP) experiments, provide evidence that RV-cyclin functions after stimulation of the MAPK pathway, and after transcription initiation of the serum-response genes to enhance the rate of transcription elongation. With this information, we suggest that RV-cyclin's interaction with CDK8 enhances transcript levels of the serum-response genes, which aids in tumor development. In conclusion, the similarities observed between CDK8's function in walleye dermal sarcoma and CDK8's function in human colon cancer and melanoma make WDSV infection an intriguing model for tumor development.

Development and validation of a method to induce and quantify local saddle pressures

Anna Brown, Melissa King, Kirk McGilvray, Eve Bassac, and Kevin K. Haussler

Poor saddle fit is considered a major contributor to equine back pain; back pain is a common clinical condition that negatively affects equine performance. Unfortunately, even after centuries of applying saddles to ridden horses, there have been no studies evaluating the effect of quantifiable increased saddle pressure on spinal motion and lameness. Therefore, this study developed an instrument that would collect pressure data from underneath the weighted saddle. The sensor incorporated a force transducer designed to measure localized saddle pressures during simulated ridden exercise on a high-speed treadmill. Our goals were to: 1) reproduce clinically-relevant, focal saddle pressures; 2) induce back pain at common sites of poor saddle fit; and 3) measure altered spinal and limb kinematics associated with poor fitting saddles. Stereophotogrammetric techniques were utilized to analyze spinal and limb movements. Back pain and favored limb patterns were monitored with pressure algometry and force plate gait analysis, respectively. This project developed a quantitative tool that can be used in future studies focused on investigating the clinical effects of poor saddle fit on musculoskeletal function and the important compensatory mechanisms in horses due to localized back pain. This study was also designed as a pilot study to help initiate critically-important research regarding the effects of poor saddle fit on performance horses, which is of practical importance to all equine athletic disciplines.

Administration of daily deslorelin acetate throughout mid-diestrus does not increase serum progesterone levels in the mare

Chelsie A Burden, Ryan A Ferris, Jennifer N Hatzel, Patrick M McCue

Purpose: Progesterone secreted from the ovarian corpus luteum is required for embryonic survival during early pregnancy. GnRH analogs have been reported to increase pregnancy rates in mares. We hypothesize that deslorelin treatment once daily from day 8 to 12 post ovulation would result in elevated serum progesterone concentrations as compared to saline placebo treatment.
Material and Methods: Four light horse mares were selected for a cross-over study comparing deslorelin treatment during mid-diestrus to a saline placebo. Estrous cycles were followed and ovulation confirmed via ultrasonography. Mares were treated with either an intramuscular injection of 50mcg of deslorelin acetate on days 8 -12 post ovulation or a single 1.0ml saline injection on day 8 post ovulation. Jugular venous blood samples were collected in empty sterile glass vacuum tubes once daily for 16 consecutive days following ovulation and serum frozen at -20ºC until analyzed. Serum samples were analyzed for progesterone using a validated RIA. Progesterone comparisons were made by repeated measure analysis of variance.
Results: There was no difference in progesterone profiles between placebo treated and deslorelin treated mares. No significant (p=0.2935) difference in peak progesterone values between deslorelin acetate treatment (14.15 +/-0.57 ng/ml) and placebo treatment (15.45 +/- 1.27 ng/ml) was observed.
Conclusions: Administration of deslorelin acetate during diestrus did not affect serum progesterone concentrations. If increased pregnancy rates are associated with the administration of a GnRH analog during diestrus, the result is possibly due to effects outside of luteal cell function. GnRH agonists may bind to GnRH receptors within the endometrium and enhance uterine histotroph production providing key enzymes, growth factors and proteins to nourish a developing embryo.

Serotype reactivity of commercial immunoassays for Salmonella enterica identification in experimentally-inoculated equine fecal samples

Brandy A. Burgess, Denise S. Bolte, Doreene R. Hyatt, Dave C. Van Metre, Paul S. Morley

Salmonella enterica can have a tremendous impact on the management of animal facilities. Comprehensive screening and rapid detection of S. enterica in relevant samples is essential for effective infection control in high-risk horse populations. The objective of this study was to characterize the reactivity of 3 commercially available immunoassays, 2 lateral flow antigen detection systems and 1 DNA hybridization detection system, using multiple isolates of S. enterica from a variety of common serotypes recovered from hospitalized patients at the Colorado State University Veterinary Teaching Hospital (CSU-VTH) and the hospital environment. A formal random process was used to select 112 S. enterica isolates, collected as part of long-term surveillance at the CSU-VTH, representing the 10 most common serotypes (6 serogroups) in this archive. One gram equine fecal samples were inoculated with 1ml of standardized inoculum (~10^2 cfu per ml) into 9ml tetrathionate broth and incubated at 43°C for 18 hr. Samples were tested in a blinded fashion. Overall, 95.6% of samples were correctly identified by at least one of these immunoassays. In general, serotype reactivity varied by immunoassay. Lateral flow detection systems had the poorest sensitivity for serotypes Cerro (Group K), Mbandaka (Group C1) and Montevideo (Group C1). The DNA hybridization immunoassay showed the best performance across serotypes tested. The findings of this study demonstrate that the utility of these commercial immunoassays varies by serogroup and serotype. This is critically important to their implementation in clinical practice as their value will be dependent upon the most common serotypes detected in a particular population or region.

Emergence of Disinfectant Resistant Mycobacteria Infections

Winona Burgess, Sara Gookin, Alyssa Margolis, Vinicius Calado Nogueira de Moura, Rafael Silva Duarte, Mary Jackson

Rapidly-growing Mycobacteria (RGM) have been associated with numerous clinical outbreaks throughout the world. These bacteria present challenges for both human and veterinary healthcare providers as not only are the infections refractory to treatment, but these organisms are found in the water supply of most hospitals and are frequently associated with biofilms. These pathogens have received increasing attention worldwide due to the development of glutaraldehyde (GTA) resistant strains of two species, Mycobacterium massiliense and Mycobacterium chelonae. In particular, M. massiliense resulted in an ongoing nosocomial outbreak in Brazil that has affected over 2,000 patients. Of particular concern is not only the fact that GTA is the most commonly used disinfectant in the world for heat-sensitive medical equipment such as endoscopes and bronchoscopes, but recent research showed that these strains have increased pathogenicity in animal models. Given the rise of globalization, it is of great concern that a disinfectant resistant strain of RGM could be introduced into the US healthcare system. Recognizing the potential need for recommendations for alternatives to GTA based disinfectants, we have quantitatively tested the susceptibility of NTM isolates and controls against 6 FDA approved disinfectants. The disinfectants were tested at their labeled Minimum Effective Concentrations (MEC) under three different testing protocols: the Quantitative Carrier Disk Method, the Quantitative Tuberculocidal Method and the Modified Quantitative Tuberculocidal Method. Our initial results show that GTA-based disinfectants that we tested are ineffective at their MEC against these resistant isolates, while other available disinfectants are effective against these resistant strains. Our results provide additional information to the healthcare community to assist with informed choices for disinfection of heat sensitive medical equipment utilized in both human and veterinary medicine.

A simple and rapid fluorescence in situ hybridization microwave protocol for reliable dicentric chromosome analysis

Ian M. Cartwright, Matthew Genet, Takamitsu Kato

Purpose: The purpose of this project was to develop a streamlined approach to staining the centromere's and telomere's of human chromosomes using PNA probes. PNA staining provides a effective way to count the number of dicentric chromosomes formed after exposure to radiation. The number of dicentrics is a great biomarker for the dose an individual received.
Methods: B70 mouse fibroblasts and human AG1521 fibroblasts cells where exposed to various doses of gamma radiation and they where stained with PNA telomere and centromere stains. Additionally, human peripheral lymphocytes were stained to show that our method is effective in both cell cultures and primary cells. Images where captured and analyzed with an Olympus BX51 fluorescence microscope equipped with Q-imaging Aqua cooled CCD camera. Two independent scores counted the number of dicentrics in 50 chromosome spreads for each does. We plotted both data sets and used a P-score to determine whether or not the results where statistically similar.
Results: We developed a protocol that effectively stained the human lymphocytes, AG1521, and B70 cells in 2min 30sec. We have statistical evidence that our protocol can be duplicated by two individuals and produce similar results.
Conclusion: Our study shows that we have modified a traditional that typically takes over 3 hours to complete and several detailed steps into a simple and effective technique that can be accomplished in roughly 3 minutes. With this new protocol we have the ability to move forward in developing a high throughput screening protocol that allows for the easily identification of dicentrics post exposure to radiation.

Perioperative changes in the Pa02/Fi02 and SaO2/Fi02 ratio in ovariohysterectomized dogs recovering on room air versus nasal oxygen insufflation

Andy Carver, Lauren Sullivan

Purpose: To retrospectively determine trends in the Pa02/Fi02 (P/F) and SaO2/Fi02 (S/F) ratios, as well as the correlation between P/F and S/F, in ovariohysterectomized dogs recovering postoperatively on room air versus 100 ml/kg/min of nasal oxygen insufflation.
Materials/Methods: Dogs undergoing ovariohysterectomy were randomized to receive 100 ml/kg/min of nasal oxygen insufflation (estimated 37% FiO2, n=9) or room air (estimated 21% FiO2, n=10) for two hours postoperatively. Baseline information was obtained one hour intraoperatively (estimated 100% FiO2), followed by three postoperative time points (10, 60 and 120 minutes). Data recorded for each time point included FiO2, PaO2, SaO2, P/F ratio, S/F ratio, PaCO2, rectal temperature, and arterial blood pH. Using the baseline value as a covariate, results were analyzed by repeated measures analysis of covariance. Correlations between P/F and S/F were determined using the Pearson correlation coefficient.
Results: The P/F ratio in dogs recovering on supplemental oxygen was significantly higher compared to those recovering on room air (516 + 28 versus 339 + 10, p <.0001). Alternatively, the S/F ratio in dogs recovering on supplemental oxygen was significantly lower compared to those recovering on room air (268 + 0.5 versus 448 + 1.4, p <.0001). The P/F and S/F ratios demonstrated high correlation for both groups at each postoperative time point. In dogs breathing room air, P/F and S/F correlations were 0.90, 0.95 and 0.93 (p <.001). In dogs receiving supplemental oxygen, P/F and S/F correlations were 0.94, 0.93, and 0.90 (p <.001).
Conclusions: The effects of surgery, anesthesia, and oxygen supplementation on the P/F and S/F ratio had not been previously evaluated in dogs. This study provides expected P/F and S/F ratios over a two hour period in postoperative ovariohysterectomized dogs, and also indicates an acceptable correlation between P/F and S/F in this population.

Use of equine bone marrow derived mesenchymal stem cells to enhance keratinocyte migration and proliferation in an in vitro model of wounding

Amanda Chang, Britta Leise

The use of bone marrow derived mesenchymal stem cells (BM-MSC), and other types of cell-based biological therapies, have great potential for their use in improving healing after an injury. The regenerative effect of stem cells is believed to be mediated through an array of mechanisms, which include the production of growth factors, anti-inflammatory mediators, promotion of cell recruitment and through direct cell differentiation. Through these suggested mechanisms, it is then possible to use stem cell therapy in the treatment of equine disorders. The purpose of this study was to evaluate the ability of equine BM-MSC and BM-MSC supernatant to enhance equine keratinocyte migration and proliferation after wounding. Equine keratinocytes were grown in culture and stimulated with either BM-MSC through a transwell system or direct application of BM-MSC supernatant. The in vitro scratch model of wounding was used to assess keratinocyte migration and proliferation over a 48 hour period. Data collected from this study will provide essential preliminary data to support the further evaluation of stem cell therapy in equine keratinocyte disorders, such as wound healing.

Androgen Exposure Leads to Global DNA Methylation and Gene Expression Changes in Sheep Placental Cells

Ellane R. Cleys, Jennifer L. Halleran, Quinton A. Winger, Jason E. Bruemmer, Colin M. Clay, Gerrit J. Bouma

Purpose: Heightened circulating androgen has been reported in serum from obese pregnant women and from patients with preeclampsia, a placental induced disorder that can lead to maternal and fetal mortality. However little is known about the role of androgen in placental development or function. Our goal is to determine the role of androgen in placental development and differentiation using an established ewe model of prenatal androgenization. We hypothesize that maternal androgenization leads to abnormal sex steroid signaling in the placenta and perturbed placental development.
Materials/methods: Pregnant ewes were treated with testosterone propionate (TP; 100mg biweekly, n=7) or cottonseed oil (2mL vehicle control, n=7) from gestational day (GD) 30 to 90. Placentomes were collected and classified by gross morphology at GD90, and processed for molecular and immunohistochemical analysis.
Results: Prenatally androgenized fetuses were growth restricted and there was a decrease in type A placentomes and an increase in type C and D placentomes in TP treated ewes. ELISA assay revealed reduced global DNA methylation in placentomes from TP compared to control treated ewes. Gene expression analysis revealed an increase in relative levels of histone demethylases *KDM4D*, a histone demethylase that complexes with androgen receptor (AR), and *LSD1* in placentomes from TP compared to control treated ewes ($p<0.05$). In addition, altered relative levels of genes involved with placental development and hormone signaling, including *VEGF* ($p<0.05$), *CYP19* ($p<0.05$), *MMP2* ($p<0.05$), *LEPR* ($p<0.05$), and *ESR2* ($P<0.05$) were observed in placentomes from TP treated ewes. Immunohistochemistry revealed that AR colocalized with ESR1, ESR2 and LSD1 to placental syncytium. KDM4D and LEPR also colocalized with AR in the caruncle epithelium.
Conclusions: Androgen is capable of altering placental DNA methylation, and changing the expression of proteins that regulate placenta differentiation and function.

Outcome of serum amyloid A and fibrinogen in horses with colic before and after surgery: A preliminary study

Madison Cloninger, Alexander Daniel, Diana Hassel, Britta Leise

Purpose: Serum amyloid A (SAA) is an acute phase protein whose degree of elevation has been correlated with outcome under many inflammatory conditions in the horse. Previous reports suggest that SAA is increases more rapidly and is more sensitive than that of fibrinogen, another acute phase protein which is commonly used clinically in the horse as an index of an inflammatory response. Therefore it was the purpose of this study to evaluate the acute phase protein response of both fibrinogen and SAA and to determine if one will provide a more sensitive measure of inflammation.
Materials/Methods: To date 6 horses, consisting of clinical cases presenting to Colorado State University for treatment of colic with completed exploratory laparotomies, were recruited for this study. Blood was drawn from the jugular vein pre-operatively (time 0) and 24, 48, 72, and 96 hours post-operatively for quantitative fibrinogen, SAA and complete blood count. SAA and Fibrinogen values were evaluated via repeated measure ANOVA.
Results: Preliminary results demonstrated a significant increase ($P<0.001$) in SAA from the 0 time compared to all post-operative values; however, there was no significant change post-operatively in SAA. There was no significant difference between any of the times for values of fibrinogen.
Conclusions: Initial evaluation suggests that SAA may be a more sensitive determinate of post-operative inflammation than fibrinogen. Additional data still needs to be collected and further evaluation of the subjects, such as type of gastrointestinal lesion, is necessary to better define the clinical relevance of increased SAA in post-operative colics.

Spatial morphology of the abdominal reproductive tract in 6 mares

Aimee C. Colbath, Eileen S. Hackett, Dean A. Hendrickson

Purpose: The study was performed to provide a description of the relative location of reproductive tract and caudal abdominal organs of the mare. The purpose of the study was to provide anatomical information to determine feasibility of a single flank ovariectomy surgery.
Materials/methods: Six adult mares were humanely euthanized. Signalment, height, weight, and number of foals was recorded. The cadavers were orientated in a standing position to mimic abdominal organ orientation during standing laparoscopy. External measurements included length from the last rib to the tuber coxae, transverse process of the spine to tuber coxae, vertical length of the paralumbar fossa, width of abdomen, length from tuber coxae to distal flank, length from withers to tail, and total circumference of the abdomen. Internal measurements included distance between the peritoneum and ovary, diameter of flank muscle and fat, dimension of ovaries, length of mesocolon, distance between ovaries, length from tuber coxae to ovary and from last rib to ovary. Range and mean were reported.
Results: The six horses ranged from 2-23 years old, mean 14.5 years. Breed distribution included TB(3), QH(2), and pony. Height ranged from 13.2–15.3 hands and mean weight of 485 kg (range 414–559 kg). Average abdomen width was 54 cm (range 51-59 cm). Distance from peritoneum to ovary ranged 4-14 cm. Muscle and fat diameters varied (range of 3.5–8 cm and 4.5–9 cm, respectively). This was reflected in the variable length between the body wall and the ovary (range 10–19 cm). The length of the mesocolon ranged from 11-16 cm.
Conclusions: The study provided the orientation of the caudal abdominal organs within a standing horse. Specifically, the orientation of the ovaries in relation to the body, the total width of the abdomen, and the length of the mesocolon of the descending colon. Distances indicate surgical instruments need to be greater than 45 cm in length to reach both ovaries from the left flank.

Local L-type Calcium Channel Signaling in alpha T3-1 Cells

An K. Dang, Nathan L. Chaplin, Christianne Magee, Dilyara Murtazina, Colin M. Clay, Gregory C. Amberg

A dramatic release of luteinizing hormone (LH) from pituitary gonadotrope cells is necessary for ovulation. Binding of hypothalamic gonadotropin releasing hormone (GnRH) to its receptor on the gonadtrope cell surface initiates multiple signaling cascades, ultimately resulting in the release of LH and induction of ovulation. We hypothesized that the signaling molecule diacylglycerol, produced by phospholipase C, could activate protein kinase C and stimulation of L-type calcium channels. To test this hypothesis we used a combination of TIRF microscopy and electrophysiology to image subplasmalemmal calcium influx in the gonadtrope cell line alpha T3-1. Using this approach we visualized discrete sites of calcium influx (calcium sparklets) which produced microdomains of elevated calcium. Following exposure of alpha T3-1 cells to GnRH, sites of localized calcium influx were identified, whereas a change in global calcium were not evident. The L-type calcium channel blocker, nicardipine (10 microM) abolished calcium influx in response to GnRH. Conversely, the L-type calcium channel agonist FPL64176 (500 nM) produced calcium influx events indistinguishable from those induced by GnRH. These data indicate that in alpha T3-1 cells, GnRH activates L-type calcium channels resulting in microdomains of elevated calcium. Interestingly, the calcium signals in alpha T3-1 cells resemble those observed in arterial smooth muscle in response to angiotensin II. Finally, the existence of calcium microdomains in alpha T3-1 cells may explain the divergent signaling cascades produced by local vs. global calcium events following GnRH receptor activation.

Speciation of Airborne Bacteria Collected by Novel and Traditional Samplers in a Cantaloupe Processing Facility: A Pilot Study

Margaret E. Davidson, Bledar Bisha, Stephen J. Reynolds, Lawrence Goodridge.

There have number of recent fatalities from cantaloupe consumption. Aerosols in open plan facilities represent a potential source of cross contamination. This poster presents data on airborne bacteria species identified during cantaloupe processing and forms part of a method development for bioaerosol sampling.
Two 2 hour sampling sessions of were conducted with NIOSH BC251 and SKC BioSamplers (control) in the packing section of a cantaloupe facility. Samplers were loaded with a resuscitation buffer. Aliquots of sampled buffer were inoculated on CHROMagar (0157 and Salmonella), RAPID'L. Mono and LPM, incubated for 24 hours at 37±2ºC and presumptive pathogens reisolated on TSA and incubated. Identification was undertaken with the Dupont Qualicon RiboPrinter system. Environmental swab samples were also analyzed.
22 presumptive Salmonella sp. were ribotyped. Of these, only 5 were weakly matched with Salmonella serovars Bovismorbificans (61%), Krefeld (47%), Orientalis (56%), Glostrup (56%) and Salmonella sp. III (49%). Presumptive E. coli 0157:H7 and Listeria sp. were isolated, but all were false positives.
The absence of E. coli was unusual given its ubiquitous nature in agriculture, and is not attributed to the sampling method because E. coli had previously been isolated from dairy samples collected in the same manner. E. coli may have been present at very low concentrations and sampling times could be lengthened to increase sensitivity. However, this may be unsuitable for the BioSamplers which were more susceptible to evaporation than BC251. None of the Salmonella sp. identified, albeit weakly, have been linked with cantaloupe food poisoning. Further testing is required to confirm Salmonella sp. because the matches were weak (<85%). Ribotyping identified Aerococcus viridans and Pseudomonas aeruginosa in aerosols. The detection of P. aeruginosa suggests that aerosols are a cross contamination source of food spoilage bacteria in cantaloupe facilities.

Effects of handling time on the leukocyte profile of wild rodents

Katie Doepker, Rhea Hanselmann, Anna Jolles

Purpose: In mammals, glucocorticoid release during stressful events can cause a change in the leukocyte profile. Here, we examined how handling time affects the leukocyte profile of wild rodents, and how different levels of forest management influence this response. We hypothesized that total leukocyte and neutrophil counts would increase linearly with prolonged handling time. We also posited that this response would be reduced in animals from poor quality habitats.
Materials/methods: Trapping occurred on forest plots that span three management intensities: undisturbed 40-50 year old stands, stands clear cut within two years, but not further managed, and recently clear cut stands intensively managed with herbicides and manual vegetation control. Rodents were bled from the retro-orbital sinus. Total leukocyte counts were obtained using a hemocytometer. Differential leukocyte counts were performed using stained blood smears. Relationships between leukocytes, handling time, and forest management level were determined using linear regression models.
Results: Rodents were captured from late June through mid-September during 2011 and 2012 (6124 trap nights). For deer mice (Peromyscus maniculatus; n=237), relationships between total leukocyte counts and handling time, as well as neutrophil counts and handling time, were complex and unexpected. Although effects were mostly weak, both habitat quality and animal sex appeared to influence these associations.
Conclusion: We demonstrate trends in the relationship between handling time and leukocyte counts, which appear to depend on cell type, habitat quality, and animal sex. These results may in part be due to the timing of our blood collection, which occurs as soon as animals are anesthetized, potentially missing the stress response to the current handling session. If this is true, the capture event in itself may not be a significant stressor for these animals.

Evaluation of the transcription factor, Nrf2, and the antioxidant response during an in vitro infection model of Mycobacterium tuberculosis

Sarah Eck, Forrest Ackart, Brendan Podell, Randall Basaraba

The host response to infection with the intracellular bacteria Mycobacterium tuberculosis (Mtb) is chronic inflammation with the generation of tissue damaging oxygen free radicals. Oxidative stress occurs when reactive oxygen species (ROS) generation exceeds the collective antioxidant capacity of the host. We hypothesize that the oxidative stress associated with Mtb infection is also due to the inability of Nrf2, a major oxidant responsive transcription factor, to successfully translocate to the nucleus leading to a deficit in a number of critical antioxidant genes. The human monocytic cell line, Thp-1, were infected for 72 hours with the H37Rv strain of Mtb and the nuclear and cytoplasmic expression of Nrf2 and several down-stream antioxidant proteins were quantified by western blot analysis. Preliminary data show there is Nrf2 expression in cytoplasmic fractions, but is absent in nuclear fractions. Data pertaining to the expression of Nrf2 regulated genes including NAD(P)H dehydrogenase quinone 1 (NQO1) and heme oxygenase 1(HO-1) are in progress. Since HO-1 is also regulated by the hypoxic response regulator HIF-1a, we also looked at the expression of this transcription factor in Mtb infected THP-1 cells. By real time qPCR we showed that Mtb infection induces an increase in HIF-1a, NQO1 and HO-1 compared to uninfected control cells. Studies to evaluate the response of Mtb infected cells to oxidative stress and whether Nrf2 and HIF-1a function normally are in progress. These findings suggest that there is a defect in Nrf2 function but that HIF-1a may contribute to host antioxidant defenses through the up-regulation of HO-1. Understanding how Mtb infection influences the expression of Nrf2 and HIF-1a is important since they can be targeted therapeutically as an adjunct to potentiate the host response in TB.

Microfluidic strategy for spatiotemporally resolved molecular sampling from organotypic tissue slices

Chad Eitel, John Wydallis, Valentina Pauna, Kelly Neinburg, Sean Morris, Cody Eslinger, Meghan Mensack, Charles Henry, David Dandy, Stuart Tobet

Advancing our understanding of organ function requires real-time, simultaneous detection of a number of key signaling molecules.
In this study we implement a microfluidic device capable of sampling multiple chemical messengers from live mouse slices. In one example, a 200 μm thick organotypic ovary slice is placed on the bottom surface of a prototype sample reservoir and immersed in growth media. The bottom of the sampling reservoir contains spatially resolved 100 μm diameter sampling ports which connect to analysis microchannels whose bottom surfaces are patterned with antibodies against specific analytes. The analysis microchannels lead to a common outlet containing multiple passive pumping reservoirs able to provide long-term, steady-state flow of effluent physiological media for spatiotemporal analysis. The flow rate through the analysis channels is linearly proportional to the number of pumping reservoirs in operation. Proof of principle experiments have been conducted under continuous flow conditions that demonstrate the ability of the system to accurately map the spatial distribution of multiple analytes within the sample reservoir as a function of time.
Current application of this microfluidic device employs immunoassay and electrochemical detection schemes to determine the characteristics of chemical signaling, organ development, and changes in cell behavior in response to a maturation factor such as specific steroid hormones, peptides or transmitters.

Misfolded Prion Protein Detection Using Real Time-Quaking Induced Conversion for Brain and Blood

Alan Elder, Davin Henderson, Anca Selariu, Amy Nalls, Candace Mathiason

Purpose: Until recently, detection of the misfolded prion protein (PrPres) has relied on the presence of large quantities of the protein to be visualized using western blots or immunohistochemistry (IHC). This large quantity of the misfolded protein is usually obtained from the brain of the animal post-mortem. Real Time-Quaking Induced Conversion (RT-QuIC) was developed as a means to detect PrPres in samples where the concentration was to low for positive identification with western blot or IHC. We hope to use RT-QuIC for the detection of PrPres in various species of animals as well as develop the assay for the detection of PrPres in the blood.
Materials/Methods: Blood was collected in heparin, EDTA and CPDA for analysis in RT-QuIC. Half of the samples underwent freeze-thaw cycles before being placed in RT-QuIC. Brain samples were made into 10% homogenates and subsequently serial diluted before being placed into RT-QuIC. Ninety-eight microliters of QuIC buffer and two microliters of sample were placed into each well of a 96 well plate. The plate was then placed in a fluorescent plate reader for 60 hours.
Results: We have been able to detect PrPres in the brain of white-tailed deer, muntjac deer, domestic cats, mice, and hamsters using RT-QuIC. Blood samples from positive animals that were collected in heparin and underwent the freeze-thaw process showed positivity. In contrast, samples collected in EDTA and CPDA were negative.
Conclusions: The RT-QuIC assay is able to detect PrPres in various species of animals, without much fluctuation of sensitivity or specificity. RT-QuIC also shows great promise for the detection of the misfolded protein in heparinized blood samples, allowing for ante-mortem diagnosis of prion disease.

Ovarian cancer cell-secreted exosomes induce molecular and phenotypic changes in cells

Vanessa A. Enriquez, Juliano C. da Silveria, Monique A. Spillman, Quinton A. Winger, Gerrit J. Bouma

Ovarian cancer is the 5th most deadly cancer among women in the United States and the most lethal gynecological malignancy in the world. Tumor cells are known to secrete vesicles called exosomes, small endosome-derived vesicles containing bioactive materials including miRNAs, and can be detected in the bloodstream and urine. Importantly, we recently described the presence of stem cell factor LIN28, as well as a number of miRNAs associated with tumorigenesis, in the ovarian cancer cell line IGROV1, as well as their secreted exosomes. We hypothesized that ovarian cancer cell-secreted exosomes are taken up by target cells and induce change in gene expression and cell behavior. Our objectives were to: 1) Determine the effects of IGROV1 cell secreted exosomes on HEK293 cell proliferation and migration, 2) Identify genes related to epithelial to mesenchymal transition (EMT) pathway that are modulated in HEK293 cell following exposure to IGROV1 secreted exosomes, 3) Identify miRNAs present in IGROV1 secreted exosomes predicted to target genes involved in EMT. Our data indicate that IGROV1 secreted exosomes are taken up by HEK293 cells. Moreover, although proliferation was not affected in HEK293 exposed to IGROV1 secreted exosomes, HEK293 cells that took up IGROV1 secreted exosomes exhibited significant increases in migration and invasion. In addition, HEK293 cells treated with IGROV1 secreted exosomes lead to increased levels of LIN28 as well as various genes involved in the EMT pathway, including TIMP1 (25-fold higher), FOXC and NOTCH1 (11-fold-higher), CDH1 (6-fold higher), MMP (5-fold higher), MMP9 (4-fold higher), and ZEB1 (3-fold higher). These genes are elevated in cancer tumors and are known to modify gene pathways involved in invasion and proliferation. Elucidating the molecular and phenotypic effects induced by ovarian cancer cell-secreted exosomes can lead to greater understanding and insight into metastatic disease.

Development of a community – based livestock syndromic recording system for animal disease surveillance in silvopastoral production system in Mexico

Jose A. Erales-Villamil, David C. Van Metre, Cristobal Zepeda, Javier Solorio-Sanchez, Robin Reid, M.D. Salman

Purpose: Develop and assess a community based livestock syndromic recording system proposed for silvopastoral (SPS) livestock producers in Tropical Mexico. This study is a proof of concept, hypothesis generating pilot study.
Materials and Methods: Five SPS farms (livestock produced by feeding from an array of trees, legumes and grasses) in Michoacan and Yucatan States in Mexico were enrolled in the study during the summer of 2012, seminars and written materials were used to educate farmers about the inherent long-term benefits of animal health care and disease surveillance to farm productivity and food safety. Farmers were also trained to recognize syndromes and to record case and treatment data in a booklet. The syndromes included: Respiratory, Digestive, Reproductive, Locomotor, Neurologic, Udder/Mastitis, Skin Lesions and Death. Calf weaning weights and milk yield will be recorded. Data will be collected by farmers, veterinarians, and animal health technicians on a daily basis and will be retrieved on January and June, 2013 Recorded data will be "triangulated", with records from one veterinarian and one technician in each State. Farmers were encouraged to perform other diagnostic tests to obtain precise diagnoses.
Results: Frequency of syndromes will be measured and the association between syndromes frequency and productivity will be estimated. Demonstrations of the use of the recording system will be presented.
Discussion: Developing countries such as Mexico are limited in economic resources to provide veterinary services to livestock producers, particularly small stakeholders in marginal communities. Furthermore, organized crime creates an unsafe atmosphere which reduces the possibility for these communities to receive veterinary advice. Approximately 70% of Mexican farmers own herds smaller than 35 cows, this units are family owned/operated and its technical level is low. Approximately 2.5 million farms can't afford private veterinary services.

U.S. Army Human Medical Event Data Collection: A Comparison of Existing Systems Using Zoonotic Disease

Rebecca Evans, Mo Salman, Karyn Havas

Purpose: Provide a comprehensive comparison of U.S. Army human medical event data collection systems to facilitate selection of the most suitable one for the developing Zoonotic Disease Report (ZDR). Seventy percent of emerging infectious disease is zoonotic in nature. Understanding and predicting the risk of these diseases must involve information from both animal and human populations. The ZDR will provide the Army critical risk assessment information regarding presence and spread of zoonotic pathogens and will create opportunities for improved preventive medicine strategies.
Methods: Phase 1: System descriptions will be compiled utilizing a template adapted from the Centers for Disease Control and Prevention (CDC) Guidelines for Evaluating a Public Health Surveillance System. The aim is to identify similarities, overlaps, and gaps for the purpose of determining the utility of these systems. Description categories include: system purpose/justification/objectives, populations included vs. excluded, data sources/feeds, and data types (laboratory, syndromes, ICD-9 codes). Phase 2: System will be queried for case count information on four specified zoonotic diseases. Comparison of the case count data will facilitate the assessment of key system traits such as data accessibility, timeliness, completeness, specificity and sensitivity, and availability of individual patient characteristics.
Results: Differences and similarities in the systems will be assessed using the standardized evaluation format and conducting the case count comparison. The differences revealed will assist in selecting the most suitable human disease data system for the ZDR.
Conclusion: This study will create standardized medical event record collection system descriptions for the Army; a valuable resource for all that currently utilizes them. The quantitative comparisons will be used to make informed decisions about which human system best suits the need of the ZDR.

Bighorn sheep sinus tumors are associated with co-infections by pneumonia-causing bacterial agents in the upper respiratory tract

Karen A. Fox, Natalie M. Rouse, Kathryn P. Huyvaert, Ivy K. LeVan, Michael W. Miller, Sandra L. Quackenbush

Purpose: Recently, we described a novel disease in bighorn sheep characterized by tumors (predominantly fibromyxomas) of the paranasal sinuses, and we have proposed a retroviral etiology for this disease. Grossly, bighorn sheep sinus tumors expand the sinus lining, obstruct the sinus cavities, and exude abundant mucus. We suspect that these features may interfere with the normal clearance of bacterial pathogens from the upper respiratory tract. Proliferation of bacteria in the upper respiratory tract may lead to bronchopneumonia, which is the leading infectious cause of death in bighorn sheep. The purpose of this project was to determine if bighorn sheep sinus tumors are associated with the presence of pneumonia-causing bacteria in the upper respiratory tract.
Materials and Methods: We examined 97 bighorn sheep carcasses post-mortem and categorized each case as tumor-positive, tumor-suspect, or tumor-negative based on specific diagnostic criteria. We collected fresh sinus lining tissue from each case and used PCR assays to screen for the presence of Mycoplasma ovipneumoniae and Pasteurellaceae bacteria, the suspected agents of fatal bronchopneumonia in bighorn sheep. We used a Fisher's exact test to compare the tumor-positive and tumor-negative groups based on the presence or absence of each bacterial pathogen.
Results: Based on PCR results for Mycoplasma ovipneumoniae and Pasterellaceae bacteria, we found a significant difference ($p<.05$) between tumor-positive and tumor-negative groups. A significantly greater proportion of tumor-positive tissues were also PCR-positive for the suspected agents of bacterial bronchopneumonia, as compared to tumor-negative tissues.
Conclusions: We conclude that bighorn sheep with sinus tumors are more likely to harbor potentially pathogenic bacteria in their upper respiratory tracts than bighorn sheep lacking sinus tumors. This may have implications for the development of bacterial bronchopneumonia in these animals.

Endoplasmic reticulum/plasma membrane junctions function as membrane protein trafficking hubs

Philip D. Fox, CJ Haberkorn, AV Wiegel, EJ Akin, MJ Kennedy, D Krapf, MM Tamkun.

Endoplasmic reticulum/plasma membrane (ER/PM) junctions are well known for their role in store-operated Ca2+ influx via the Stim/Orai complex. We provide evidence for a novel role of ER/PM junctions as trafficking hubs for insertion and removal of plasma membrane proteins in HEK cells and neurons. By simultaneously visualizing ER/PM junctions and various transmembrane protein cargoes with total internal reflectance (TIRF) microscopy, we demonstrate that the vast majority of exocytotic delivery events for a recycled membrane protein, or for a membrane protein being delivered to the PM for the first time, occur at ER/PM junctions. Likewise, we observed stable clathrin clusters and functional endocytosis of PM proteins preferentially at EM/PM junctions. Thus, ER/PM junctions serve to organize the molecular machinery for both insertion and removal of cell surface proteins, highlighting a novel role for these unique cellular microdomains in neuronal secretory trafficking.

Histologic Characterization of Experimental Brucellosis Infection in Elk (Cervus canadensis)

Alana Garner, Pauline Nol, Jack Rhyan

Purpose: Brucellosis is an important zoonotic disease, and the transmission between elk and cattle is of great concern in the greater Yellowstone area. The purpose of this study was to characterize the microscopic lesions resulting from experimental infection of elk with Brucella abortus to aid in the disease surveillance and diagnosis of natural infections.
Materials/Methods: Archived tissues from post-mortem examination of 10 elk cow-calf pairs were examined via histopathology. All cows had been inoculated with 1.18x10^8 colony-forming units of Brucella abortus strain 2308 into the conjunctival sac.
Results: Infection was confirmed in 8/10 cows and 6/10 calves by PCR of blood and various tissues. The most prominent microscopic lesions were found in the mammary glands, spleen, submandibular lymph node, and placenta of the cow, and the lung and spleen of the fetus. Mammary glands of all cows were affected, with 3/10 displaying marked glandular atrophy and degeneration, with dilation and inspissation of secretory material, surrounded by mixed chronic interstitial inflammation. The spleens of all cows were affected by mild to marked suppurative splenitis and lymphoid hyperplasia. Submandibular lymph nodes of 8/10 cows displayed mild to moderate suppurative lymphadenitis with lymphoid hyperplasia. Maternal caruncles in 9/10 cows were affected by mild to marked diffuse suppurative placentitis. Lungs from 9/10 calves displayed mild to moderate suppurative interstitial pneumonia. Spleens from 5/10 calves displayed mild to moderate suppurative splenitis.
Conclusion: Microscopic lesions in the mammary glands, spleen, lymph nodes, and placenta of elk suggest a similar pattern of dissemination of brucellosis to those seen in other livestock species, including cattle. Additional studies are needed to thoroughly characterize the pathogenesis of brucellosis in elk.

Survey Assessment of Empirical Antimicrobial Use by Veterinarians

M. Brandon Gates, Paul S. Morley, David C. Van Metre

Antimicrobial prescribing factors and their role in contributing to resistance is one of the most pressing issues currently facing veterinary and human health. The use of antimicrobials in veterinary medicine, especially in food animals, has important implications for the development of resistant organisms and is considered to be an important contributing factor. Imprudent use of antimicrobials can lead to resistance causing increased morbidity and mortality, and decreased efficacy in the treatment of disease. There are limited data regarding prescribing practices of veterinarians and the role these may play in the development of resistant organisms. It is important to be able to compare actual antimicrobial prescribing practices with empirical prescribing practices. We hypothesize that empirical use of antimicrobial drugs by veterinarians is strongly correlated to actual use. To address this question, we designed a survey to assess empirical antimicrobial drug use by veterinarians given a set of scenarios specific to bovine, equine, or canine practice. We asked licensed veterinarians to provide demographic information and to select one of three species with which they work most often. Three common disease scenarios are presented for each species and practitioners choose an antimicrobial drug or combination of drugs to treat each case. We also collect information about the duration of treatment, route of administration, and the proportion of cases that fail to respond to initial treatment. We will analyze these data to quantify empirical antimicrobial drug use to later compare to actual use data in order to confirm or deny a direct correlation between the two. We expect to find a strong correlation between empirical antimicrobial drug prescribing factors with actual drug use by veterinarians. This will allow us to characterize and quantify antimicrobial prescribing factors which will eventually aid in the development of prudent antimicrobial use guidelines.

The Dengue Virus NS5 RNA Capping Enzyme is Activated by Redox Conditions

Rebekah C. Gullberg, Jia J. Long, Brian J. Geiss

Flaviviruses are single-stranded positive sense RNA viruses which replicate on the ER membrane. The environmental conditions required and their roles in regulating viral replication within the host cell are not fully understood. The NS5 flavivirus protein adds a 5' type 1 RNA cap to the viral genome to prevent its degradation by host exonucleases. A critical step in the addition of a cap structure to viral RNA is the transfer of a GMP moiety from the viral NS5 enzyme to the RNA. Prior to this transfer, the enzyme forms a covalent enzyme-GMP intermediate. We sought to test the effects of an oxidizing environment on the formation of the covalent enzyme-GMP intermediate with the dengue capping enzyme. This was measured by the addition of a fluorescently labeled GTP-680 to the capping enzyme. We observed that the fluorescent signal was augmented with increasing concentrations of H2O2 and diamide indicating increased formation of the enzyme-GMP intermediate in an oxidizing environment. We further observed the formation of NS5 dimers with increased guanylation activity compared to the monomer form in the presence of strong oxidizers. Di-sulfide bonds are readily formed in oxidizing environments and could contribute to dimer formation, thus we hypothesize that di-sulfide bonding is a critical component of activating the capping enzyme to form the enzyme-GMP intermediate. Furthermore, the redox balance may act as an environmental switch driving positive strand synthesis.

Functinal Genomics of Hybrid Vigor

Theodore M. Gurol, Lucas Argueso, Aline Rodriguez, Fabiana Duval

Hybrid vigor (heterosis) is defined by the improved function of any biological quality in a hybrid offspring. It's been noted by Shull that "the more numerous the differences between the uniting gametes… the greater on the whole is the amount of stimulation [of physiological vigor]". However, the genetic basis for the observed increase in vigor has been continuously debated. According to the dominance hypothesis, superiority of hybrids is due to the suppression of undesirable recessive alleles from one parent by the dominant alleles from the other, indicating that inbred strains perform poorly due to the loss of beneficial alleles. However, the overdominance hypothesis attributes the increase in vigor to combinations of alleles that are especially advantageous when paired in heterozygous individuals, a hypothesis that is not restricted to hybrid lineages and can explain the persistence of alleles that are harmful when homozygous. In this proposal, we describe the use of the yeast Saccharomyces cerevisiae as a model to investigate the effects of heterozygosity on fitness using strain JAY270, a industrial bioethanol producing yeast with a highly heterozygous genome (Argueso et al 2009). We plan to investigate the effects of heterosis by systematically selecting for Loss of Heterozygosity (LOH) mutants. In previous yeast studies larger tracts of homozygosity correlated with decreased growth rates and reduced fitness (Abbey et al 2011). However, LOH has also been characterized as a driving force in evolution and adaptation through the sudden appearance of previously masked recessive phenotypes caused by mutation on only one chromosome arm (Rosenberg 2011). We have developed a counter-selectable cassette with a regulatable promoter that can be inserted anywhere in the known genome. Through the systematic creation of a LOH strain library, we will create a community resource for the collaborative investigation of the complex mechanisms involved in hybrid vigor.

Effectiveness of monosodium alpha-luminol (Galavit or GVT) as an adjunctive medication in the treatment of chronic superficial keratitis

Angela D. Gwynn, Tomo Wiggans, Juliet Gionfriddo

Purpose: Chronic superficial keratitis (CSK) is a progressive, immune-mediated, inflammatory disease of the canine cornea. If left untreated, loss of vision generally results. Presently there is no cure for CSK and the mainstay pharmaceutical therapies are topical steroids and cyclosporine. Alpha-luminol (GVT) has anti-inflammatory and immunomodulatory effects. The hypothesis in this study is that alpha-luminol as an adjunct to standard therapy will be more effective than standard therapy alone at controlling CSK. Materials/methods: Twelve dogs with newly diagnosed or uncontrolled CSK were enrolled in the year-long study. Dogs were examined at enrollment (week 0) and at 2, 4, 12, 26, and 52 weeks. Exams include a complete ocular exam and digital image capture of both eyes. In addition to standard therapy, each patient received a drop of GVT in one eye and a placebo drop in the other. Neither the client nor investigator was aware of which eye received which treatment. Pigmentation and neovascularization were analyzed using a combination of Photoshop and ImageJ. Angiogenesis was scored using previously established techniques. Results: 5 dogs have completed the study and 7 dogs are still enrolled. No dog has had any ocular deleterious effects from the GVT. There have been no clinically important changes in intraocular pressures or Schirmer tear test results between control and treated eyes or from baseline values. Empirical results suggest improvement in the degree of inflammation in one eye more than the other but because the study is double-blinded no conclusions can yet be made as to the benefits of adding alpha-luminol to the standard therapy compared to standard therapy alone. Conclusion: This study builds upon past clinical research which has investigated using alpha-luminol to treat inflammatory ocular diseases. Here we have established a framework for gaining conclusive evidence on the efficacy of alpha-luminol as an adjunctive medication.

Prenatal androgenization and its effects on the placenta

Jennifer Halleran, Ellie Cleys, Juliano Da Silveira, Quinton Winger, Jason Bruemmer, Gerrit Bouma

Environmental factors have been hypothesized to play a role in fetal programming, a phenomenon where the fetus responds to environmental changes by altering tissue growth and differentiation. These alterations ultimately can affect postnatal development and health. Understanding how environmental factors affect fetal development is important not only for livestock, but human reproductive health as well. Prenatal androgenization in pregnant ewes is a well characterized model to study fetal programming and adult reproductive function, allowing parallels to human diseases such as intrauterine fetal growth restriction, preeclampsia, and polycystic ovaries syndrome. In this study, we tested the hypothesis that sex steroid receptors, androgen (AR) and estrogen receptors (ESR1 and ESR2) play a critical role in placental development and function. We used two groups of sheep, one group acting as our control and one group receiving biweekly testosterone injections starting at gestational day 30 until day 90. Blood samples were collected throughout gestation and blood and tissue samples were collected on day 90. Western blots, immunohistochemistry, and real time PCR analysis was performed on placentomes collected on gestational day 90 from treated and control ewes. AR was present in caruncles and cotyeldons according to western blot analysis. Furthermore, ESR1 and ESR2 levels both were significantly ($P<0.05$) increased in cotyledons collected from treated ewes compared to controls. Real time PCR data indicates a significant ($P<0.05$) increase in levels of ESR1 and ESR2 in caruncles compared to cotyledons collected from control ewes. This data reveals a role for sex steroid signaling in placental development and function.

Characterization of immunity against Mycobacterium tuberculosis in C3Heb/FeJ and C3H HeOuJ mice

Marcela Henao-Tamayo, Andres Obregon, Elizabeth Creissen, Ian M. Orme, Diane J. Ordway

The global epidemic caused by the bacterial pathogen Mycobacterium tuberculosis continues unabated. The available animal models which mimic the pulmonary pathology in human tuberculosis are limited. In this study, we evaluated immune reponses and pathology in mice exposed to a low dose aerosol of the W-Beijing family Mycobacterium tuberculosis strain in C3Heb/FeJ and C3H HeOuJ mice. Both C3Heb/FeJ and C3H HeOuJ mice resulted in a progressive M. tuberculosis infection. However tracking the T cells cells in these different strains of mice demonstrated clearly that these mice utilized different immunity in reponse to infection with M. tuberculosis. In addition, the immunity induced by these two different mouse models impacted the pulmonary pathology formed.

Genetic Analysis of a Quarantined Yellowstone National Park Bison Herd

Julia A. Herman, Antoinette J. Piaggio, Jack C. Ryan, Natalie D. Halbert, Mo D. Salman

As part of the Bison Quarantine Feasibility Study (BQFS) implemented by the Interagency Bison Management Plan (IBMP), 89 bison (Bison bison) from Yellowstone National Park (YNP) were quarantined and tested to qualify as free of brucellosis. These animals will be reintroduced to areas of their historic range as satellite herds of YNP bison for conservation purposes. It is important to understand the genetic diversity of the herd and to determine if any genetic characteristics such as cattle DNA introgression or low genetic diversity may threaten the protected status of this herd. We evaluated genetic diversity at 42 microsatellite loci representing each of the nuclear chromosomes in the bison genome. We found no detectable evidence of cattle DNA introgression in this herd through nuclear markers and mitochondrial DNA analysis. Parentage analysis of the BQFS herd indicated that the majority of mature adults were actively breeding and contributing offspring to the herd. Genetic diversity levels in the quarantined herd were high and comparable to the parent herd, suggesting a low risk of inbreeding in the near future. Based on these analyses, the genetic diversity currently available within the BQFS herd will provide a strong foundation for bison satellite herds and for the preservation of the species.

Characterizing the Dose Fields of the Radionuclide Cu-64-ATSM in Canines using PET

Hetrick L, Kraft S, Kato T, McMillan D, Petefish K, Arceneaux B, Stewart J, Johnson T, Zhang D

The radionuclide Cu-64-ATSM has been shown to have the capability to identify and treat hypoxic tumor regions, which have strong radiation resistance and typically cause tumor recurrence after radiotherapy. As an effective PET imaging agent to locate the hypoxic tumor regions, the Cu-64-ATSM radionuclide can help improve the radiotherapy treatment plan by optimizing a larger dose delivery to the dose resistant regions. There have been studies with Cu-64-ATSM on various small-sized animals (rodents). In this pioneering study with medium-sized animals (canines), imaging and radiation dosimetry data will be collected and evaluated to prepare the Cu-64-ATSM radionuclide for use in human clinical trials. Four canine patients will be recruited in this study for a PET scan with Cu-64-ATSM. The internal dosimetry will be characterized by the studying the effective active decay of the radionuclide. The external dose will be measured using a collection of electronic personal dosimeters set up in a grid around the patient. These results will be simulated and cross referenced with the software OLINDA and compared to validate the results. Currently, the project is only in the simulation stage but some preliminary results have been calculated for the internal dosimetry for Cu-64-ATSM. Using a phantom similar to the mass of an medium sized canine (15kg), it was found that when the radionuclide resided in the kidneys, that the absorbed dose was approximately 0.102 mSv/MBq. In a similar experiment done with a single baboon (25kg) in 1999, it was recorded that the baboon experienced an absorbed dose in the kidneys of 0.337 mSv/MBq. The difference in the dose absorbed by the kidneys in the simulation and the experiment could be attributed to the fact that a higher activity of Cu-64-ATSM was injected to the baboon thus exposing the baboon's kidneys to more radiation. Over the next few months, more simulations will be run and compared to the data collected from the actual patients.

Mitigation of Prion Pathogenicity by Heat Shock Protein 72 in Vitro

Clare E. Hoover, Michael J. Oglesbee, Mark D. Zabel (co-advisor), Edward A. Hoover (co-advisor)

Purpose: Prions are the causative agents of transmissible spongiform encephalopathies, including chronic wasting disease, scrapie, and human Creutzfeld Jakob disease. These fatal diseases are caused by the conversion of the native prion protein, PrPc, to a misfolded, protease-resistant form, PrPsc. The major inducible member of the 70 kDa heat shock protein family (hsp72) is a molecular chaperone that functions during cellular stress to maintain correct protein conformations. Hsp72 overexpression has been shown to protect against the pathologic effects of some neurodegenerative diseases, including spinocerebellar ataxia and Alzheimer's disease, however its role in prion diseases is unknown.
Methods: Murine neuroblastoma cells stably transfected with an hsp72 expression plasmid to constitutively express hsp72 (N2a-HSP) and their vector transfected controls (N2a-V) were exposed to either mouse-adapted scrapie (RML) brain homogenate or normal FVB mouse strain brain homogenate.
Results: After RML prion exposure, the N2a-V cells exhibited a reduced growth rate compared with the RML-exposed N2a-HSP cells and the normal FVB brain-exposed cells. In addition, the RML-exposed N2a-V cells displayed a cytopathic effect characterized by cytomegaly, cytoplasmic vacuolation, and increased cell death when compared with N2a-HSP RML-exposed cells and the normal FVB brain-exposed controls.
Conclusion: These results suggest that hsp72 expression mitigates the pathologic effects of prion infection in neuroblastoma cells. We are currently extending these observations in vivo by studying RML inoculation in hsp72 transgenic C57BL/6 mice engineered to constitutively express the chaperone protein in neurons.

Regulation of zinc finger protein mRNA stability in induced pluripotent stem cells

Aimee L. Jalkanen, Ashley T. Neff, Ju Youn Lee, Bin Tian, Jeffrey Wilusz, Carol J. Wilusz

Purpose: Messenger RNA decay is an important determinant of mRNA abundance, particularly for genes that exhibit rapid changes in expression in response to cellular signals. A global analysis of mRNA decay rates in human induced pluripotent stem (iPS) cells and genetically matched human foreskin fibroblast (HFF) cells revealed that a large group of mRNAs encoding C2H2 zinc finger proteins (ZNFs) are stabilized in iPS cells. In addition, it has been reported previously that numerous C2H2 ZNF mRNAs have unusually short poly(A) tails in stem cells. As the C2H2 ZNF protein family represents a large group of transcription factors with important roles in development, differentiation and tumor suppression, understanding their regulation in stem cells is vital. Our long term goal is to identify the mechanism by which ZNF mRNA decay is regulated in stem cells and fully differentiated fibroblasts. We hypothesize that this regulation may be achieved through differential regulation of poly(A) tail length in the two cell types. Materials/methods: Poly(A)+ and poly(A)- mRNAs from iPS and HFF cells were separated using oligo(dT)25 magnetic beads. Quantitative reverse transcription PCR was performed to assess abundance of ZNF mRNAs and control transcripts in the poly(A)+, and poly(A)- fractions and also in the input samples. Results: Preliminary results suggest that a larger proportion of ZNF mRNA is polyadenylated in iPS cells than in HFFs. As the poly(A) tail generally has a stabilizing influence this is consistent with these transcripts being more stable in iPS cells. Additionally, ZNF280B, which is destabilized in iPS cells appears to be polyadenylated to a similar extent in both cell types. Conclusions: Poly(A) tail length may have a key role in determining mRNA decay rates in C2H2 zinc finger proteins. We are currently investigating the sequence elements that confer differential regulation of ZNF mRNA stability in stem cells through experimental and bioinformatic approaches.

Evaluation of Immunogenicity of Prion Vaccine Administered Together with Vaccine Enhancing Agent

Valerie Johnson, Steve Dow, Mark Zabel

Transmissible spongiform encephalopathy (TSE) is a neurodegenerative disorder characterized by pathologic accumulation of a misfolded form of a normal cellular protein in neurons. Emergence of TSEs in wildlife populations and the ability of some TSEs to cross species barriers have prompted concern regarding the lack of treatment options or prevention strategies. Efforts at vaccine development have been hampered by the difficulty of overcoming self-tolerance. Studies in our lab have demonstrated that vaccine induced immunity is often diminished due to the recruitment of anti-inflammatory myeloid cells. We hypothesized that utilizing an effective antigen while simultaneously inhibiting monocyte migration could elicit a more effective anti-prion response . The vaccine was formulated using a peptide fragment of the human prion protein (PrP106-126). This peptide spontaneously forms fibrillar aggregates and is thought to mediate the conversion from the normal cellular prion protein (PrPC) to the pathogenic form (PrPSC). To enhance vaccine efficacy, a monocyte migration inhibitor was administered (RS102895). Wild type mice were divided into three groups consisting of a control group, a vaccine group and a group receiving the vaccine plus RS102895. Antibody responses were assessed using ELISA and Western Blot. Vaccinated mice treated with RS102895 exhibited significantly increased vaccine titers when compared to vaccinated mice that did not receive this compound. This group also exhibited increased concentrations of antibodies against both PrP 106-126 and PrPC. This vaccination regime shows great promise in eliciting an immune response, thus overcoming self-tolerance. Our results suggest that this strategy could overcome the limitations that have thus far prevented successful development of a prion vaccine.

IGF2 mRNA Binding Protein 1 Drives Growth, Metastasis and Chemoresistance in Osteosarcoma

Brian T. Kalet, Liza E. O'Donoghue, Dawn L. Duval

Osteosarcoma (OSA) is the most common bone tumor in children. Patients with metastasis at diagnosis display only a 20% survival rate. The availability of OSA samples for study is extremely limited; however, over 10,000 canine patients spontaneously develop OSA annually and canine tumors share common histological features, genetic mutations and gene expression profiles with human OSA. We assessed the gene expression signatures of normal bone and groups of primary canine OSA tumors surgically resected from dogs with short and long disease free intervals (DFI) following standard treatment of amputation and therapy with doxorubicin or platinum-based drugs and identified IGF2 mRNA binding protein 1 (IGF2BP1) as a gene with elevated expression in osteosarcomas from patients with a DFI300 group and normal bone. IGF2BP1 is an oncofetal protein that binds multiple mRNA targets to regulate their nuclear transport, stability, translation and subcellular localization. In 5 human OSA cell lines we measured an average 14-fold increase in IGF2BP1 mRNA transcripts compared to normal human osteoblasts. Next, we measured elevated mRNA transcripts and protein levels in the MG63.2 cell line, a metastatic variant of the MG63 human OSA cell line. IGF2BP1 knockdown in shRNA-expressing MG63.2 clones reduced cell invasion. In addition, IGF2BP1 knockdown in MG63.2 cells resulted in a 3-fold decrease in cellular proliferation compared to cells stably expressing a non-targeted shRNA construct. A similar experiment was performed in vivo using a subcutaneous model in nude mice where the IGF2BP1 knockdown tumors from 2 independent shRNA constructs displayed delayed tumor appearance and reduced tumor volume compared to control at days following tumor cell inoculation. Finally, IGF2BP1 knockdown resulted in a two-fold increase in doxorubicin sensitivity in MG63.2 cells. Overall, these data suggest IGF2BP1 drives OSA growth, metastasis and chemotherapeutic resistance.

Immunophenotypic Characterization of Canine CD8 T cell Lymphoproliferative Disorders

Elena Kaplan, Janna Yoshimoto, Teckla Webb, Anne Avery

Canine T cell lymphoproliferative disorders are immunophenotypically diverse diseases with a variety of clinical signs and outcomes. Previous research by this laboratory established that a presenting lymphocyte count of >30,000 lymphocytes/uL is associated with significantly decreased mean survival time in CD8+ T cell lymphoma/leukemia, although there was significant heterogeneity within the good and poor prognosis groups. We hypothesize that clinically relevant subsets of CD8 T cell neoplasia can be identified based on expression patterns of cytokines and surface antigens, which may also be useful therapeutic targets. In a retrospective analysis of 804 dogs presenting with CD8+ lymphocytosis, we identified a unique subset of CD8 lymphoproliferative disorder characterized by loss of the pan-leukocyte phosphatase CD45. In addition, 122 out of 134 (91%) of samples in this subset also express the CD21 complement receptor on CD5+ T cells. Dogs within the CD45-loss subset presented with significantly lower lymphocyte counts compared with cases that retain CD45 ($p=0.0116$), and 62 out of 91 (68%) show counts below 30,000 cells/uL. Breed predisposition analysis showed that 41% (52 out of 128) dogs within the CD45-loss subset were identified as Golden Retrievers. Further molecular characterization of the CD45-loss subset revealed a significant increase in CD25 expression ($p <0.0001$), suggesting the possibility of elevated Il-2 levels that could serve as a potential target for cyclosporine therapy. While levels of serum IL-2 were not significantly higher in the CD45-loss subset, we also assessed Il-2 production by mitogen-stimulated lymphocytes and RNA message levels by gene expression profiling in order to obtain a more complete expression profile of this potential therapy target. Finally, our assays also allowed the evaluation of expression levels of several other cytokines that further characterize this subset of T cell neoplasia and provide potential prognostic markers.

The role of CCDC3 in canine osteosarcoma cell proliferation, clonogenicity, and chemotherapeutic resistance

Dorna S. Khamsi, Dawn L. Duval

Osteosarcoma (OSA) is the most common bone cancer in dogs, occurring frequently in giant and large breeds with nearly all patients eventually succumbing to metastatic disease. We previously found Coiled-Coil Domain Containing 3 (CCDC3) to be significantly downregulated in tumors from patients with a disease free interval (DFI) of less than 100 days versus greater than 300 days. Other research has found CCDC3 may be involved in mesenchymal cell metabolism and differentiation, and down-regulation of CCDC3 has been associated with ifosfamide resistance. We hypothesize CCDC3 down-regulation contributes to the metastasis and/or chemotherapeutic resistance in OSA. To further elucidate this role, we have thus far investigated cell proliferation, clonogenicity, and chemotherapeutic resistance in canine OSA cell lines with CCDC3 over-expression.
Two CCDC3 shRNA knockdown constructs and a mammalian expression construct expressing V5-tagged human CCDC3 were made and transfected into Abrams cells. Significant gene knockdown was confirmed by qRT-PCR in several clonal cell populations and pooled selectants. Overexpression in clonal cell populations was confirmed by western blot analysis and immunocytochemistry. Immunocytochemical staining of the V5-tagged protein also localized CCDC3 to the cytoplasm. In cell proliferation assays, two CCDC3 over-expressing clones grew significantly faster than the control. Clonogenicity assays showed one of the highly proliferative clones to also have a consistent relative increase in clonogenicity. In drug sensitivity assays, the same clone showed significant sensitivity to doxorubicin. Findings from this research will lead to a better understanding of the role of CCDC3 in the progression of canine OSA and has the potential to improve prognostication as well as aid in treatment strategy development.

Instrumentation and Technique for Improved Implantation of Osteochondral Grafts

Brenda L. Kick, Ferris M. Pfeiffer, Aaron M. Stoker, James L. Cook

Purpose: Currently osteochondral allografts (OCA) are used to treat osteochondral dissecans and focal lesions of osteoarthritis. Cylindrical grafts require significant force to seat in the patient which can negatively impact cell viability and long term graft stability. Our goal is to compare the insertion force and extraction strength of cylindrical verses tapered OCAs ex vivo. Further, the effect of graft seating on immediate (1 hour) and short term (3 day) chondrocyte viability will be evaluated. We hypothesize tapered OCAs will require significantly less insertion force and energy and will have significantly higher cell viability compared to current cylindrical OCAs.
Methods: All procedures were approved by the ACUC and performed on canine cadavers euthanatized for reasons unrelated to this study. Five cylindrical and tapered grafts created from femoral condyles were measured for the insertion force and energy required to seat the graft and the extraction strength of the graft after implantation using an Instron. Cylindrical and tapered grafts from humeral heads and femoral condyles were surgically implanted ex vivo and tested for cell viability at day 0 and 3 after implantation. Cell viability was tested using fluorescent microscopy with sytox blue (dead cell stain) and calcein AM (live cell stain) stains.
Results: As theorized tapered grafts require significantly less insertion energy for seating compared to cylindrical grafts. The taper and cylinder OCAs had average insertion energies of 0.03J and 0.14J respectively, $p<0.5$. Further, the extraction strength of the tapered OCA (13.44N) was not significantly lower than the cylindrical OCA (13.85N), $p=0.88$. There was not a significant difference in the time 0 cell viability between the two graft systems; the day 3 cell viability data is currently being evaluated.
Conclusion: Our data leads us to believe tapered grafts improve cell viability due to the decreased insertion force required to seat the graft.

Optimization of Electroretinogram Parametric Amplitudes through Monochromatic Filter Combination Challenge in the Normal Dichromatic New Zealand White Rabbits

Pamela P. Ko, Robert Sun, Ricardo A.P. de Carvalho

Purpose: To characterize the optimal settings of full-field electroretinogram (ERG) based on the background/filter stimulus color combinations on a dichromatic species. To further characterize the normal ERG A, B waves and photopic negative response (PhNR) amplitudes in normal New Zealand White (NZW) rabbits.
Materials/Method: Six female NZW rabbits aged between 15 weeks to 6 months and weighing at least 2.5 kg were dark-adapted for 30 minutes prior to LKC™ ERG recordings. ERG was performed after anesthetizing with an intramuscular injection of ketamine/xylazine (50mg/mL,10 mg/mL). Animals were dark-adapted for another 10 minutes under a fixed blue background paired with each filter stimulus(green, red, white, yellow) at 0.6-13.6 cd-s/m2 flash intensity range. Each combination was repeated in triplicate in 10 days apart. Optimal settings were considered as background/stimulus combinations which yielded the most discernible and reproducible responses. Statistical analysis included correlation and goodness-to-fit (R^2) was applied. Results: Blue background with green stimulus produced the most consistent, reliable and optimal B wave and PhNR amplitudes, 133 and 40 mcV at 13.6 and 2.44 cd-s/m2 flash intensities respectively. Optimal A wave amplitude of 115 mcV was achieved with white stimulus at 13.6 cd-s/m2. The PhNR amplitudes declined as flash intensity increased from 4.1 to 13.6 cd-s/m2 with green and yellow stimuli. PhNR reached its peak amplitude at 0.378 cd-s/m2 and declined afterwards with white stimulus. Red stimulus produced the lowest PhNR amplitudes.
Conclusions: The most appropriate filter combination for evaluating B wave and PhNR amplitudes was blue background with green stimulus. Optimal A wave amplitudes were achieved with white stimulus. The blue and green color-coded rod and cone photoreceptors, retinal ganglion cells and protanopic character in the dichromatic rabbit appear to provide the physiological bases of these results.

Development of a New Transgenic Line of Mice for Evaluating Ovine GnRH Receptor Expression in vivo

Jennifer E. Kouri, Christianne Magee, Jeremy D. Cantlon, Colin M. Clay

Estrogen (E2) regulation of the Gonadotropin Releasing Hormone Receptor (GnRHR) is observed in women and most domestic species. When 9100 bases of proximal promoter of the ovine GnRHR gene are fused to luciferase (-9100oGnRHR-Luc), E2 regulation of the GnRHR promoter is not observed in transient transfection of immortalized murine pituitary gonadotrope cell lines, but expression is observed in specific tissues of transgenic mice carrying the -9100oGnRHR-Luc transgene. In primary cultures of sheep pituitary cells, the cyclic AMP response element (CRE) of the -9100 promoter appears essential for oGnRHR regulation. In order to assess the contribution of CRE to oGnRHR expression in vivo, the CRE binding domain in the -9100 promoter was mutated and used to create a new line of transgenic animals. Following pronuclear injection of the -9100uCREoGnRHR-Luc plasmid (UC Denver, Transgenic Core), 3 males (A-C) and 1 female (D) expressing the transgene in an FVB background were identified. Animals were bred to wild-type FVB mice, and males A-C produced transgenic litters. Offspring were assessed for luciferase expression in pituitary, brain, gonad, liver, kidney, lung, heart, and spleen. Absolute light units (ALU) were normalized to protein (ALU/mg) in each sample. F-tests of each line (A-C), by sex, for each of the tissues were performed to evaluate ALU/mg as Luc expression in positive vs. negative animals. Luc expression was significantly higher in pituitary, brain, and gonad of positive as compared to non-transgenic animals ($P<0.05$). These results are consistent with the -9100oGnRHR-Luc phenotype and confirm tissue-specific activity of the mutated promoter. Using ovariectomized transgenic females treated with a GnRHR antagonist, the contribution of the CRE binding domain to oGnRHR regulation can now be elucidated in the context of E2, other estrogen receptor (ER) agonists/antagonists, as well as a pituitary-specific ERa knockout.

Demonstration and Analysis of a Safe, Novel, Human-baited Tent Trap for the Collection of Anthropophagic Culex and Anopheles Disease Vectors

Benjamin J. Krajacich, Jeremiah R. Slade, Timothy Burton, Wojciech Nowak, Jonathan Seaman, Massamba Sylla, Brian D. Foy

Purpose: Currently, there exists a deficit of safe, active trapping methods for the collection of human host-seeking mosquitoes and other disease-causing arthropod vectors. The “gold standard” approach for mosquito collection is the “Human Landing Catch (HLC)”, in which an individual exposes bare skin to possibly infected vectors. Previous collection designs that protect the individual have had considerable difficulty in replicating the success and efficiency of the HLC technique, and utilize older, less versatile materials. Here, we present the initial results of a novel human-baited vector collection method utilizing modern camping tent construction design and materials coupled with a volatile-distributing, active-trapping apparatus. Materials/methods: The trapping tent was designed and engineered at Infoscitex, Corp. using computational fluid dynamics data, and input from CSU scientists on features needed to properly and efficiently capture host-seeking vectors. This design was validated in CSU insectaries against multiple anthropophagic vectors using HLC vs. tent sampling bioassays. After redesign, the tent was subsequently deployed in the Kedougou region of southeastern Senegal to demonstrate “real-world” field efficacy compared to HLC and to other trapping alternatives.
Results: In the laboratory, the tent caught significantly fewer mosquitoes than HLC. However, in the field it caught significantly more human host-seeking mosquitoes than the CDC Light Trap with Bed net and equivalent to the HLC. It had high efficiency at sampling Culex and Anopheles populations, with high mosquito quality. Finally, there was a significant reduction in the amount of effort necessary for sampling and a marked increase in safety. Conclusions: In the field, the tent caught disease-transmitting mosquitoes as or more efficiently than the alternative techniques, its low labor and high degree of safety enhance its usefulness in sampling anthropophagic vectors.

Oral, Subcutaneous and Intravenous Pharmacokinetics of Ondansetron in Healthy Cats

Renee C. Lake, Ryan J. Hansen, Dan L. Gustafson, Jessica M. Quimby

Purpose: Ondansetron is a 5-HT3 receptor antagonist that is an effective anti-emetic in cats. It is used in the treatment of nausea and vomiting associated with chemotherapy and chronic illness such as chronic kidney disease. However, pharmacokinetic studies in cats have not previously been performed. The purpose of this study was to evaluate the pharmacokinetics of ondansetron in healthy cats.
Materials and Methods: Six healthy cats with unremarkable complete blood count, serum biochemistry and urinalyses were utilized. Jugular catheters were placed under ketamine/butorphanol sedation 12 hours prior to sampling. Each cat received 2 mg oral (mean 0.43 mg/kg), subcutaneous (mean 0.4 mg/kg) and intravenous (mean 0.4 mg/kg) ondansetron in a cross-over manner with a 5 day wash out period. Serum samples were obtained prior to, and at 0.25, 0.5, 1, 2, 4, 8, 12, 18, and 24 hours after administration of ondansetron. Ondansetron concentrations were measured using liquid chromatography coupled to tandem mass spectrometry. Non-compartmental pharmacokinetic modeling was performed. Repeated measures ANOVA was used to compare parameters between administration routes. Parameters that are significantly different ($p < 0.05$) are denoted with (IV vs. PO - 1;IV vs. SQ - 2;PO vs. SQ - 3). Results: Bioavailability of ondansetron was 32% for oral administration and 75% for subcutaneous administration. Half-life of ondansetron was 1.84 ± 0.58 hr (intravenous), 1.18 ± 0.27 hr (oral) and 3.17 ± 0.53 hr (subcutaneous)(significance: 2,3). Tmax of ondansetron was 0.83 ± 0.26 hr (oral) and 0.38 ± 0.14 hr (subcutaneous)(significance: 1,3). Cmax of ondansetron was 447 ± 426 ng/ml (intravenous), 87 ± 54 ng/ml (oral) and 98 ± 48 ng/ml (subcutaneous).
Conclusions: Subcutaneous administration of ondansetron to healthy cats is more bioavailable and has a longer half-life than oral administration. This information may be helpful for management of patients with chronic disease.

Examining the role of Dengue Virus NS4B as a potential suppressor of RNAi in Aedes aegypti

Chris Larson, Brian Foy, Alexander Franz, Kenneth Olson

Arbovirus-vector interactions are modulated by the mosquito's RNAi response. Triggered by dsRNA, an intermediate of +ssRNA virus replication, the exogenous RNAi pathway works to combat viral replication via Dcr-2 and Ago2 activity. Dengue virus (DENV) infections of Aedes aegypti are minimally pathogenic and persistent in the mosquito vector. Although, RNAi is induced during dengue virus (DENV) infection the continued ability of the virus to replicate suggests that a viral suppressor of RNAi (VSR) exists. Of the seven DENV non-structural proteins, NS4B is a strong VSR candidate due to its association with dsRNA and its role in viral RNA synthesis. This work aims to elucidate the potential role of DENV NS4B as a VSR by comparing the RNAi responses in Aedes aegypti to that of B2 (FHV) a known and well characterized VSR. In order to determine whether NS4B alters RNAi in the mosquito vector a ds SINV ATS construct was generated using TE/3'2J as a viral expression vector. TE/3'2J, TE/3'2J-NS4B (DENV), and TE/3'2J-B2 (FHV) were intrathoracically injected into Aedes aegypti (HWE 4-11 post emergence) at a target dose of 5x103 PFU/mL n= 20. Five days post injection saliva was extracted and mosquito bodies were pooled into groups of ten for plaque assays. Three experimental replicates yielded similar titers ~8 log10 PFU/mL in mosquito bodies. However, titers of saliva extracts interestingly showed a similarity between TE/3'2J-NS4B (DENV) and TE/3'2J-B2 (FHV) a PFU/mL ~3 logs, zero plaques were observed in all three replicates with TE3'/2J. This observation could potentially be due to enhanced midgut escape, which would increase the extrinsic incubation period of the virus or possible suppression of RNAi.

Detection of pulmonary vascular micro-hemorrhages in PECAM-1 deficient FVB/n mice using hemosiderin-positive macrophages and deposition of fibrin.

Marta Lishnevsky, Lena C. Young, Steven J. Woods, Todd A. Bass, Alan R. Schenkel

Platelet Endothelial Cell Adhesion Molecule 1 (PECAM-1) deficient mice in the FVB/n strain exhibit fatal chronic pulmonary fibrotic disease. The illness occurs in the absence of a detectable proinflammatory event. PECAM-1 is important for controlling vascular permeability, leukocyte extravasation, clotting of platelets, and clearance of apoptotic cells. We show here that the spontaneous disease development in PECAM-1 deficient FVB/n mice is characterized by loss of vascular integrity in pulmonary and alveolar capillaries, resulting in spontaneous microbleeds. Building on our previous findings, and looking into the early events and contribution of PECAM-1 to the integrity of the vascular barrier function, we observed hemosiderin-positive macrophages in tissue and bronchoalveolar lavage (BAL) fluid in relatively healthy animals. The presence of hemosiderin-positive alveolar and interstitial macrophage populations in the tissue and bronchoalveolar lavage (BAL) fluid is a useful diagnostic method for the detection and quantification of microbleeds. Using this method, we observed a gradually increasing presence of hemosiderin-positive macrophages and fibrin deposition in the advanced stages of disease, corresponding to the accumulation of collagen and smooth muscle actin (SMA)-positive myofibroblasts. Together with the growing evidence that pulmonary microbleeds and coagulation play a role in human fibrotic diseases, this data further supports our hypothesis that PECAM-1 expression is critical to the regulation of vascular barrier function and maintenance of normal coagulation events in the pulmonary environment.

Risk Factors Associated with Colic in Horses Undergoing Elective Procedures Under General Anesthesia

Elizabeth E. Lordan, Brad B. Nelson, Diana M. Hassel

Purpose: To identify risk factors associated with post-operative development of colic following elective procedures requiring general anesthesia in horses.
Methods: Medical records were collected from horses undergoing general anesthesia from January 1, 2008 to December 31, 2010. Horses less than six months of age and those not hospitalized for at least 24 hours following general anesthesia were excluded. Signalment, physical exam, complete blood count, medications, details of anesthesia and the surgical procedure performed as well as post anesthetic parameters including fecal output or visible signs of colic were collected. Univariable screening was performed with logistic regression using a limit of a $p < 0.25$. Through backward elimination, the final multivariate model was created. Statistical significance was set at $p < 0.05$.
Results: Colic or decreased fecal output was reported in 37 out of 416 (8.9%) horses undergoing general anesthesia in the study period. In the final multivariable model, horse breed ($p=0.03$), peripheral blood lactate ($p=0.02$), recumbency during general anesthesia ($p=0.04$), rectal temperature collected post-anesthesia ($p=0.03$), and hours to first passage of manure ($p=0.007$) were statistically significant between horses that had colic compared to those that did not. Arabians were more likely to colic compared with other horse breeds (4/13, 31%). Horses that had colic on average passed their first pile of manure later than those that did not (7.3+/-0.82 hrs and 5.5+/-0.2 hrs, respectively). As blood lactate increased, the odds of colic also increased (OR:1.4).
Conclusions: This study demonstrated the prevalence of colic in horses undergoing elective general anesthetic procedures in our hospital population. Arabian horses, lateral recumbency, increasing blood lactate, decreased rectal temperature post-operatively and a delayed passage of manure was significantly associated with an increased risk of colic.

Genomic instability and telomere fusion of canine osteosarcoma cells

Junko Maeda, Charles R. Yurkon, Hiroshi Fujisawa, Masami Kaneko, Stefan C. Genet, Erica J. Roybal, Garrett W. Rota, Ethan R. Saffer, Barbara J. Rose, William H. Hanneman, Douglas H. Thamm, Takamitsu A. Kato

Canine osteosarcoma (OSA) is known to present with highly variable and chaotic karyotypes, including hypodiploidy, hyperdiploidy, and increased numbers of metacentric chromosomes. The spectrum of genomic instabilities in canine OSA has significantly augmented the difficulty in clearly defining the biological and clinical significance of the observed cytogenetic abnormalities. In this study, eight canine OSA cell lines were used to investigate telomere fusions by fluorescence in situ hybridization (FISH) using a peptide nucleotide acid probe. We characterized each cell line by classical cytogenetic studies and cellular phenotypes including telomere associated factors and then evaluated correlations from this data. All eight canine OSA cell lines displayed increased abnormal metacentric chromosomes and exhibited numerous telomere fusions and interstitial telomeric signals. Also, as evidence of unstable telomeres, colocalization of γ-H2AX and telomere signals in interphase cells was observed. Each cell line was characterized by a combination of data representing cellular doubling time, DNA content, chromosome number, metacentric chromosome frequency, telomere signal level, cellular radiosensitivity, and DNA-PKcs protein expression level. We have also studied primary cultures from 10 spontaneous canine OSAs. Based on the observation of telomere aberrations in those primary cell cultures, we are reasonably certain that our observations in cell lines are not an artifact of prolonged culture. A correlation between telomere fusions and the other characteristics analyzed in our study could not be identified. However, it is important to note that all of the canine OSA samples exhibiting telomere fusion utilized in our study were telomerase positive. Pending further research regarding telomerase negative canine OSA cell lines, our findings may suggest telomere fusions can potentially serve as a novel marker for canine OSA.

Does tensile strain induce cellular proliferation in cultured mitral valves?

Derek Matthews, Carla Lacerda E. Christopher Orton.

Degenerative mitral valve disease is an important cause of heart failure and death in dogs and humans. The disease shows remarkable pathologic similarity in both species, including deposition of glycosaminoglycan, net catabolism of the fibular ECM, and increased cellular density. The specific mechanism for increased cellular density is unknown. Mitral valve leaflets cultured under cyclic strain initiate molecular processes that mimic myxomatous mitral valve disease. Specifically, locally-synthesized serotonin mediates cyclic strain-induced phenotype transformation, matrix degeneration, and glycosaminoglycan synthesis in cultured sheep mitral valves. Studies have also shown that increased tensile strain results in local serotonin production by mitral valves and that can be inhibited pharmacologically. We hypothesize that high tensile strain on valve leaflets induces proliferation of valve interstitial cells through a serotonin dependent mechanism. This study addressed the following questions: 1) Does cyclic tensile strain induce local cellular proliferation? 2) Does blocking serotonin signaling result in decreased cellular proliferation? Cultured sheep mitral leaflets were subjected to 0, 10, and 20% cyclic strain for 72 h in the presence of Bromodeoxy-uridine (BrDU). Immunohistochemistry and flow cytometry methods were used to detect incorporation of BrDU and quantify new cells (BrDU positive). Preliminary data show cell proliferation to occur in leaflets grown in culture medium supplemented with serum in the presence and absence of serotonin inhibition. These findings further implicate tensile loading in mitral degeneration, functionally link the pathogeneses of serotoninergic (carcinoid, drug-induced) and degenerative mitral valve disease, and have therapeutic implications.

Prion Strain Adaptation: Breaking and Building Species Barriers

Crystal Meyerett Reid, Mark D. Zabel

Purpose: Chronic Wasting disease (CWD) is one of many prion-mediated diseases known as transmissible spongiform encephalopathies (TSEs). There is ever-increasing biological and biochemical evidence that prion pathogenesis is caused by the conversion of the normal host protein (PrPC) into an abnormal disease causing conformation (PrPRES). How prions encipher heritable strain properties without nucleic acid remains unclear. We hypothesized that mice co-expressing both mouse and cervid PrPC would have a delayed onset of clinical disease upon prion inoculation due to the interference of heterologous substrate with PrPC conversion to PrPRES. Materials and Methods: We further assessed strain differences by generating a mouse that co-expressed mouse and cervid prion protein. Through intracranial inoculation of various mouse and cervid adapted prion strains, we assessed which of the competing normal host cellular prion proteins would allow conversation of the infectious prion strain. Results: Our findings show that normal cervid prion protein is more promiscuous than mouse prion protein and therefore, is more easily converted into an infectious, protease resistant prion. While mouse PrPC-expressing mice were only susceptible to mouse-adapted prions, cervid PrPC-expressing mice were susceptible to both mouse and cervid prions. Mice co-expressing mouse and cervid PrPC were susceptible to both mouse and cervid prions, similarly to mice expressing only cervid PrPC. Conclusion: We conclude that prion strain adaptation and evolution is highly dependent upon host factors and host encoded PrPC primary sequence. These data suggest that cervid prion protein is more promiscuous and easily converted than mouse prion protein, and animals expressing cervid PrPC may be more susceptible to a wider range of prion strains. Therefore, cervid prion protein is less efficient at building species barriers, and more efficient at breaking them.

NF-kB Activation in the Hippocampus During Multiple Sub-threshold Exposures to Seizuregenic Compounds

James A. Miller, Kelly A. Kirkley, Yogendra H. Raol, Manisha Patel, Russell A. Bialecki, Ronald B. Tjalkens

Drug-induced seizures have been documented for broad classes of pharmaceuticals including CNS and Non-CNS targeted drugs. A better understanding of the early molecular signaling events involved in promoting seizures is necessary to identify potential proconvulsive liability of new pharmacologic agents earlier in the development process. The NF-kB pathway is involved in regulating a number of stress genes and its activation may conceivably be an early indicator of potential seizure liability. Presently, we employed a NF-kB-dependent GFP reporter mouse to investigate the role of NF-kB signaling in rendering hippocampal neurons hyper-excitable. Utilizing EEG recordings and video documentation we established a sub-threshold dose level of the seizurogenic compound kainic acid (KA). Transgenic reporter mice were exposed to multiple sub-threshold doses of KA and regional and cell specific NF-kB activity was assessed after each dose. Under control levels reporter expression was absent in the hippocampus except for a slight basal expression in the CA3 pyramidal layer. Upon multiple exposures to KA, a pronounced expression of the GFP reporter was observed in the stratum moleculare, dentate gyrus molecular layer and in the dentate hilus. Additionally we exposed reporter mice to multiple low levels of a different seizurogenic compond, pentylenetetrazole (PTZ). After multiple doses of PTZ, a global increase in GFP expression was observed. Comparison of the two compounds suggests a regionally selective expression consistent with the distinct mechanisms of action for each compound. Utilizing cultured slices from the reporter mice we observed similar selective GFP expression in response to the two compounds demonstrating the potential utility of this method for the assessment of proconvulsive properties of new pharmacologic compounds.

Coxiella burnetii in Northern Fur Seals and Steller Sea Lions of Alaska

Cody Minor, Gilbert J. Kersh, Tom Gelatt, Ashley V. Kondas, Kristy Pabilonia, Christina Weller, Bobette R. Dickerson, Colleen Duncan

Coxiella burnetii (C. burnetii), a zoonotic bacterium, has recently been identified in several marine mammal species on the Pacific Coast of North America, but little is known about the epidemiology, transmission, and pathogenesis in these species. To address this knowledge gap, we tested sera archived from northern fur seals (NFS, Callorhinus ursinus; n=236) and Steller sea lions (SSL, Eumatopias jubatus; n=72) sampled in Alaska for presence of C. burnetii antibodies, and vaginal swabs from NFS (n=40) for C. burnetii by qPCR. The seroprevalence of NFS samples from 1994 was 49%, while the prevalence in samples from 2009 and 2011 was 69%, and this difference was significant. The seroprevalence of SSL samples from 2007-2011 was 59%. All NFS vaginal swabs were negative for C. burnetii, despite an 80% seroprevalence of the matched sera. The significant increase in seroprevalence in NFS from 1994 to 2011 suggests that the pathogen may be increasingly common, or that there is marked temporal variation, within the vulnerable NFS population. The high seroprevalence in SSL suggests that this pathogen may also be significant in the endangered SSL population. These results confirm that C. burnetii is more prevalent within these populations than previously known; more research is needed to determine how this bacterium may affect individual, population, and reproductive health of marine mammals.

This research was supported by funding from Merial and the USDA, NIFA Animal Health and Disease Program.

Dysregulation of host mRNA stability by flaviviruses: implications for pathogenesis

Stephanie L. Moon, Shelton S. Bradrick, John R. Anderson, Carol J. Wilusz, Alexander A. Khromykh, Jeffrey Wilusz

Purpose: Members of the Flaviviridae—including Dengue virus (DV), West Nile virus (WNV), and Hepatitis C virus (HCV)—are of major public health concern worldwide. In order to maintain a productive infection, we hypothesize that these viruses specifically inactivate the host RNA decay machinery through the production of highly structured RNAs during infection. The goal of these studies was to determine if flaviviruses manipulate host gene expression by sequestration and or inactivation of host nucleases including Xrn1, Dicer, and Argonaute 2 (Ago2). Materials/Methods: Changes in host cell gene expression were assessed in tissue culture cells infected with HCV, WNV or DV. Transcript abundances, mRNA half-lives, levels of uncapped mRNAs (to indicate a block in the 5'-3' RNA decay pathway) and the efficacy of the host RNA interference response during infection were analyzed using a variety of molecular assays. Results: The accumulation of a highly structured non-coding RNA (sfRNA) produced in all arthropod-borne flavivirus infections directly correlated with changes in host mRNA stability. This sfRNA was shown to sequester the 5' exonuclease Xrn1. The Xrn1-mediated 5'-3' decay pathway was also found to be dysregulated in HCV infected cells. Finally, the sequestration of Dicer and Ago2 by sfRNA was associated with dysregulation of the host RNA interference response. Conclusions: Manipulation of host mRNA stability appears to be a conserved mechanism by which flaviviruses promote the stability of viral transcripts. Furthermore, the dramatic stabilization of cellular mRNAs during viral infection may represent a highly significant but to date underappreciated aspect of viral pathogenesis as mRNAs that encode many regulators of innate and acquired immunity are regulated via their mRNA stability. Future studies will assess the role of dysregulated mRNA stability in the onset hepatocellular carcinoma in HCV infections as well as immunopathogenesis in DV and WNV infections.

Differential regulation of mRNA stability in human induced pluripotent stem cells

Ashley Neff, Ju Youn Lee, Bin Tian, Jeffrey Wilusz, Carol Wilusz

Purpose: Induced pluripotent stem cells are able to proliferate indefinitely while maintaining the capacity to differentiate into other cell types given the correct stimuli. These properties reflect a unique gene expression program. We are interested in characterizing mRNA decay in these cells in order to better understand how they differ from differentiated cell types. We also hope to find ways to increase reprogramming efficiency and fidelity for future medical applications.
Materials/Methods: Using microarray-based global analyses of mRNA decay rates, we recently identified three classes of mRNAs whose stability is differentially regulated in human induced pluripotent stem cells compared to the fully differentiated fibroblasts (HFFs) they were derived from.
Results: We find that replication-dependent histone mRNAs are more abundant and more stable in iPS cells. C2H2-type ZNF mRNAs are also stabilized, possibly through reduced expression of miRNAs targeting their ORFs. Finally, mRNAs containing C-rich elements in their 3'UTR are significantly destabilized in iPS cells. Interestingly, we also identified two members of the poly(C)-binding protein family, PCBP3 and PCBP4 that exhibit differential expression and may be responsible for regulating C-rich element containing transcripts.
Conclusions: We are now examining how these novel pathways contribute to achievement and/or maintenance of pluripotency.

In Vitro Comparison of V-Loc™ vs Biosyn™ in a One-Layer End-to-End Anastomosis of Equine Jejunum

Brad B. Nelson and Diana M. Hassel

Purpose: To compare a unidirectional barbed suture (V-Loc™) to its suture material equivalent (Biosyn™) in a single-layer end-to-end anastomosis of equine jejunum.
Methods: Jejunal sections from adult horses (n = 5) without gastrointestinal disease were collected. Jejunal end-to-end anastomoses (n = 9) were performed for each group (V-Loc™, Biosyn™) with a continuous Lembert pattern with an interruption every 120º. Anastomosis construction time, luminal diameter, and number of suture bites were recorded as a mean +/- SEM. Anastomosis constructs were distended with fluid at 1L/min until failure. Location and intraluminal pressure at failure were recorded and all measurements were compared between groups with a student's paired t-test and significance was set at $P<0.05$.
Results: V-Loc™ anastomoses were significantly faster to perform (13.1±0.35 minutes) when compared to the Biosyn™ group (15.6±0.72 minutes; P =.0004). No differences were observed for anastomotic index or number of suture bites. V-Loc™ anastomosis construct had a significantly decreased bursting pressure (160±11.6 mmHg) compared to Biosyn™ constructs (184 ±16.9 mmHg; P=.01).
Conclusions: V-Loc™ allowed faster construction time and did not cause a decreased anastomosis luminal diameter when compared with Biosyn™. V-Loc™ had a decreased bursting strength compared with Biosyn™, albeit well above pathologic pressures encountered clinically. Use of V-Loc™ may be beneficial for decreasing the amount of exposed suture material because of the absence of knots after construction and has the potential to result in decreased adhesions.

Use of a cationic contrast agent predicts glycosaminoglycan content in equine femoropatellar joint cartilage in horses undergoind contrast enhancing computed tomography

Brad B. Nelson, Rachel C. Stewart, Mark W. Grinstaff, Brian Snyder, Alejandro Valdés-Martínez, Natasha M. Werpy and Laurie R. Goodrich

Purpose: To use previously developed contrast enhanced computed tomography (CECT) methods to compare cationic (Ca4+) and anionic (HexabrixTM) contrast agent uptake within equine femoropatellar joint articular cartilage. With loss of GAG content an early hallmark of osteoarthritis, a further aim is to develop correlations between CECT and glycosaminoglycan (GAG) content in cartilage.
Methods: A 2 year-old horse was humanely euthanized for reasons unrelated to joint disease. Each femoropatellar joint was injected with a contrast agent (Ca4+ or HexabrixTM). A CECT scan was performed of both joints. Seven mm cartilage plugs were harvested (n=36) from multiple joint surfaces and analyzed with microCT. The cartilage was removed from subchondral bone and GAG content quantified with a 1,9-dimethylmethylene blue colorimetric assay. The microCT and CECT scan attenuation were correlated with GAG content. Univariate linear regression was performed to express CT attenuation as a function of GAG content and ANCOVA to compare regression parameters. Statistical significance was set at $P<0.05$.
Results: The cationic contrast material had more consistent uptake within the articular cartilage compared to HexabrixTM on the CECT scans. The Ca4+ microCT attenuation effectively predicted the GAG content present in the cartilage with attenuation increasing proportionally with GAG content ($R2 = 0.79$). Similarly, the findings of the HexabrixTM samples were also correlative, but to a lesser degree ($R2 = 0.42$). The microCT and CECT scans were compared and demonstrated a weak correlation ($R2 = 0.20$-0.24). Conclusions: Increasing Ca4+ CECT attenuations are well correlated with increasing GAG content. The disparity between CECT and microCT is likely due to the improved resolution with the latter method. Clinical application of this technique appears promising. Horses that have early osteoarthritis may be more effectively identified and treated at an earlier stage in the disease process.

Validation of a novel radiographic method for tibial plateau angle measurement in large and giant breed dogs

Adam Nylund, Kurtis M. Hazenfield, Alex Valdes-Martinez, Lynn Griffin, Clara Goh, Chris Mackay, Colleen Duncan, Ross Palmer, Felix Duerr

Purpose: Accurate tibial plateau angle (TPA) measurement is crucial for proper TPLO execution. Centering the x-ray beam over the stifle and collimation to include the tarsus results in the most accurate TPA measurement. Tibial length in large and giant breed dogs prevents inclusion of both the stifle and tarsus in a stifle-centered radiograph. Contemporary digital imaging software permits 'stitching', or combining two separate radiographs, a stifle-centered and a tarsus-centered, into a single image analogous to a properly centered and collimated image. We hypothesized that the novel image 'stitching' technique would result in more accurate TPA measurements when compared to the traditional method in large and giant breed dogs.
Materials/Methods: Three medio-lateral radiographic projections were obtained from 34 paired pelvic limbs. Each of eight observers performed image stitching and traditional (tTPA) and stitched (sTPA) measurements. Anatomic TPA (aTPA) was measured as previously described. The mean measured TPA angle for tTPA and sTPA was compared between all eight observers using ANOVA. TPA angles from all dogs measured using the tTPA and sTPA technique were compared to the aTPA using ANOVA.
Results: There was no statistically significant difference between observers for tTPA and sTPA measurements. No significant difference was observed in the mean TPA between the tTPA, sTPA, and aTPA.
Conclusion: This novel method produced radiographic TPA measurements consistent with the aTPA. However, no difference was shown between this technique and a tibia-centered view. Regardless, this novel digital imaging technique provides an alternative method for measuring TPA without the need for the traditional TPLO view. This may be useful in large and giant breed dogs because of their size, or in patients where visualization of the tibial plateau is difficult due to severe osteoarthritis or angular limb deformities.

Ultrasound guided transversus abdominus plane block in routine ovariectomies in dogs

Amber M. R. Orr, Sandra I. Allweiler, Gregg M. Griffenhagen.

Purpose: Transversus abdominus plane (TAP) block has been used in human medicine for a number of years but has yet to be evaluated as a pain management option in veterinary patients. Local anesthetics have been used extensively in limb and spinal analgesia in veterinary patients to great success. Extending this technique to the abdomen would be a useful tool for both specialty and general practice veterinarians. We hypothesized the TAP block would decrease the intra-operative and post-operative analgesic requirements of canine patients undergoing routine ovariectomies.
Materials/Methods: 24 dogs were pre-medicated with morphine, atropine and acepromazine SQ. Dogs were induced with propofol IV. TAP block was performed with ultrasound guidance in the fascial plane between the transversus abdominus and internal oblique muscles. 0.75ml/kg of either 0.375% bupivacaine (high dose), 0.25% bupivacaine (low dose), or physiologic saline (control) was injected. Inhalant isofluorane was then reduced to 1.5% and surgery was performed. Any dog that had an increase in heart rate, blood pressure or respiratory rate of greater than 20% over baseline received a rescue dose of fentanyl IV. Dogs received carprofen at the end of the procedure. Post-operatively dogs were evaluated using the short form of the Glasgow pain scale at 15 minutes, 60 minutes and 4 hours post extubation. If at any point a dog received a total score greater than 8 or greater than 1 in any single category they received a dose of morphine SQ.
Results: Number of doses of rescue analgesia was not found to be significantly different between the three groups. Glasgow pain scores were not found to be significantly different between the three groups.
Conclusions: While these results do not support the use of this technique in ovariectomies it does suggest that this is a safe procedure that can be considered for other procedures more invasive within the skin and musculature of the abdominal wall.

Equine Mesenchymal Stem Cell Characteristics; differences in sternum and ilium

Karla G. Penman, Jennifer N. Phillips, John D. Kisiday, Audrey Ruple, C. Wayne McIlwraith, Laurie R. Goodrich

Purpose: Osteoarthritis is a major cause for loss of athleticism and chronic pain in horses. Equine mesenchymal stem cells (MSCs) have been a primary focus for tissue regeneration. The two sites of marrow aspiration in the horse are the sternum and ilium, each offering a rich supply of MSCs that have similar growth rates in vitro. The next question is if MSCs from either site differ in cell characteristics. These qualities are MSCs tri-lineage potential (adipogenic, osteogenic and chondrogenic), cell surface markers and gene transduction efficiencies. We hypothesized that MSCs acquired from sternum and ilium in horses will have a similar in vitro characteristics.
Methods: Bone marrow was aspirated from the sternum in 8 horses. Cells were cultured and passaged three times and treated with appropriate differentiation media for tri-lineage evaluation. Flow cytometry was conducted on cells looking for CD11/18a, CD34, CD44, CD90 and MHC1 cell surface markers. Viral gene transduction efficiencies were calculated using a green fluorescent protein.
Results: Differentiation assays yielded MSCs with desired morphologic changes, confirming tri-lineage differentiation (lipid deposition, GAG halos and blocky osteogenic appearance). Chondrogenic and osteogenic propensity were not found to be significantly different between the two aspirate locations for alkaline phosphatase, GAG or qPCR of osteogenic gene markers. Cell surface markers were not significantly different between the two groups. Gene transduction efficiencies were also not statistically significant difference between aspiration location.
Discussion: There was no significant difference between the aspiration location on MSCs differentiation capacity in vitro, expression of cell surface markers, osteogenic gene expression, or gene transduction efficiencies. Thus, clinicians can collect bone marrow from either sternum or ilium and either should have similar regenerative capabilities.

In vitro differentiation of canine mesenchymal stem cells into cells with functional hepatocyte-like properties

Michelina Petri, MS, BS, David Twedt DVM, Allison Bradley, DVM, MS, Pei-Yi Tai, Tracy Webb DVM, PhD, Steven Dow DVM, PhD

Mesenchymal stem cells (MSC) can be derived from adipose or bone marrow tissues. Recent studies suggest that the MSC can be differentiated into functional hepatocytes using the right combination of growth factors in vitro. Given the large unmet need for new approaches to treat chronic hepatic disease and failure in dogs, we have investigated the ability of canine MSC to be differentiated into cells with hepatocyte-like properties, with the goal of using these cells to help regenerate functional hepatic tissue in vivo. We hypothesized that canine MSC cultured in the presence of EGF, FGF, HGF, and dexamethasone will assume hepatocyte-like properties in vitro. Canine MSC were derived from adipose biopsies obtained from healthy young dogs. Early canine MSC cultures were grown in the presence of a cocktail of growth factors including 5-azacytidine, epidermal growth factor (EGF), fibroblast growth factor (FGF), hepatocyte growth factor (HGF), and dexamethasone, demonstrated to promote hepatocyte lineage development in rodent and human stem cells. Hepatocyte differentiation was assessed using NH3 production, alkaline phosphatase release, periodic acid-Schiff (PAS) stain, and low density lipoprotein uptake. In addition, the ability of labeled MSC to reach the liver following intra-splenic injection was assessed in anesthetized research dogs. We found that culturing in a cocktail of EGF, FGF, HGF, and dexamethasone promoted to acquisition of PAS staining. Intrasplenic injection of a low number of MSC resulted in efficient uptake in the liver. We concluded that culture of canine MSC in a cocktail of growth factors promoted the development of cells with hepatocyte-like properties. These preliminary findings, therefore, suggest that it may be possible to use short-term culture to generate hepatocyte “educated” MSC for intrasplenic injection and liver seeding in clinical patients with advanced liver disease.

Increased severity of tuberculosis in a guinea pig model of type 2 diabetes

Brendan K. Podell, David F. Ackart, Andres Obregon-Henao, Sarah P. Eck, Marcela Henao-Tamayo, Elizabeth Creissen, Jes Kuruvilla, Kristie Capson, Michael Richardson, Ian M. Orme, Diane Ordway, Randall J. Basaraba

Diabetes is an established but poorly understood risk factor for tuberculosis (TB). Since 80% of the global diabetic population resides in countries where TB is endemic and 95% of diabetics have type 2 diabetes, a relevant model of TB-diabetes comorbidity is needed. Consistent with human type 2 diabetes progression, we have developed a guinea pig model to mimic the increased susceptibility of human type 2 diabetics to Mycobacterium tuberculosis (Mtb) infection. Guinea pigs were fed either a normal diet (non-diabetic) or a high fat, high sugar diet for 8 weeks to induce insulin resistance (pre-diabetic) as confirmed by decreased glucose tolerance. Type 2 diabetes was induced in a subset of insulin resistant guinea pigs with a single dose of streptozotocin yielding sublethal pancreatic beta cell cytotoxicity. Type 2 diabetics, confirmed by exacerbated glucose intolerance, remained hyperglycemic for 3 weeks prior to infection with the H37Rv strain of Mtb. Progression of TB was measured by stereologic histopathology, tissue bacterial culture, and cytokine gene expression by qRT-PCR. Diabetic guinea pigs were highly susceptible to Mtb resulting in 67% mortality before day 30 of infection compared to non-diabetic guinea pigs ($p<0.001$). Pulmonary pathology was more severe in diabetic guinea pigs (29.3% vs. 10.8% in non-diabetics ($p<0.01$)) with increased granulocyte infiltration. More severe TB disease in diabetic animals was accompanied by higher bacterial burden with 1.5 to 2 Log10-CFU/ml increases in lung, spleen, lymph node and liver ($p<0.001$). Diabetic guinea pigs infected with Mtb had 8.8-fold higher IL-17 ($p<0.05$), 7.5-fold higher IFN gamma ($p<0.001$), and 17.2-fold higher IL-10 ($p<0.01$) transcript levels. Despite an elevation in IFN gamma, type 2 diabetics display marked susceptibility to TB and unrestricted bacterial growth where heightened pathology may be due to increased IL-17 production and an inability to limit infection due to early onset of IL-10 production.

Evaluation of coliphage dynamics in bighorn sheep, domestic sheep and cattle: implications for bacteriophage therapeutics

Sheridan Potter, Claudia Gentry-Weeks, Michael W. Miller

Mannheimia haemolytica is a significant bacterial pathogen of the respiratory disease complex contributing to population declines of bighorn sheep, and costing the beef industry a billion dollars annually. As both antibiotics and traditional vaccination attempts have been largely unsuccessful, novel bacteriophages for treatment and prevention are being developed in our laboratory. Phages are ideal agents given their ability to self-propagate, although little data are available regarding their population dynamics in mammals, and none for bighorn sheep. Therefore, this study was conducted to assess the ecology of "natural" coliphages in domestic sheep, cattle, and bighorn sheep, as well as their respective habitats. Nasal and rectal swabs were collected from domestic sheep and cattle housed at the CSU Agricultural Research Development and Education Center (ARDEC), captive bighorns at the Wildlife Research Center (WRC) of Colorado Parks and Wildlife, and from wild bighorns near Granite, CO. Soil, feed, vegetation, and water samples were also collected from each habitat. Isolation of viable coliphages from these samples was determined by visualization of plaque forming units (PFU) using a host *E. coli* strain in a double agar overlay technique. ARDEC livestock contained a significantly greater abundance and prevalence of coliphages than either WRC or Granite bighorns, correlating strongly with the presence of coliphages in their respective habitats. The majority of environmental coliphages were isolated from hay and vegetation, an unexpected result as most literature documents their presence in water and soil, indicating that delivery of the M. haemolytica therapeutic phages via livestock feed can be a highly efficient method. Additionally, coliphages were present in a milk sample acquired from an ARDEC ewe, demonstrating that maternal transmission of phages to offspring is possible, an aspect critical to treatment as the majority of wild bighorn deaths occur in lambs.

Production of non-ping pong dependent PIWI RNA-like small RNAs in the mosquito midgut in response to West Nile virus infection

Abhishek N. Prasad, Doug E. Brackney, Faye D. Schilkey, Jimmy E. Woodward, Gregory D. Ebel

Purpose: The role of small-interfering RNAs (siRNAs) in response to viral infection in invertebrates has been well-characterized; however, the involvement of other small RNA (sRNA) pathways is poorly understood. Evidence suggests that members of the PIWI family of proteins can also participate in antiviral defense in mosquitoes. In this study, we profiled the anti-West Nile virus (WNV) sRNA response in Culex quinquefasciatus.
Materials/Methods: Two field populations of Cx. quinquefasciatus were infected with WNV. After 14 days, midguts were harvested, and total RNA extracted. Groups of 5 infected midguts were pooled and used as the input for sRNA sequencing libraries. Data was aligned to the WNV genome, and sRNA profiles of the two field-collected groups were compared to existing data we had for our colonized mosquitoes.
Results: As in our colonized mosquitoes, we found a stereotypical siRNA response. However, there was variation in viral genome targeting, intensity, and size classes of sRNAs produced. In particular, 24-30 nt sRNAs consistent in size with products of the piRNA pathway showed significant variation across groups. While exhibiting the expected strand-bias seen in piRNAs, 24-30 nt RNAs in our libraries lacked the expected nt bias seen in piRNAs produced in a ping-pong dependent manner.
Conclusions: Studies with alphaviruses (Togaviridae) in Aedes sp. mosquitoes and cells have described the production of viral-derived piRNA-like sRNAs that exhibit ping-pong amplification. In this study, we characterized 24-30 nt piRNA-like sRNAs produced in response to WNV (Flaviviridae) infection in Cx. quinquefasciatus. Interestingly, while exhibiting a strong bias for (+)-sense orientation, viral-derived piRNA-like RNAs did not exhibit signatures indicative of ping-pong amplification. Studies with dengue virus-infected Ae. aegypti support this observation, suggesting that the piRNA pathway may respond differently to flaviviruses compared to alphaviruses.

Evaluation of an outpatient protocol in the treatment of canine parvoviral gastroenteritis

Karolina Preisner, Lauren Sullivan, Kayla Harding, Tracy Keppel-Kolb, Jennifer Perez, Claire Ortega, Pedro Boscan, David Twedt

Purpose: Canine parvovirus is a highly infectious disease affecting young dogs, with treatment often being cost prohibitive for many owners. Establishment of an outpatient treatment protocol may provide an alternative for dogs that may otherwise die or be euthanized. We hypothesized that dogs with naturally occurring parvoviral gastroenteritis may be successfully managed using an outpatient treatment protocol, as determined by clinical response to therapy and overall outcome, when compared to dogs receiving traditional inpatient treatment.
Materials/Methods: Forty naturally infected dogs with no vaccine history or prior treatment intervention were enrolled following a positive snap ELISA parvoviral test. Dogs were resuscitated with intravenous fluids and then randomized to an inpatient (n=20) or outpatient (n-=20) treatment protocol. Inpatients received intravenous fluids, maropitant (1 mg/kg IV q24h) and cefoxitin (22 mg/kg IV TID). Outpatients received subcutaneous fluids, maropitant (1 mg/kg SQ q24h) and cefovicin (8 mg/kg SQ once). Parameters monitored during treatment included clinical severity scoring, body weight, blood work, hydration status, caloric intake, length of hospitalization and outcome.
Results: Overall outcome and intermediate health measures between treatment groups were similar. No difference in survival rate was observed (18/20 inpatients vs. 16/20 outpatients, p=0.66). There was also no difference in duration of hospitalization, changes in body weight, hydration status, caloric intake, clinical severity scoring, nausea or visceral pain scoring between groups.
Conclusions: A modified outpatient protocol may be a reasonable alternative for dogs whose owners cannot afford hospitalization for treatment of canine parvovirus. Such a protocol should be considered under the appropriate circumstances, but should not be considered a substitute for inpatient care when such care can be provided.

Cellular Localization of PenA ß-lactamase in Burkholderia pseudomallei

Linnell B. Randall, Herbert P. Schweizer

Burkholderia pseudomallei (Bp), a Gram-negative soil bacterium found tropical regions, is the etiologic agent of melioidosis. Bp is intrinsically resistant to many antibiotics, and melioidosis treatment involves prolonged antibiotic therapy. PenA, a chromosomal ß-lactamase in Bp, confers resistance to many ß-lactams. Point mutations in penA leading to PenA amino acid changes can cause resistance to ceftazidime and amoxicillin-clavulanate, which can result in treatment failure. Typically ß-lactamase enzymes are found the periplasm of Gram-negative bacteria. Previous studies have shown that PenA is secreted via the twin arginine translocase system, but failed to demonstrate periplasmic localization. The purpose of this study is to determine the sub-cellular localization of PenA in Bp. By using alkaline phosphatase (AP) as a periplasmic marker we have optimized a method for extracting periplasmic proteins from Bp. Further, by generating mutants expressing PenA or AP with either their native or switched signal sequences and evaluating them through subcellular fractionations, immunoblotting, colorimetric enzyme assays, and ß-lactam susceptibility assays, we are examining the localization of PenA within the cell envelope of Bp. These experiments give us a better physiological understanding of PenA, an important antibiotic resistance mechanism in Bp.

Streptococcus agalactiae Mastitis: a Molecular Approach to Investigating Re-emergence in the Dairy Industry

Amanda Rauhauser and Dr. Ruth Zadoks

A recent rise in the incidence of Streptococcus agalactiae (Group B Streptococci, GBS) mastitis in the dairy industry has prompted investigation into the cause of its re-emergence. This trend has been noted internationally and follows a twenty year period of eradication in some countries. Historically, Streptococcus agalactiae clonal complex 67 (CC67) is indicated as the most bovine-adapted strain and was the target of eradication protocol.

Humans are also reservoirs of this pathogen as it causes severe invasive disease in infants and is subclinically carried in the gastrointestinal and reproductive tracts of adults. Previous research indicates that the populations of human and bovine strains of GBS overlap, which would allow for the possibility of re-emerging strains to be of human origin. If this is the case, significant genetic crossover could lead to dissemination of new strains within both populations and ultimately alter disease patterns.

The primary objective of this study was to investigate the distribution of bovine-origin Streptococcus agalactiae samples in Italy. Specifically, aims were to 1) discover the genetic origin of countrywide re-emergence and 2) compare it to patterns within other European locations such as Denmark, France, and the United Kingdom. Multi-locus sequence typing and eBURST analysis of Streptococcus agalactiae isolates were used to compare genotypes of bacterial isolates from Italy and Denmark. Further comparison would increase understanding of the altered epidemiology of Streptococcus agalactiae mastitis in dairy cattle and may suggest necessary control methods.

To accomplish this, fourteen isolates previously obtained from bulk tank milk samples at individual dairies in Italy were analyzed using multi-locus sequence typing of the seven pre-determined housekeeping alleles. This project is part of a larger, ongoing study of 500+ international Streptococcus agalactiae isolates conducted at the Moredun Research Institute.

Investigation into the role of Aedes aegypti in the transmission of Bartonella clarridgaie and Mycoplasma hemofelis to cats

Krystle L. Reagan, Lorelei Clarke, Michael Lappin

Purpose: Bartonella clarridgeiae (BC) and Mycoplasma haemofelis (Mhf) both have complex transmission cycles with Ctenocephalides felis as a primary vector. However, alternative routes of transmission have not been fully investigated. Our objective was to determine whether Aedes aegypti takes up BC or Mhf in the blood meal and is capable of transmitting the organism amongst cats.
Materials/methods: Four laboratory reared cats were used, with institutional IACUC approval. One cat was infected with either BC or Mhf by IV inoculation. Aedes aegypti (n = 200/cat) were placed in a feeding chamber with each sedated cat for 30 minutes. At that time, 2 fed mosquitoes from each group were collected to be analyzed for mechanical uptake of the bacteria and the remaining fed mosquitoes were housed under insectary conditions for 7 days. The mosquitoes were then allowed to feed on an additional BC naïve cat or a Mhf naïve cat as described. Blood was collected weekly for performance of BC and Mhf PCR assays.
Results: DNA of BC or Mhf was not amplified from the mosquitoes that fed on the infected cats even though the infection level was estimated to be high. The previously naïve kittens were negative for BC or Mhf DNA in 10 weekly samples collected after exposure to the mosquitoes.
Conclusions: These results fail to support the hypothesis that mosquitoes act as a mechanical or biological vector for either pathogen. However, variables such feeding time, number of feeding events, and the species of mosquito species may have influenced the results.

ATM Mouse Strain-Dependent Variations in Sensitivity to Induction of Gamma-H2AX Foci after Continuous Low Dose-Rate Irradiation

Ashley Romero, John R. Brogan, Hatsumi Nagasawa, Justin Bell, Christina Fallgren, T. Wade, Paula C. Genik, John B. Little, Joel S. Bedford, Michael M. Weil, Takamitsu A. Kato

Purpose: A sensitive low dose rate gamma-H2AX assay was developed to distinguish differences from normal ATM (Ataxia Telangiectasia Mutated)+/+(mouse) or ATM +/+(human), and the phenotypes associated with the corresponding heterozygous genotypes as well as distinguishing mild hypersensitivities for cells from a proportion of apparently normal individuals. This assay was used to determine whether the genetic background of four inbred mouse strains showed any differences in radiosensitivity and whether the ATM -/- genotype resulted in a uniformly increased radiosensitivity that might further add to or reduce sensitivity.
Materials and Methods: Fibroblast cultures established from ear clips from three separate mice of each mouse strain and cells in chamber flasks were allowed to grow to a confluent monolayer with isoleucine deficient medium. After 48 hours, in a G0/G1 state, the cultures were irradiated with Cesium-137 gamma-rays at a dose rate of approximately 8.6cGy/h for 24 hours. Cells were then fixed and immunostained to detect gamma-H2AX foci by fluorescence microscope using a Metamorph system to capture images for analysis.
Results: For the C57BL/6J, A/J, and 129S6 mouse strains there was a significant difference between the mean foci per cell for the ATM +/+ vs. ATM -/- genotypes but no significant difference for the two ATM genotypes of the Balb/c strain background. The number of foci per cell from the Balb/c ATM +/+ mice were of the PRKDC defect, a DNA double strand break rejoining deficiency, which was significantly higher than that for cells from the other ATM +/+ strains.
Conclusion: The number of foci per cell from the Balb/c ATM +/+ mice was significantly higher than that from the other ATM +/+ strains. For all other cell strain mutations, ATM knockout increased the average number of foci per cell. Measured foci size has a distinct distribution, possibly showing discrete foci formation patterns based on cell strain mutation and ATM status.

Delivery of interferon-tau into the uterine or jugular vein induces genes hypothesized to protect the corpus luteum from luteolysis

Jared J. Romero, Alfredo Q. Antoniazzi, Hanna L. Baird, Natalia P. Smirnova, Brett T. Webb, John S. Davis, Jose R. Sereno, Thomas R. Hansen

Ovine interferon-tau (IFNT) is secreted from the conceptus by day 12 of pregnancy. IFNT silences the up-regulation of endometrial estrogen receptor alpha, oxytocin receptor and pulsatile release of prostaglandin F2 alpha (PGF). Microarray analysis and RTPCR revealed interferon stimulated gene 15 (ISG15) and myxovirus (influenza virus) resistance 1 (MX1) in the corpus luteum (CL) were up-regulated in response to early pregnancy; and luteinizing hormone receptor (LHR) and pentraxin 3 long (PTX3) were down-regulated in response to luteolysis. Infusion of roIFNT for 3 days into the UV (200 or 20 mcg/day) or into the JV (200 mcg/day), beginning on day 10 of the estrous cycle (EC), followed 24 h later by an injection of the luteolytic agent PGF, blocks the PGF-induced decline in serum progesterone (P4) concentration. Subcutaneous (SQ) delivery of roIFNT was hypothesized to cause luteal resistance to PGF by up-regulation or maintenance of antiluteolyic genes in the CL. Osmotic pumps loaded to deliver 20 mcg/day of roIFNT subcutaneously into the neck or 200 mcg bovine serum albumin (BSA) into the uterine vein (UV); control)/ for 3 days were installed on day 10 of the EC. PGF (4 mg/58 kg) was injected on day 11 of the EC to allow for 24 h pre-exposure to roIFNT or BSA. Serum P4 concentrations were determined twice daily until day 13. In ewes treated with BSA, PGF caused a 70% decline in serum P4 concentrations from days 11-13, which was blocked by 24 h roIFNT pre-treatment. Based on RTPCR roIFNT induced ISG15 and MX1 mRNA in the CL regardless of mode of delivery. PGF caused a decline in concentration of LHR and PTX3 mRNA, which was blocked for LHR by 200 mcg roIFNT/day (JV) and attenuated for LHR and PTX3 by 20 mcg roIFNT/day (SQ and UV). In summary systemic delivery of roIFNT blocks the decline in serum P4 concentrations in response to PGF challenge. IFNT may induce luteal resistance through induction of ISGs and prevention of down-regulation of genes encoding LHR and PTX3.

Plasma exosomes as a diagnostic tool for canine iron deficiency, hemangiosarcoma, and osteosarcoma

Emily D. Rout, Susan E. Lana, Christine S. Olver

Exosomes are 50-100 nm vesicles secreted by mammalian cells. Exosomes in the plasma contain proteins from distant sites, allowing exosome proteins to serve as biomarkers in noninvasive diagnostic tests. Purpose: We performed a preliminary evaluation of using exosomes diagnostically for three canine conditions: hemangiosarcoma (HSA), osteosarcoma (OSA), and iron deficiency (ID). Methods: Cases for the HSA study included dogs with HSA or splenic hematomas, confirmed by histopathology. OSA cases were selected based on a disease free interval (DFI) 300 days, which was defined by the time to metastasis. ID cases included normal dogs and dogs with microcytic anemia. Exosomes were isolated by ultracentrifugation. Exosome protein levels were determined by Western blot and densitometry analysis. Results: First, we investigated CD146, an adhesion molecule present on endothelial cells and canine HSA cell lines, as a biomarker to help distinguish HSA from splenic hematoma. CD146 expression was greater in HSA exosomes compared to exosomes from dogs with splenic hematomas. Second, we investigated Ezrin and IGF2BP1 expression to help determine prognosis in newly diagnosed OSA patients. Differential expression of both of these molecules in primary tumors has shown promise to predict prognosis in previous studies. Ezrin levels did not correlate with the disease free interval. Early studies suggest IGF2BP1 levels may be higher in plasma exosomes from dogs with a shorter DFI. Third, transferrin receptor, a protein involved in iron hemostasis, was evaluated for diagnosis of ID. Preliminary studies suggest that transferrin receptor is elevated in dogs with microcytic anemia and may be useful in differentiating iron deficiency from anemia of chronic disease. Conclusions: These exosome markers may provide a noninvasive method to guide diagnosis of iron deficiency and hemangiosarcoma and prognosis of osteosarcoma.

Therapeutic plasma lidocaine concentrations in horses

Aileen L. Rowland, Lauren K. Luedke, Shaylynn G. Magditch, Eileen Hackett, Luke Wittenburg, Lutz Goehring

Lidocaine-HCl (LDO) is a commonly used prokinetic agent in horses. To have therapeutic effects a plasma concentration between 980 – 1600 ng/mL has to be achieved. As LDO has a short half-life the drug is first administered as an i.v. bolus (1.3mg/kg b.w.), then followed by an intravenous constant rate infusion (CRI) at (0.05mg/kg b.w./ min). In this study we aimed to evaluate how often target concentrations (TC) are met in clinical, usually post-operative, cases following gastro-intestinal tract surgery. Owner's consent was obtained at all times. Plasma samples from a total of 12 horses were collected at constant time points 0, 1, 2, 3 hrs after LDO bolus administration and start of a CRI; then, at 3 randomly selected time points between 12-24 hrs, twice between 24-48hrs, and once every 24 hrs until LDO CRI was discontinued. Plasma samples were stored frozen until analysis. Total LDO concentrations were determined using high-pressure liquid chromatography. Results showed that overall 30 of the 41 samples reached the target range. During the first 24 hours of sampling TC were reached in 16 of 25 samples. In samples collected after 24 hours TC were reached in 14 of the 16 samples. While the first 24 hours post-operatively is the period where benefits of LDO administration are considered most important an effective plasma concentration of LDO was only achieved in 16 of 25 samples. However, 9 'below TC' samples were obtained from 5 horses. These results indicate that further optimization of LDO therapy post-operatively is warranted. More precisely calculated doses based on body weight may need to be re-calculated more frequently, and hydration status has to be more thoroughly assessed.

Meiotic Spindle Configurations in Metaphase II Oocytes from Young and Old Mares

E. Ruggeri , L.J. Maclellan PhD, D.F. Albertini PhD, E.M. Carnevale DVM, PhD

With increasing mare age, embryo collection rates decline, and recovered embryos are often delayed in development and competence. The incidence of aneuploidy has not been determined in old mares, but could represent a cause of age-associated early embryo loss. We hypothesized that alterations in the meiotic spindle and chromosomal alignment occur more frequently in the oocyte of old versus young mares. Oocytes were collected from the dominant follicles of young (4-11 yr, n=7) and old (=20 yr, n=8) estrous mares and fixed at 44 h after administration of a GnRH analog to the donor. Oocytes were stained for DNA (Hoechst 33258) and microtubules (mouse anti a and ß tubulin and goat anti-mouse-alexa488). Confocal images of the oocytes' meiotic spindles were analyzed to determine spindle integrity and alignment of chromosomes. Spindle conformation was considered normal when the following criteria were observed: bipolar organization, microtubules converging at both poles, and chromosomes evenly aligned at the equatorial plate. Atypical meiotic spindle morphology was observed in more oocytes from old versus young mares (7/8 and 0/7, respectively; $P<0.05$, Fisher's Exact Test), with oocytes from old mares having normal chromosomal alignment (n=1), nonaligned chromosomes (n=5), or a disarrangement of the spindle (n=2). Results of our study support that advanced mare age is associated alterations in morphology of the meiotic spindle and an increase in misalignment of chromosomes, which could affect embryo viability and developmental competence.

Risk factors for the development of malignant histiocytosis in Bernese Mountain Dogs

Audrey Ruple-Czerniak, Paul S. Morley

Purpose: Bernese Mountain Dogs are at an increased risk of developing malignant histiocytosis when compared to other breeds. In order to elucidate which exposure variables affect the outcome of malignant histiocytosis in Bernese Mountain Dogs the influence of genetics must be accounted for. The purpose of this study was to examine multiple factors that may be associated with the outcome of malignant histiocytosis while taking the genetic influences into account.
Materials/methods: The study was conducted as a cross-sectional survey. The eligible study population consisted of Bernese Mountain Dogs registered with the Berner-Garde Foundation. Owners who elected to participate were invited to complete an electronic survey. Mixed effects logistic regression and conditional logistic regression were used in parallel to examine associations between potential risk factors (exposure variables) and the occurrence of malignant histiocytosis.
Results: Data were collected for a total of 216 Bernese Mountain Dogs, representing 140 different litters. When controlling for litter of origin (as a surrogate for genetics), dogs diagnosed with orthopedic conditions were 2.5 times more likely to develop malignant histiocytosis. These data also show that dogs receiving long-term medications are at a considerably lower risk of developing malignant histiocytosis than are dogs that do not receive long-term medications. The most common medications reported by owners to have been used long-term for their dogs were anti-inflammatory medications.
Conclusion: The results of this study suggest the use of anti-inflammatory medication may be a modifiable risk factor for development of malignant histiocytosis in Bernese Mountain Dogs. More research in this area is warranted.

A novel role for Bouvardin as an inhibitor of canine tumor cell proliferation

Abbey R. Sadowski, Barbara J. Rose, Douglas H. Thamm.

Drug therapies are constantly evolving to target various aspects of cancer cell proliferation. Bouvardin has recently been identified in a Drosophila screen as an agent that enhances the effect of ionizing radiation. As a protein synthesis inhibitor, Bouvardin has been shown to enhance the effects of chemotherapeutic agents and radiation in human cancer cells and human cancer xenografts in mice. We proposed to evaluate the sensitivity of a panel of canine tumor-derived cell lines to Bouvardin. A panel of more than 20 cell lines were treated with Bouvardin at concentrations ranging from 10 mcM to 0.0625 mcM for 72h. Cell proliferation was quantified after 72h using Alamar blue cell viability assay. Bouvardin dose-dependently inhibited canine tumor cell proliferation. A striking difference in sensitivity was observed between and within cell lines of different cancer types, with 50% inhibitory concentrations ranging from 10 mcM. Examining the gene expression profiles of the individual cell lines may provide insight into the mechanisms behind the sensitivity or resistance to Bouvardin. These results highlight the future potential for Bouvardin to be used as an effective single agent growth inhibitor or in combination drug therapy with other chemotherapeutic agents.

A Similar Role for LIN28 in Placental and Cancer Cells

Analisa Schilling, Gerrit Bouma, Quinton Winger

Placental and cancer cells have similar phenotypes in that they are proliferative, migratory, and invasive. In this study, we explored the possibility that these cell behaviors are regulated by a common genetic network involving LIN28. When overexpressed, pluripotency factor LIN28 leads to lower levels of let-7 miRNA, and possibly is associated with higher levels of migration, proliferation, and invasion in placental and cancer cells specifically. Related to pregnancy, LIN28 overexpression can be linked to trophoblast cell invasion and shedding, leading to preeclampsia and placental insufficiency. Similarly, cancer cells with high levels of LIN28 are more metastatic in nature. Based on this knowledge, we examined relative levels of LIN28A, LIN28B, and the let-7 miRNAs in ACH3P and BeWo trophoblast cell lines, as well as OV420, IGROV1, and SKOV3 human ovarian cancer cell lines using real time PCR and Western Blot assays. We also examined LIN28 and let-7 miRNA content in cell-secreted vesicles (i.e. exosomes) from placental and ovarian cancer cells. MiRNA content in these exosomes appears to correlate with migratory, proliferative, and invasive behavior of the cells. It is speculated that increased intracellular LIN28 expression leads to a lower level of let-7 miRNA in cells and their secreted exosomes. Our hypothesis is that miRNA expression in secreted exosomes may serve as a predictive marker for medical conditions such as preeclampsia and cancer.

Evidence for vertical transmission of chronic wasting disease (CWD)

Anca Selariu, Amy Nalls, Dean Hendrickson, Richard Bowen, Jennifer Barfield, Mark Stetter, Jeannette Hayes Klugg, Kelly Anderson, Kelly Walton, Erin McNulty, Clare Hoover, Amber Mayfield, Monica Brandhuber, Stephenie Fullaway, Candace K. Mathiason

Transmissible spongiform encephalopathies (TSEs) are infectious progressive neurodegenerative diseases that affect several mammalian species, including humans (Creutzfeldt-Jakob disease), cattle (mad cow), sheep (scrapie) and cervids (chronic wasting disease - CWD). TSEs are caused by the accumulation of a misfolded form (PrPRes) of a normal and ubiquitously expressed membrane protein – PrPC. CWD, the only TSE of a native wildlife population, can be easily transmitted horizontally via direct or indirect contact with infectious CWD prions found in bodily fluids, excreta, or environmental contaminants. What remains unknown is the role maternal or vertical transmission plays in the perpetuation of this TSE in nature. Evidence for vertical transmission of infectious prions has been demonstrated directly only in sheep, whose placentas can accumulate large amounts of PrPRes. Our previous studies in a small cervid model, the Reeves muntjac deer, have suggested that infection is likely to occur before birth. Moreover, the rate of stillbirths to CWD positive does is 4x higher than that of naïve does (80% vs 20%). We hypothesize that infectivity is passed to the fetus in utero via multinucleated trophoblasts – a subset of specialized, migratory cells that make up the epithelial layer of the embryonic sac and mediate the exchange of nutrients between mother and fetus. We have designed a trophoblast barrier cell culture model derived from placental cells harvested from transgenic mice expressing the cervid PrP, as well as from our muntjac deer model. This culture system aims to mimic the in vivo feto-maternal interface in order to demonstrate that trophoblasts are responsible for the uptake of PrPCWD and the consequent infection of the fetus. We aim to employ the protein misfolding cyclic amplification (PMCA) assay, a robust in vitro prion amplification technique, as well as immunohistochemistry and immunofluorescence assays to elucidate the mechanism of PrPCWD transfer.

Altered gene expression in equine granulosa cells associated with aging

Dawn R. Sessions-Bresnahan, Elaine M. Carnevale

Maternal aging is associated with a decline in fertility but the exact reasons are unknown. Follicle growth, selection, and ovulation require complex endocrine and paracrine signaling. Ovulation and oocyte maturation is initiated by LH (or hCG) binding to receptors on granulosa cells. The aim of this study was to determine age-related differences in the expression of genes associated with follicle and oocyte maturation in response to ovulation induction. Light-horse mares in a clinical assisted reproductive program were used with owner permission. Mares were divided into three age groups: young (n=12, 4-14 yr), middle-aged (n=9, 15-19 yr), and aged (n=14, 20-27 yr). A GnRH analog (SucroMate™, 0.9-1.4 mg, IM) and hCG (Chorion®, 1500-2000 IU, IV) were administered to mares with a follicle > 32 mm to induce follicle maturation. Between 22 and 24 h later, granulosa cells were collected by ultrasound-guided, transvaginal aspirations. Expression for 32 genes related to follicular maturation and ovulation were examined using qPCR. Genes of interest were normalized to the geometric mean of two housekeeping genes, log-transformed and evaluated using ANOVA. Young mares had greater ($P < 0.05$) expression of TNF when compared to aged mares and TNFAIP6 and MMP2 when compared to middle-aged mares. Aged mares had greater ($P < 0.05$) expression of FSHR, LHCGR, ADIPOR2, IL6 and IL6R than young mares, STAR than middle-aged mares, and IL6ST and INSR than young and middle-aged mares. Middle-aged mares had lower ($P < 0.05$) PLAT expression than both young and aged mares. Young mares had lower ($P < 0.05$) expression of PPARG than both middle-aged and aged mares. Expression of genes associated with inflammation, metabolism, tissue remodeling, and hormone receptors and synthesis were altered by age. These disruptions could alter follicular maturation pathways that could affect the oocyte, possibly contributing to the decline in fertility associated with age.

The Role of Synaptotagmin in Asynchronous Vesicle Release

Mallory Shields, Noreen Reist

Understanding the mechanisms mediating information transmission across a chemical synapse is essential to understanding brain function. During synaptic transmission, membranous vesicles within neurons are loaded with neurotransmitter, docked to the presynaptic cell membrane, primed for release, and fused with the presynaptic membrane to release neurotransmitter onto the next, or postsynaptic, cell. The vesicle membrane and proteins are recycled back into the presynaptic cell to be utilized later. There are three types of neurotransmitter release, one being a Ca2+ dependent, prolonged, asynchronous release, which has recently been proposed to play a role in synaptic plasticity, the basis for learning and memory mechanisms. These release processes are tightly regulated by a number of key synaptic proteins, including Ca2+ sensors and the fusion machinery complex. One such protein, synaptotagmin, is proposed to be the low-affinity Ca2+ sensor that, upon Ca2+ binding, triggers fast, synchronous release of neurotransmitter. In addition, studies have shown interplay between synaptotagmin and a currently unidentified and controversial high-affinity Ca2+ sensor responsible for the prolonged, asynchronous neurotransmitter release mechanism. At this time, it is postulated that synaptotagmin is directly inhibiting this second Ca2+ sensor due to synaptotagmin knockout studies and point mutations preventing Ca2+ binding by synaptotagmin's C2A Ca2+ binding domain. However, what this interplay entails is currently unknown and poorly understood. Using specific point mutations in vivo, the interaction between the C2A domain of synaptotagmin and its role in modulating asynchronous release will be investigated.

Evaluation for associations between Leptospire species antibodies and azotemia in client-owned cats

Shropshire SB, Morris AK, Lappin MR, Veir JK

Purpose: Leptospire spp. are commonly associated with acute renal failure in dogs and have been hypothesized to be a cause of canine chronic kidney disease (CKD). While CKD is common in cats, they have been considered to be resistant to development of leptospirosis. However, recently Leptospire spp. DNA was amplified from 10 of 85 shelter cats showing that cats may harbor the organisms. The purpose of this study was to determine if there are associations between anti-Leptospire spp. antibodies (L-Abs) in cats with or without azotemia.
Materials/Methods: To validate the microscopic agglutination test (MAT) for use in cats, two SPF laboratory cats were vaccinated using a canine leptospiral vaccine on days 0 and 14. Serum collected on days -7, 0 and weekly thereafter for 12 weeks was evaluated for presence of L-Abs (6 serovars) using a commercial MAT. Sera from 71 client-owned azotemic cats and 90 client-owned non-azotemic cats enrolled in a previous study were tested for L-Abs. The prevalence of positive results and mean titers for L-Abs was determined. A chi-square test was used to analyze the data with significance set at $p < 0.05$.
Results: Both SPF cats seroconverted by week nine. In the client owned cats, the prevalence (1/71; 1.4%) and mean titers for Leptospira grippotyphosa were higher in azotemic vs. non-azotemic cats (0/90; 0.0%). In contrast, the prevalence (4/90; 4.4%) and mean titers for Leptospira canicola were higher in non-azotemic versus azotemic cats (0/71; 0.0%). However, the differences did not achieve statistical significance and the prevalence and mean titers for other serovars were similar in both groups of cats.
Conclusions: Though no significant association between L-Abs and azotemia was found in these cats, the presence of other risk factors was not known and not all cats may seroconvert. Thus, further studies using a combination of serology and PCR assay results are needed in order to determine if leptospirosis contributes to feline CKD.

Evaluation of the association between Bartonella species antibodies and azotemia in client-owned cats

Shropshire SB, Morris AK, Veir JK, Lappin MR

Purpose: Chronic kidney disease (CKD) is a common cause of morbidity and mortality in cats that is often due to unknown causes. Bartonella henselae DNA has been amplified from renal tissues from experimentally inoculated cats with concurrent mild lymphocytic interstitial nephritis. The purpose of this study was to determine if there are associations between Bartonella species antibody assay results and azotemia in client-owned cats.
Materials/Methods: Sera from 71 cats with creatinine concentrations > 2 g/dl (azotemia) and 90 cats with creatinine concentrations < 2 g/dl enrolled in a previous study were tested for Bartonella species IgG using a previously reported enzyme-linked immunosorbent assay with a positive cutoff value of = 1:64. The state of origin was used to classify each case as having low flea risk (AK, AZ, CO, ID, MT, NM, NV, UT, WY) or high flea risk (all other states). Associations between proportions of positive Bartonella spp. IgG assay results and azotemia were evaluated using logistic regression with $P > 0.05$ considered significant. The initial logistic model controlled for age and flea risk but age was removed from the model as it was not significant.
Results: Overall, cats from high flea risk states were more likely to be positive for Bartonella spp. IgG than cats from low flea risk states. Prevalence rates for Bartonella species IgG in cats with azotemia (23.5%, SE = 5.4%) or without azotemia (33.7%, SE = 5.8%) were not significantly different ($p = 0.14$) and there were no differences in titer magnitude between groups.
Conclusions: Bartonella spp. IgG antibodies were not associated with azotemia in this sample set. However, Bartonella spp. IgG antibodies do not indicate current infection and high prevalence rates can mask statistical associations. Future studies should also include culture or polymerase chain reaction on blood or renal tissues to further evaluate for associations between current Bartonella spp. infection and feline CKD.

Regulation of Human Trophoblast Cell Differentiation by LIN28A and LIN28B

Erin E. Soisson, JL Seabrook, RV Anthony, QA Winger

MicroRNAs (miRNA) are 19-22 nucleotide strands of RNA that regulate gene expression by degradation of mRNA or inhibition of translation. The let-7 family of miRNAs is involved in regulation of cell differentiation and is detected in trophoblast cells. LIN28 is an RNA binding protein involved in maintaining pluripotency in human stem cells by selectively inhibiting let-7 miRNA biogenesis. As cells differentiate, LIN28 decreases allowing mature let-7 to increase. LIN28A and LIN28B both inhibit mature let-7 processing by distinct mechanisms. In the current study we investigate how LIN28A and LIN28B regulate trophoblast cell differentiation. LIN28A and LIN28B mRNA and protein are both detected in the ACH3P, human early trimester trophoblast cell line. We constructed LIN28A and LIN28B shRNA-knockdowns (KD) ACH3P cells, and a non-target scramble shRNA control. Human chorionic gonadotropin (hCG) is released from trophoblast cells and is a marker for differentiated syncytiotrophoblast. Media hCG levels were determined via ELISA and found to be significantly increased in LIN28A KD but not in LIN28B KD vs. control. Relative mRNA levels for differentiation marker genes; human endogenous retrovirus-1 (ERV-1), placental protein-13 (PP13), and human leukocyte antigen G (HLAG) were all significantly increased in LIN28A KD but not the LIN28B KD cells. The effect of the LIN28 KD on let-7 levels was assessed. Relative levels of let-7a, e, f, and i were significantly increased in LIN28A KD cells and let-7e, f, g, and i miRNA level was significantly increased in LIN28B KD cells compared to controls. Interestingly, two miRNAs expressed in the placenta miR-9 and miR-30 were significantly increased in the LIN28A KD but were not different in the LIN28B KD ACH-3P cells. These data suggest that both LIN28A and LIN28B regulate the level of let-7 in trophoblast cells however; a decrease in LIN28A may be necessary to induce trophoblast differentiation.

Genes relevant to left ventricular hypertrophy are differentially expressed according to dietary fatty acid composition

Spencer K, Jeckel K, Bouma GJ, Hess A, Petrilli E, Frye M

Background/Aims: Obesity increases the risk for cardiomyopathy in the absence of hypertension, diabetes or myocardial ischemia. Not all obese individuals develop heart failure; obesity may provide protection in some populations. The diet-modulated fatty acid milieu may alter myocardial gene expression relevant to structure/function, lending partial explanation for the cardiomyopathic phenotypy in obese individuals. Our aim was to define myocardial gene expression profiles with consumption of a Western diet and subsequent modification with DHA supplementation.
Methods: Adult male Wistar rats (n=10) were assigned to 1 of 3 diets for 3 months: control (CON), Western (WES) and Western supplemented with DHA (WES+DHA). Left ventricular myocardial tissue was subjected to RNA isolation, biotinylated cRNA targets were hybridized to the GeneChip Rat Genome 2.0 probe array. Signal intensity was determined with the GeneChip 3000 scanning system. Six genes with a log2FC>0.9 were chosen for real-time PCR validation based on relevance to hypertrophy, extracellular matrix remodeling and contractile proteins.
Results: Microarrays revealed 66 genes that were differentially present in 1 or more group comparisons ($p<0.001$). There was agreement between relative transcript levels determined by microarray and PCR. Transcript expression patterns and pathway analysis revealed hypertrophy in WES rats compared to CON, and antihypertrophic processes in WES+DHA rats compared to WES. Compared to CON, WES+DHA rats had variable changes in gene expression relevant to hypertrophy and changes favoring modification of contractile proteins.
Conclusions: Dietary fatty acid composition modulates myocardial gene expression in dietary obese rats. Genes favoring myocyte hypertrophy appear to be upregulated in response to WES feeding and may be attenuated with DHA supplementation. Future studies will focus on identifying changes in protein levels consistent with observed changes in gene expression.

Subgenomic Reporter RNA System for Detection of Sindbis Virus Infection in Live Mosquitoes

J. Jordan Steel, Alexander W.E. Franz, Irma Sanchez-Vargas, Ken E. Olson, Brian J. Geiss.

Alphaviruses are mosquito-borne pathogens that can cause severe human disease, several of which are considered potential biological weapons. Defining how alphaviruses infect their mosquito hosts and transmit to mammalian hosts is a critical area of research for understanding how infection may occur, but the tools for monitoring alphavirus infection in mosquitoes has relied largely on alphaviruses engineered to express virus encoded reporter proteins. These drastic modifications to the viral genome, sometimes increasing the genome size by over 10%, have large effects on viral replication and virulence in their hosts. To better visualize how wild type alphaviruses infect, disseminate, and transmit from mosquitoes, we are developing a transgenic mosquito system where reporter constructs encoded within the mosquito's genome is activated only during infection. We have developed a sindbis virus (SINV) mini-genome style expression system that can produce an RNA species in mosquito cells that is recognized and replicated by trans-complemented viral non-structural proteins. This sindbis-based reporter RNA is expressed in cells containing our construct and only upon SINV infection is subgenomic RNA transcribed and a mCherry fluorescent reporter protein produced. The fluorescent reporter protein provides a simple method for visually tracking SINV infection. These results represent the first time a replication-competent RNA genome structure has been launched from DNA in mosquito cells, and opens the way for further work into mosquito DNA-launch systems. Based on our success in vitro, we are in the process of developing transgenic Ae. aegypti mosquitoes that will constitutively express the reporter RNA. The Higgs White-Eye strain of Ae. aegypti were transduced with a Mariner Mos1 transposon containing a Sindbis reporter RNA expressing mCherry from the subgenomic promoter. We have established 7 transgenic families that we are currently analyzing for reporter RNA activity.

Endothelial cell apoptosis following stereotactic radiation therapy in canine soft tissue sarcomas

Katy L. Swancutt, James T. Custis, Susan M. LaRue

While traditional, fractionated radiation therapy has achieved only palliation in certain types of cancer such as osteosarcoma or oligometasteses of liver and lung, the more recent innovation called stereotactic radiation therapy (SRT) has been shown to achieve tumor control above 90% in these "resistant" tumor types. Unlike fractionated radiation therapy, STR is administered in large doses in only one to three fractions under conditions that provide for sharp demarcation between tumor and adjacent normal tissues. Previous research has shown that apoptosis in vascular endothelium is inhibited in mice that are deficient in the enzyme ASMase, which is a critical component of the ceramide-mediated pathway for radiation-induced apoptosis, following exposure to large doses (15-16Gy) in single fractions. Significant endothelial cell apoptosis was observed in both tumor xenografts as well as in normal murine intestinal villi of the wild-type litter mates of the ASMase deficient mice. We hypothesize that tumor control following SRT may be achieved via ceramide-mediated apoptosis of endothelial cells within the radiation field. In this study, eight dogs with soft-tissue sarcomas were treated, half with at a low dose of 3Gy and half with a high single fraction dose of 18Gy. Biopsies taken from each dog's tumor pre- and post-treatment were stained with markers for endothelial cells as well as with a TUNEL stain for apoptotic events. Apoptotic endothelial cells were observed in tumor samples treated with 18Gy to a greater extent than in the tumor samples treated with only 3Gy.

Quantification of Feline Immunodeficiency Virus Proviral Load in FIVpco subtype A infected Puma (Puma concolor) and Bobcat (Lynx rufus)

Sahaja Templin-Hladky, Justin Lee, Ryan Troyer, Sue VandeWoude

Feline immunodeficiency virus (FIV) is a lentivirus that naturally infects domestic and wild feline species. Individual feline species typically carry genetically-distinct species-specific FIV strains. One notable exception includes sympatric populations of puma (Puma concolor) and bobcat (Lynx rufus) in California and Florida, which are both infected with FIV-Puma concolor subtype A (FIVpcoA). In contrast, FIVpco subtype B is found only in pumas. We hypothesize that FIVpcoA may be a bobcat-adapted virus, which has more recently been transmitted to pumas. Host-adapted lentiviruses typically replicate to high viral load in their natural host species. Thus, if FIVpcoA is a bobcat-adapted virus, we expect FIVpcoA viral loads to be higher in bobcats than pumas. In order to test this hypothesis, we developed a quantitative polymerase chain reaction (qPCR) assay to compare FIVpcoA proviral loads in infected bobcats and pumas. This assay targets highly conserved sequences in the FIVpcoA envelope (env) gene and employs FIVpcoA env plasmid standards for proviral quantification and verification of assay efficiency. We compared proviral load for 6 pumas and 18 bobcats using DNA extracted from whole blood. We found that bobcats had significantly higher FIVpcoA proviral loads than pumas ($p = 0.0006$). Furthermore, we found that pumas infected with FIVpcoA had lower proviral loads than pumas infected with FIVpcoB (Blake et al., 2006). These preliminary data support the hypothesis that FIVpcoA evolved to replicate efficiently in bobcats but has lower fitness in pumas. In the future we plan to expand the number of bobcat and puma samples to further investigate this hypothesis.

Neuroprotective efficacy and pharmacokinetics of novel para-phenyl substituted diindolylmethanes in a model of Parkinson's disease

Briana R. Trout, James A. Miller, Ryan J. Hansen, Paul J. Lunghofer, Stephen Safe, Daniel L. Gustafson, Dorothy Colagiovanni, Ronald B. Tjalkens.

Currently, no approved therapeutics exist for use in treating progressive, neurodegenerative disease with a glial-derived inflammatory component. This is partially because distribution to the central nervous system can be difficult to achieve for therapeutic compounds that demonstrate efficacy in vitro. This study examined selected para-phenyl subsitiuted diindolylmethane (C-DIM) compounds, derived from 3-3'-diindolylmethane (DIM), a naturally occurring condensation product of indole-3-carbinol found in cruciferous vegetables. These selected C-DIMs have shown the ability in vitro to decrease glial-based inflammatory cytokines (NOS2). We postulated that pharmacokinetic characterization of the C-DIM compounds would enable us to better determine the efficacy of C-DIMs in a progressive, in vivo murine Parkinson's disease (PD) model. Pharmacokinetics and metabolism of 1,1-bis(3'-indolyl)-1-(p-methoxyphenyl)methane (C-DIM5), 1,1-bis(3'-indolyl)-1-(p-hydroxyphenyl)methane (C-DIM8), and 1,1-bis(3'-indolyl)-1-(p-chlorophenyl)methane (C-DIM12) were determined in plasma and brain of C57Bl/6 mice. Intravenous (1 mg/kg) and oral (10 mg/kg) doses were given to determine the optimal route of administration and putative metabolites were measured in plasma, liver, and urine. Oral dosage of C-DIM compounds displayed greater AUC, Cmax, and Tmax levels than intravenous administration. C-DIM12 exhibited the most favorable pharmacokinetics of the selected C-DIMs, with an oral bioavailability of 42% in comparison of C-DIM8 (6%). Following pharmacokinetic studies, efficacy of C-DIM5, C-DIM8, and C-DIM12 (50 mg/kg, oral) was established using a progressive, neuroinflammatory PD model employing MPTP and probenecid (MPTPp) over a period of 14 days. By first creating a lesion in the region of the brain affected in PD and then treating with anti-inflammatory C-DIMs, we were able to establish that C-DIM5 and C-DIM12 demonstrate the maximum ability of attenuating progressive dopamine neuron loss.

Effects of xylazine on normal and interleukin-1 conditioned equine articular cartilage explants in vitro

Jeffrey J. Ullmer, David D. Frisbie, Khursheed Mama, Christina M. Lee

Purpose: There is continued interest in developing alternate methods of pain control in both horses and humans. The use of intra-articular alpha-2 agonists has been proposed, but their effects on articular cartilage are not known. This study was conducted to determine the effects of xylazine (XY) on normal and recombinant equine interleukin-1b (IL-1b) conditioned articular cartilage. Materials/methods: Articular cartilage was collected from the trochlea and femoral condyles of 4 skeletally mature horses with no concurrent joint disease and sectioned to a wet weight of 60 to 100mg. Explants were stabilized for 48 hours before the start of the experiment and then cultured for 8 days. The treatment groups investigated were: no XY (control), 1%, 2% and 10% XY and each of the previous + 10ng/ml IL-1b. Each explant was exposed to each treatment for 15, 30 and 60 minutes. Total DNA was quantified using Hoechst 33258 dye and the explants were evaluated using calcein and ethidium bromine and a fluorescent microscope to subjectively assess living vs. dead cells. Statistical analysis was conducted to determine the differences in total DNA content accounting for both treatment group and exposure using Proc GLIMMIX. Predictive F-values were used to determine statistical differences between treated and untreated or between time points with specific comparisons made using a least squares mean procedure both with significance set at 0.05. Results: There was a significant difference ($P < 0.05$) in the total DNA content between control and all XY treatments(controls were at least 38% higher than treated); 1% XY differed further from both 2 and 10% XY (20% higher) suggesting an influence of dose on cartilage viability. Conclusions: XY has a dose dependent deleterious effect on normal and IL-1b treated cartilage in-vitro.

Detection of Chronic Wasting Disease Prions in Cerebrospinal Fluid by In Vitro Amplification

Alexandra D. Van de Motter, Nicholas J. Haley, Davis M. Seelig, Candace K. Mathiason, Davin Henderson, Glenn C. Telling, Edward A. Hoover

Purpose: Transmissible spongiform encephalopathies (TSEs), or prion diseases, are a uniformly fatal family of neurodegenerative diseases in mammals that includes chronic wasting disease (CWD) of cervids. The early and ante-mortem identification of TSE-infected individuals using conventional western blotting or immunohistochemistry (IHC) has proven difficult, as the levels of infectious prions in readily obtainable samples (e.g. cerebrospinal fluid, CSF) are typically beyond the limits of detection. This has necessitated the development of assays employing amplification of the abnormal prion protein for detection of low levels of infectious prions.
Materials/methods: In the present study, we evaluated the CSF of CWD-exposed and naïve deer (n=49) for CWD prions using two amplification assays: serial protein misfolding cyclic amplification with PTFE beads (sPMCAb) and real-time quaking induced conversion (RT-QuIC). Samples were evaluated blindly in parallel with appropriate positive and negative controls. Results from amplification assays were compared to one another and to obex IHC, the “gold standard” diagnostic test for CWD, using Spearman correlation. Experimental results were correlated to a number of variables including CWD inoculum source (e.g. saliva, blood), genotype, and duration of clinical signs.
Results: We found that both sPMCA and RT-QuIC were capable of amplifying CWD prions from cervid CSF. Experimental results correlated highly with each other, and ultimately to obex IHC scores. We observed a statistically significant relationship between the likelihood of amplifying CWD prions in CSF and both date of first tonsil biopsy positivity and incubation period.
Conclusions: Based on our findings, we expect that both sPMCAb and RT-QuIC may prove to be useful diagnostic assays for the detection of prions in CSF. Based on its ease of use, repeatability, and quantitative nature, RT-QuIC may prove more valuable in a diagnostic setting.

Pulse Toceranib plus Lomustine for the Treatment of Unresectable Canine Mast Cell Tumors

Rachel Venable, Douglas Thamm, Jenna Burton, David Vail, Laurel Williams, Sandra Axiak

Introduction: Pulse administration of a tyrosine kinase inhibitor (TKI) with chemotherapy may effectively chemosensitize canine mast cell tumors (MCT) while reducing toxicity and owner cost. Our hypothesis was that the combination of pulse-administered toceranib and lomustine will be well tolerated and efficacious. The purpose of this phase-1/2 multicenter clinical trial was to determine the maximum tolerated dose (MTD) and adverse effect profile of combined treatment, as well as describe the objective response rate and progression-free interval.
Methods: Client owned dogs with measurable MCT were eligible to participate; previous therapy was permitted with the exception of lomustine or TKIs. Toceranib was given on days 1, 3, and 5 of a 21-day cycle at set dose of 2.75 mg/kg. Lomustine was given on day 3 of the 21-day cycle. All dogs were concurrently treated with oral diphenhydramine, omeprazole and prednisone. Dose escalation of lomustine was determined using a 3+3 cohort schema, with expansion once an MTD was established.
Results: Thirty dogs have been enrolled with 18/30 (60%) treated previously. The MTD of lomustine combined with pulse-administered toceranib was established at 50 mg/m2; neutropenia was the dose limiting toxicity. Other adverse events include increased ALT, vomiting, diarrhea, thrombocytopenia, and anemia. The overall response rate was 50% (3 CR, 9 PR). The overall median progression free interval was 47 days.
Conclusions: Lomustine at 50 mg/m2 combined with pulse-administered toceranib is well tolerated in dogs with MCT and appears to have activity with neutropenia as the dose-limiting toxicosis.

The effects of an oral recuperation fluid on the clinical recovery of dogs with parvoviral gastroenteritis

Emilee Venn, Lauren Sullivan, Mike Deogracias, Katie Osekavage, Cord Brundage, Pedro Boscan, David Twedt.

Purpose: To prospectively determine if administration of an oral recuperation fluid to dogs recovering from parvoviral gastroenteritis would improve caloric intake, water intake, body weight and fecal scores during the first five days at home when compared to dogs receiving placebo.
Materials/Methods: Dogs with naturally occurring parvoviral gastroenteritis, treated at Colorado State University's Veterinary Teaching Hospital, were randomized at discharge to either a control or study group. Dog owners, blinded to treatment, administered their dog either 30 ml/day of Viyo Veterinary (study group) or 30 ml/day of water (placebo group) for five days. All dogs were offered, at a minimum, their calculated daily energy requirement of canned Purina EN and 100 ml/kg/day of water. Body weight, total amount of food and water intake, and fecal scoring were recorded daily. Repeated measures analysis of covariance was used to compare changes in body weight, caloric intake (kcal/kg/day) and water intake (ml/kg/day) between groups. Chi Square analysis was conducted on daily fecal scores, and the percentage of prescribed food and water consumed.
Results: A total of 26 dogs (Viyo n=13, placebo n=13) were included. No significant differences were observed between the groups as determined by caloric intake, water intake, percentage of prescribed food or water intake, change in body weight, or Day 2-5 fecal scoring. The Viyo group demonstrated a lower fecal score for the first day ($p<0.004$), interpreted as more formed stool, compared to the placebo group.
Conclusions: Viyo Veterinary was found to be highly palatable and well tolerated by this group of dogs with no adverse side effects noted. Based on the variables measured, we were unable to identify any differences in the clinical recovery of dogs with parvovirus when administered Viyo versus placebo. Further studies may be warranted due to the small group size and reliance on owners to record a majority of data in this study.

Treatment of Chronic Implant-Associated S. aureus Infections with Therapeutic Staphylococcal Protein A Vaccination

Kelly D. Walton, Margie Sutherland, Valerie Johnson, Lon V. Kendall, Steve Dow

Staphylococcus aureus is a leading cause of nosocomial and community-acquired infections, and the appearance of antimicrobial resistance continually presents new treatment challenges. In addition, S. aureus is a biofilm-producing pathogen that is commonly implicated in implant-associated infections. Vaccination has been proposed as a potential therapeutic strategy for chronic infections, however recent attempts to develop an effective vaccine have been met with marginal success. One of the most important virulence factors used by S. aureus is the membrane-bound protein Staphylococcal Protein A (SpA), which functions to inhibit both the innate and adaptive immune responses of the host. The majority of clinically relevant strains of S. aureus express SpA, making this protein a natural target for novel immunotherapeutics. In the present study, we demonstrated that mice treated with SpA vaccination following subcutaneous placement of S. aureus-coated mesh implants harbored lower bacterial numbers than untreated mice following the treatment period. Using in vivo bioluminescent imaging, we also showed that over the course of the study, the bacterial burden declined more rapidly in vaccinated mice. These experiments suggest that SpA vaccination may be an effective tool for the treatment of implant-associated S. aureus infections.

The effect of rotational positioning of the canine tibia on radiographic measurement of frontal plane angulation

David Wilson, Emily Mehlman, Clara SS Goh, Ross Palmer

Purpose: The objective of this study was to evaluate the effect of internal rotational deviation of the tibia from a true caudal-cranial (Cd-Cr) radiographic projection on tibial frontal plane angular measurements.
Materials and methods: Cadaveric limbs (n=8) of large breed dogs were secured for standard and tangential view radiography in a custom apparatus with tibae in precise Cd-Cr orientation followed by quantifiable internal tibial rotational deviation (iARD) of 0, 5, 10, 15, 20, 25, 30, 35, and 40 degrees. Three observers, blinded to the iARD, measured mechanical medial proximal tibial angle (mMPTA) and mechanical medial distal tibial angle (mMDTA) on each radiograph. An ANOVA for repeated measurements evaluated the effect of increasing iARD on mMPTA and mMDTA. In addition, we evaluated the influence of investigator upon the effect of iARD on mMPTA and mMDTA. Significance was set at $p<0.05$.
Results: The effect of each sequential iARD increase was a significant increase in mMPTA for both standard ($p<0.01$) and tangential views ($p<0.01$). In contrast, the effect of increasing iARD was a significant increase in mMDTA ($p<0.01$) for standard and a significant decrease in mMDTA for tangential view ($p<0.01$) radiographs. The effect of iARD on mMPTA and mMDTA was not statistically different between investigators for standard or tangential views.
Conclusions: Tibial rotational deviation from a Cd-Cr image altered measured frontal plane angles. Progressive increases in internal rotational deviation resulted in artifactual proximal tibial valgus in standard and tangential projections and was particularly pronounced in the latter. These findings demonstrate the importance of close scrutiny to insure that true frontal plane (Cd-Cr) radiographs are used to measure frontal plane tibial angulation.

Quantitative and Facile Analysis of the ATP-binding Proteome of Mycobacterium tuberculosis

Lisa M. Wolfe, Susan Idicula-Thomas, Robert Reynolds, Stephan Schürer, Karen M. Dobos

Beyond their function in cancer immune evasion and dysregulated growth, ATP dependent catalytic pathways are being scrutinized for their roles in pathogen biology in order to identify novel drug targets. A new use of biotin-tagged acyl-phosphates of ATP is presented that allows rapid and efficient profiling of ATP-dependent processes over different metabolic states. In particular, we have analyzed the ATPome of M. tuberculosis (Mtb) H37Rv in actively growing and “latent” (hypoxic) cells. A profile of 63 differentially abundant ATP-labeled proteins reveals essential gene products critical to survival, adaptation and the development of drug resistance. Mtb is an ideal prototype organism, as it exists in a variety of metabolic states during infection. With the goal of identifying critical and potentially druggable ATP dependent pathways, these studies lay the groundwork for profiling the ATPome across diverse infectious diseases within multiple and dynamic metabolic states.

Bioassay detection of chronic wasting disease prions in soil

A. Christy Wyckoff, Kurt C. VerCauteren, Mark D. Zabel

Studies suggest that environmental deposits of Chronic Wasting Disease (CWD) prions play an important role in the transmission and persistence of CWD among captive and wild cervids. Furthermore, studies indicate that the prion molecule forms a close association with clays and other types of soil, enhancing its persistence and surprisingly, enhancing the transmissibility of the infectious agent. Investigation of PrPCWD presence in soil has been particularly challenging due to limited sensitivity of existing laboratory assays. To date, detection of naturally occurring prions in field soil samples have not been successful, and as such, estimates of prion contamination in the environment are difficult to make due the lack of sensitive assays. Our objective was to use an existing bioassay technique with CWD susceptible transgenic mice to demonstrate presence, and estimate amount, of PrPCWD in soil. A prion-soil titration curve was created by orally inoculating mice with one of 5 dilutions of PrPCWD positive elk brain homogenate (E2) mixed with 10% whole soil in sucrose. Second, additional groups of mice were either orally inoculated with, or housed on, untreated soil originating from captive cervid research facilities where CWD occurred in herds. These soil types, one from the Colorado Division of Wildlife research facility and the other from the Wyoming Fish and Game research facility, were considered “naturally contaminated” with PrPCWD. Preliminary results from time point sacrifices and clinically ill mice indicate that the use of a mouse bioassay successfully demonstrated the presence of prions in naturally contaminated soil samples. Eventually, when data collection is completed, we will estimate the amount of infectious PrPCWD present in these naturally contaminated soils as compared to our bioassay titration curve established in this project.

The influence of CELF 1 on myogenin expression during differentiation of C2C12 myoblasts

Annie Zhang, Jerome Lee, Carol Wilusz

Purpose: CELF1 is associated with several transcripts encoding proteins essential for effective myogenesis, including Myogenin, MyoD and Cdkn1a mRNAs. Studies have shown that CELF1 can bind GU-rich elements in 3’UTRs and accelerate mRNA decay. Although the myogenin mRNA has a GU-rich element (GRE) in its 3’UTR and is associated with CELF1, the specific role of CELF1 in modulating the expression of myogenin is unclear. Methods: To investigate this, we developed a Renilla Luciferase reporter system to assess post-transcriptional mechanisms acting through 3’UTR of Myogenin in mouse C2C12 cells. This system will be utilized to investigate the role of CELF1 in regulating myogenin expression during muscle differentiation. Results and conclusions: The 3’UTR of myogenin induces mRNA decay and represses translation of the reporter in proliferating C2C12 myoblasts. Future experiments will investigate how this regulation is impacted by depletion of CELF1 through RNA interference. We will also determine whether the role of CELF1 changes during muscle cell differentiation.

2013 CVMBS Research Day

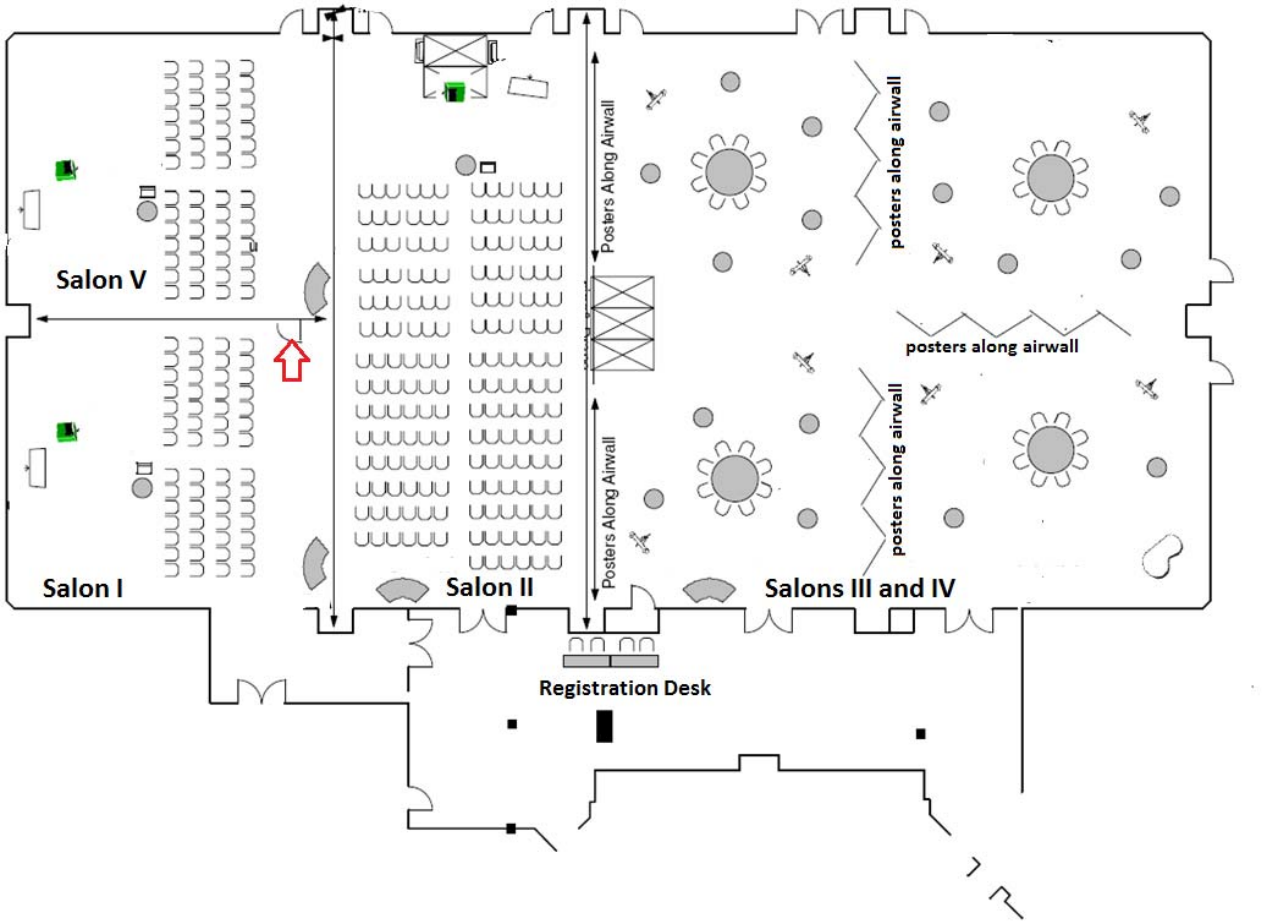

Floorplan Colorado State Ballroom
Fort Collins Hilton